



TECHNICAL REPORT M-71-10

(Supersedes Technical Report M-70-15)

# PERFORMANCE OF BOEING LRV WHEELS IN A LUNAR SOIL SIMULANT

Report I

## EFFECT OF WHEEL DESIGN AND SOIL

by

A. J. Green, K.-J. Melzer



N72-28845

Unclas  
36012

(NASA-CR-127695) PERFORMANCE OF BOEING LRV  
WHEELS IN A LUNAR SOIL SIMULANT. REPORT 1:  
EFFECT OF WHEEL DESIGN A.J. Green, et al  
(Army Engineer Waterways Experiment  
Station) Dec. 1971 83 p  
CSSL 03B G3/30



December 1971

Prepared for **George C. Marshall Space Flight Center**  
**National Aeronautics and Space Administration, Huntsville, Alabama**

Conducted by **U. S. Army Engineer Waterways Experiment Station**  
**Mobility and Environmental Division**  
**Vicksburg, Mississippi**



TECHNICAL REPORT M-71-10

(Supersedes Technical Report M-70-15)

# PERFORMANCE OF BOEING LRV WHEELS IN A LUNAR SOIL SIMULANT

Report 1

## EFFECT OF WHEEL DESIGN AND SOIL

by

A. J. Green, K.-J. Melzer



December 1971

Prepared for **George C. Marshall Space Flight Center**  
**National Aeronautics and Space Administration, Huntsville, Alabama**

Conducted by **U. S. Army Engineer Waterways Experiment Station**  
**Mobility and Environmental Division**  
**Vicksburg, Mississippi**

ARMY-MRC VICKSBURG, MISS.

APPROVED FOR PUBLIC RELEASE; DISTRIBUTION UNLIMITED

~~PRECEDING PAGE BLANK NOT FILMED~~

#### FOREWORD

The study reported herein was conducted by personnel of the Mobility Research Branch (MRB), Mobility and Environmental (M&E) Division, U. S. Army Engineer Waterways Experiment Station (WES). The study was sponsored by the Apollo Program Office, National Aeronautics and Space Administration, Washington, D. C., and it was under the technical cognizance of Dr. N. C. Costes of the Space Sciences Laboratory, George C. Marshall Space Flight Center (MSFC), Huntsville, Alabama. The work was performed under NASA - Defense Purchase Request No. H-68683A, dated 9 April 1970.

The tests were conducted under the general supervision of Messrs. W. G. Shockley and S. J. Knight, Chief and Assistant Chief, respectively, of the M&E Division; and under the direct supervision of Mr. A. J. Green and Dr. K.-J. Melzer of the Research Projects Group, MRB. This report was prepared by Mr. Green and Dr. Meizer.

The Lunar Rover wheels used in this study were furnished by the A. C. Electronics Division of General Motors Corporation in cooperation with the Boeing Company (Huntsville, Alabama) and MSFC. The wheels were modified by the WES without their basic characteristics being altered.

Acknowledgment is made to Dr. D. R. Freitag, Assistant Technical Director, WES, for his advice and assistance during this study.

COL Levi A. Brown, CE, and COL Ernest D. Peixotto, CE, were Directors of WES during the conduct of this study and preparation of this report. Mr. F. R. Brown was Technical Director.

MISSING PAGE READING NOT AT ALL

CONTENTS

	<u>Page</u>
FOREWORD . . . . .	v
NOTATION . . . . .	ix
CONVERSION FACTORS, BRITISH TO METRIC AND METRIC TO BRITISH UNITS OF MEASUREMENT . . . . .	xi
SUMMARY . . . . .	xiii
PART I: INTRODUCTION . . . . .	1
Background . . . . .	1
Purpose and Scope . . . . .	1
PART II: TEST PROGRAM . . . . .	3
Soil . . . . .	3
Wheel-Soil Interaction Test Equipment . . . . .	7
Wheel-Soil Interaction Test Procedures . . . . .	9
PART III: PRESENTATION AND ANALYSIS OF RESULTS . . . . .	10
Data Presentation . . . . .	10
Wheel-Soil Performance Evaluation . . . . .	11
PART IV: CONCLUSIONS AND RECOMMENDATIONS . . . . .	17
Conclusions . . . . .	17
Recommendations . . . . .	17
LITERATURE CITED . . . . .	18
FIGURES 1-27	
TABLES 1-5	
APPENDIX A: WES SINGLE-WHEEL DYNAMOMETER SYSTEM	A1

## NOTATION

$c_b$	Cohesion determined from bevameter tests, psi
$c_c$	Cohesion determined from sheargraph tests, psi
$c_{tr}$	Cohesion determined from trenching tests, psi
$C_u$	Coefficient of uniformity of the soil = $d_{60}/d_{10}$
$d_{50}$	Grain diameter at 50 percent finer by weight, in.
$D'$	Compactibility, % = $100 \left( \frac{e_{max} - e_{min}}{e_{min}} \right)$
$D_r$	Relative density, % = $100 \left( \frac{e_{max} - e}{e_{max} - e_{min}} \right)$
$e$	Initial void ratio
$e_{max}$	Maximum void ratio
$e_{min}$	Minimum void ratio
$G$	Penetration resistance gradient, pci*
$k_c, k_\phi, k_n$	Bekker soil values
$M$	Wheel torque, ft-lb
$M/Wr_e$	Torque coefficient, dimensionless
$M_x/Wr_e$	Value of $M/Wr_e$ at a given percentage of wheel slip $x$ (e.g. 20 or 50 percent)
$P$	Pull (drawbar pull), lb
$PN$	Power number $M_w/Wv_a$ , dimensionless
$PN_{sp}$	Value of $PN$ at self-propelled point ( $P/W = 0$ )
$PN_{15}$	Value of $PN$ when $P/W = 0.27$ (corresponds to 15-deg slope)
$PN_{20\%}$	Value of $PN$ at 20 percent slip
$PN_{50\%}$	Value of $PN$ at 50 percent slip

---

\* pci = lb/in.<sup>3</sup>

$P/W$	Pull coefficient, dimensionless
$P_T/W$	Value of $P/W$ when torque = 0
$P_x/W$	Value of $P/W$ at a given percentage of wheel slip $x$ (e.g. 20 or 50 percent)
$s_b$	Shear stress determined from bevameter tests, psi
$s_c$	Shear stress determined from sheargraph tests, psi
$v_a$	Translational (carriage) speed, fps
$w$	Moisture content, % (percent of dry density)
$W$	Wheel load; weight, lb
$\gamma$	Wet density, $g/cm^3$ (pci)
$\gamma_d$	Dry density, $g/cm^3$ (pci)
$\gamma_s$	Specific gravity
$\sigma_1$	Major principal stress, psi
$\sigma_3$	Minor principal stress, psi
$\sigma_n$	Normal stress, psi
$\phi_b$	Angle of internal friction determined from bevameter tests, deg
$\phi_c$	Angle of internal friction determined from sheargraph tests deg
$\phi_{pt}$	Angle of internal friction determined from in situ plate, tests, deg
$\phi_s$	Secant friction angle determined from triaxial tests, deg
$\omega$	Angular velocity of the wheel, radians/sec

CONVERSION FACTORS, BRITISH TO METRIC AND METRIC  
TO BRITISH UNITS OF MEASUREMENT

British units of measurement used in this report can be converted to metric units as follows:

<u>Multiply</u>	<u>By</u>	<u>To Obtain</u>
inches	2.54	centimeters
feet	0.3048	meters
pounds (force)	4.4482	newtons
pounds per square inch	6.8948	kilonewtons per square meter
pounds per cubic inch	0.2714	meganewtons per cubic meter
foot-pounds	1.3558	meter-newtons

Metric units of measurement used in this report can be converted to British units as follows:

<u>Multiply</u>	<u>By</u>	<u>To Obtain</u>
grams per cubic centimeter	62.43	pounds per cubic foot
newtons	0.2248	pounds (force)
kilometers	0.6214	miles

PRECEDING PAGE BLANK NOT REPRODUCED

#### SUMMARY

Six versions of the Boeing-GM wire-mesh wheel were laboratory tested in a lunar soil simulant, consisting of a crushed basalt with a grain-size distribution similar to that of samples collected during Apollo 11 and 12 flights, to determine their relative performance. The consistency of the soil was varied to cover a range of cohesive and frictional properties to simulate soil conditions assumed to exist on the moon.

Programmed-slip and constant-slip tests were conducted with the U. S. Army Engineer Waterways Experiment Station single-wheel dynamometer system. The performance of the wheel covered with a metal chevron tread over 50 percent of its contact surface was slightly superior to that of other tread designs.

The amount of soil accumulated in the wheels during the tests varied linearly with slip. Less soil accumulated in the 50 and 75 percent chevron-covered wheels than in the open-mesh one.

Pull/load increased rapidly with increasing slip to a near maximum at 15 to 25% slip for all wheels, then increased slowly with increasing wheel slip to 100% slip. This behavior suggests that the operation of a vehicle at slips higher than 25% for protracted periods would result in immobilizing the vehicle, as would be the case if the vehicle were required to negotiate a soft soil spot or a steeper slope section. Specific power requirements for all wheels tested, as depicted by the power number, also rose rapidly at slips beyond 15 to 25%. These trends indicate that the wheel performance at 20% wheel slip provides a reasonable measure for comparing the limiting mobility performance capabilities of several versions of the basic GMC (wire-mesh) Lunar Roving Vehicle (LRV) wheel type.

Following the selection of the Boeing-GMC wheel for the LRV, additional wheel-soil interaction tests were conducted in the lunar soil simulant and are reported in Report 2 of this series.

Appendix A describes in detail the WES dynamometer system in which the LRV wheel was tested.

PERFORMANCE OF BOEING LRV WHEELS IN A LUNAR SOIL SIMULANT  
EFFECT OF WHEEL DESIGN AND SOIL

PART I: INTRODUCTION

Background

1. Following the award of the contract for the Manned Lunar Roving Vehicle (MLRV) system to the Boeing Company, its subcontractor, General Motors Corporation (GMC), fabricated two new<sup>\*</sup> 32-in.<sup>\*\*</sup>-diam wheels, one with inner and outer wire-mesh surfaces separated by a layer of fabric and with traction spikes attached to the outer surface, and the other of open-wire mesh and chevron metal treads covering 50 percent of its contact surface. At the request of the George C. Marshall Space Flight Center (MSFC), the U. S. Army Engineer Waterways Experiment Station (WES) conducted tests to evaluate the performance of these two wheels in a fine, uniform sand, the cohesive and frictional properties of which spanned a range believed to embrace the probable range of lunar soil properties. The report (Green and Melzer, 1970) on these tests was furnished to MSFC in March 1970 and was subsequently furnished to the Boeing Company and GMC.

2. In the interim, GMC prepared other wheel designs in an effort to optimize the traction performance, increase the durability, and minimize the weight of the LRV mobility system. Subsequently, the WES was requested to conduct tests with several of these wheel versions in a lunar soil simulant (LSS) consisting of a crushed basalt with a grain-size distribution very similar to that of the lunar soil samples collected during the Apollo 11 and 12 flights (Costes, et al., 1969; Scott, et al., 1970). The results of these tests are reported herein.

Purpose and Scope

3. The purpose of this test program was to determine and compare the quantitative performance of several of the basic wheel designs and

---

\* Boeing-GM VII and VIII; wheels I-VI had been tested previously (Freitag, Green, and Melzer, 1970a and 1970b).

\*\* A table of factors for converting British to metric and metric to British units of measurement is included on page xi.

modified versions of the GM<sup>\*</sup> LRY wire-mesh wheel (paragraph 24). To meet these objectives, a series of single-wheel, programmed-slip tests was conducted in the crushed basalt.<sup>\*\*</sup> As had been done in earlier tests in sand, the soil was prepared at various consistencies (LSS<sub>1</sub>, LSS<sub>2</sub>, LSS<sub>3</sub>, and LSS<sub>4</sub>) to cover the range of cohesive and frictional properties of the actual lunar soil as assessed from the Apollo 11 and Apollo 12 manned lunar landings and earlier unmanned missions (Scott and Roberson, 1968; Costes, et al., 1969; Scott, et al., 1970). Three programmed-slip tests were conducted with the 50 percent chevron-covered (GM X) wheel at the design load of 57 lb on each of the four soil conditions. Two programmed-slip tests usually were conducted with the other wheels on each soil condition. The soil, wheel, and wheel-performance parameters measured and the test equipment and procedures used in this test program were the same as those employed in the earlier tests.<sup>†</sup>

---

\* For convenience, the Boeing-GMC wheels are called "GM wheels" in this report.

\*\* The terms basalt, lunar soil simulant, LSS, and soil are used interchangeably in this report.

† See Freitag, Green, and Melzer (1970a and 1970b) and Green and Melzer (1970).

## PART II: TEST PROGRAM

### Soil

#### Description

4. The soil used in this study was crushed basalt purchased from the Basalt Rock Company, Napa, California. Gradation and classification data and density and void ratio values are given in fig. 1. This soil is granular with angular to subangular grains, but it exhibits a small amount of cohesion when moist and/or compacted.

#### Preparation

5. The desired soil consistency of the air-dry basalt (LSS<sub>1</sub>, LSS<sub>2</sub>, and LSS<sub>3</sub>) was obtained in the following manner: The test bins were filled, and the soil was plowed with a seed fork to a depth of 12 in. For loose conditions, no compaction was necessary, so the surface of the plowed section was screeded level; for the denser conditions, the soil was compacted with a vibrator applied at the surface before screeding. The relation between dry and relative densities for the material is shown in fig. 2.

6. To prepare the wet basalt (LSS<sub>4</sub>), a sufficient quantity of water was added to the material to raise the moisture content to 1.4%. The material was then thoroughly mixed in the test bin. The mixing process was repeated with an additional quantity of water, yielding a material with a very nearly uniform moisture content with an average value of 1.8% ( $\pm 0.1\%$ ). This moisture content was held constant by covering the test section when not in use and occasionally spraying the surface very lightly with water to compensate for evaporation. The wet soil was processed in place before each test. During the testing cycles in this test program, uniformity in soil conditions was ensured by frequent determination of moisture content and density and by measurements with the cone penetrometer.

7. Four soil conditions were used in these tests, designated as LSS<sub>1</sub>, LSS<sub>2</sub>, LSS<sub>3</sub>, and LSS<sub>4</sub>. The ranges of soil properties for each test condition and their average values are given in table 1.

## Soil tests

8. Vacuum triaxial tests.\* To obtain at least qualitative knowledge of the shear strength characteristics of the soil at low normal stresses, three series of vacuum triaxial tests were conducted on samples 2.8 in. in diameter and 5.9 in. high. Each series consisted of two tests conducted at constant relative density and confining pressures of 0.5 and 1.0 psi; initial relative densities for the three series were 38, 51, and 85%.

9. In situ plate shear tests. During this test program, two series of in situ plate shear tests were conducted on prepared test sections with a specially developed test device.\* Each series consisted of four tests conducted at constant relative densities and normal pressures of 0.16, 0.51, 0.75, and 1.06 psi; initial relative densities were 25 and 58%, respectively, and moisture content for both series was 1.1%.

10. Trenching tests. To determine the cohesion of the soil, two trenching tests were conducted in each of the four soil conditions. A vertical wall was very carefully excavated in the material, its height at failure was measured, and the failure patterns were observed. On the basis of the data collected and known density-friction angle relations, the soil cohesion was determined from a slope stability analysis (Taylor, 1948).

11. Density and moisture content determinations. Density and moisture content were determined gravimetrically by means of a "density box."\* Two measurements of density were usually made before and one after each test. The surface moisture of the soil was measured occasionally (table 2) by standard procedures. In some cases the relative density and dry density, respectively, were monitored only by measuring the penetration resistance of the soil with the WES cone penetrometer and converting to relative density or dry density through calibration diagrams.

12. Cone penetration resistance. The standard WES mechanical cone penetrometer was used throughout this study to measure the penetration resistance gradient  $G$ .\* During the single-wheel tests,  $G$  usually was determined at five points on the center line of a test section prior

---

\* Freitag, Green, and Melzer (1970a).

to testing (tables 1 and 2). Two additional penetrations were made in the middle part of the test section (except during the later part of the program), one 10 in. to the left and one 10 in. to the right of the center line. In a three-pass test, data were also taken at four points along the center line upon the completion of the first and third passes.

13. An alternative method of determining dry density  $\gamma_d$  from cone penetration resistance gradient  $G$  values was developed\* as follows: Soil with the desired moisture content was placed into molds 15 in. in diameter and 12 in. high and was compacted to the desired dry density. The density was determined volumetrically for the total mold, and  $G$  was measured. Two test series were conducted at moisture contents of 0.8 and 1.8 percent, respectively. The data were evaluated statistically, and the two regression equations are (fig. 3)

a. For  $w = 0.8$  percent :

$$\gamma_d = 1.531 + 0.152 \log G ; \gamma_d \text{ in g/cm}^3, G \text{ in pci}$$
$$\text{Standard error of estimate} = \pm 0.037 \text{ g/cm}^3$$
$$\text{Correlation coefficient} = 0.959$$

Number of points = 11

b. For  $w = 1.8$  percent :

$$\gamma_d = 1.420 + 0.176 \log G ; \gamma_d \text{ in g/cm}^3, G \text{ in pci}$$
$$\text{Standard error of estimate} = \pm 0.002 \text{ g/cm}^3$$
$$\text{Correlation coefficient} = 0.998$$

Number of points = 6

14. Special soil tests. A number of special soil tests were conducted during this study at the request of the sponsor. Bevameter plate penetration, bevameter ring shear, and Cohron sheargraph tests were conducted during a large part of the single-wheel tests before and after each test (table 2).

#### Analysis of soil test data

15. Values of the following soil parameters pertinent to the tests are presented in table 1: penetration resistance gradient  $G$  ; bevameter

---

\* Green, Smith, and Murphy (1964) and Freitag, Green, and Melzer (1970a and 1970b) showed that the evaluation of  $\gamma_d$  of sand from a relation between  $G$  and  $\gamma_d$  established from few carefully controlled tests often led to more reliable  $\gamma_d$  values than the evaluation of  $\gamma_d$  from routine tests with the density box, especially for wet sand. The same was found to be true for the LSS.

values  $k_c$ ,  $k_\phi$ ,  $v$ ,  $\phi_b$ , and  $c_b$ ; cohesion from trenching tests  $c_{tr}$ ; secant friction angle from triaxial tests  $\phi_s$ ; friction angle from in situ plate shear tests  $\phi_{pl}$ ; density  $\gamma$ ; relative density  $D_r$ ; and moisture content  $w$ .

16. Angle of internal friction. The results of the vacuum triaxial tests were plotted in a  $(\sigma_1 - \sigma_3)/2$  versus  $(\sigma_1 + \sigma_3)/2$  relation in fig. 4. In such plots each Mohr circle appears as a point. As shown in fig. 4, the relation between  $(\sigma_1 - \sigma_3)/2$  and  $(\sigma_1 + \sigma_3)/2$  is not linear for a given relative density, but is a curved line, i.e. the angle of internal friction is not constant for a given relative density, but depends on the normal stress  $\sigma_n$ , at least within the  $\sigma_n$  range tested (0.85-1.65 psi); the influence of  $\sigma_n$  seems to decrease with decreasing relative density.

17. To assess the dependence of the angle of internal friction on relative density and density, respectively, the secant friction angles  $\phi_s$  (fig. 4)\* were evaluated for each test and two normal stress levels, and were plotted versus relative density  $D_r$  and dry density  $\gamma_d$  (fig. 5). Based on these results, the angles of internal friction for the soil conditions tested were roughly as follows:

$\phi_s$  Values, deg

Soil	LSS <sub>1</sub>	LSS <sub>2</sub>	LSS <sub>3</sub>	LSS <sub>4</sub>
$D_r$ , %	29.0	40.0	51.0	32.0
$\sigma_n = 0.85$ psi	38.5	39.0	40.0	38.6
$\sigma_n = 1.65$ psi	37.0	37.5	38.3	37.1

The results of the in situ plate shear tests, which were more-or-less exploratory-type tests during this program, showed qualitatively the same influence of normal stress on the angle of internal friction as that observed in the triaxial tests. Within the normal stress range tested (0.16-1.06 psi), the  $\tau$ - $\sigma_n$  relation was a curved line for a given relative density, i.e. the angle of internal friction was not constant. The influence of  $\sigma_n$  decreased with decreasing  $D_r$ . Based on the results

\* Freitag, Green, and Melzer, op. cit., p 4.

of the two tests series with  $D_r = 25$  and 58 percent, the angles of internal friction  $\phi_{pl}$  (secant friction angles) can only be estimated for the soil conditions tested during the wheel program. They are tabulated for the two extreme normal stresses as follows:

$\phi_{pl}$  Values, deg

Soil	LSS <sub>1</sub>	LSS <sub>2</sub>	LSS <sub>3</sub>	LSS <sub>4</sub>
$D_r$ , %	29.0	40.0	5.10	32.0
$\sigma_n = 0.16$ psi	37.5	38.5	39.0	37.5
$\sigma_n = 1.06$ psi	34.0	35.0	35.5	34.0

18. Apparent cohesion. On the basis of trenching tests, the apparent cohesion of the soil was computed by the Coulomb wedge or graphic method, and by slope stability analysis.\* The average values of apparent cohesion  $c_{tr}$  for LSS<sub>1</sub>, LSS<sub>2</sub>, LSS<sub>3</sub>, and LSS<sub>4</sub> soils were 0.03, 0.05, 0.08, and 0.11 psi, respectively.

19. Relative density and moisture content. The minimum, maximum, and average values of dry density, moisture content, and relative density for the various soil conditions evaluated from the volumetric (density box) and cone penetration resistance measurements are given in table 1. The values determined for each single-wheel test are given in table 2.

20. The relative density and density values determined volumetrically were erratic, especially for the loose soil conditions. Accordingly, the  $D_r$  and  $\gamma_d$  values evaluated from the relations between relative and dry density with cone penetration resistance gradient (fig. 3) are considered to be more representative of the actual soil conditions used in these tests.

### Wheel-Soil Interaction Test Equipment

#### Dynamometer

21. The dynamometer system (see Appendix A) used in these tests can accommodate loads from approximately 15 to slightly more than 200 lb, and

\* Ibid., p 6.

wheels ranging from 18 in. to 45 in. in diameter. Vertical load, horizontal force (drawbar pull), torque, sinkage, carriage speed, and wheel speed were continuously measured during testing by instrumentation on the dynamometer carriage (fig. 6). The load cell used to measure torque was manufactured by the Baldwin-Lima-Hamilton Corporation and has a maximum rated capacity of 200 lb. The two vertical sensor bars and two horizontal sensor bars have a maximum capacity of approximately 150 lb each. These were machined and gaged by the WES. Each bar has a full Wheatstone bridge with two active arms. The average translational speed of the wheel at zero percent slip was approximately 2.5 fps; the angular velocity was held constant and it, too, was roughly 2.5 fps. A schema of the system is shown in fig. 7.

Recording systems (see fig. A11)

22. The primary data recording system is an in-line digital computer. With this system the electrical signals (analog) reach the computer in a raw form with no signal conditioning, such as filters, galvanometer circuits, etc. When the computer functions in an off-line capacity, the signals are converted to digital form and then stored on magnetic tape for subsequent data processing. The data output system includes an IBM 35 teletypewriter. Representative data output from this system is shown in table 3.

23. The secondary recording system is a 36-channel direct-writing light-beam oscillograph, which requires signal conditioning in the form of filters and galvanometers. Care is taken to ensure that the filters and galvanometers do not distort the signal to the extent that significant time lags occur or that significant transient pulses are not "smoothed out." This secondary system gives the test engineer an opportunity, if necessary, to take a quick look at the data when planning subsequent tests and a means to rapidly determine whether all circuits are functioning properly during a given test. These records are used in data analysis only when the digital recording system cannot be used; only one test (test 28) of the group in this report was analyzed from the oscillograph record.

### Test wheels

24. Six 32-in.-diam metal-elastic wheels were tested,

Name	Surface
GM IX	75% chevron-tread cover*
GM X	50% chevron-tread cover*
GM XI	GM IX covered with inner tube*
GM XII	GM XI with rubber grousers added*
GM XIII	50% chevron-tread cover*
GM XIV	Open mesh (GM X with chevron-tread removed)

\* Over the portion of the wheel normally in contact with the ground.

The GM IX and GM X wheels are shown in fig. 8; the GM X is shown in the soil bin in fig. 9.

25. The GM X and GM XIII were essentially alike. The GM XI was formed by covering the 75 percent chevron-covered version with a 9.00-14 inner tube. Because air pore pressure development was suspected, aggressive grousers were glued to the rubber surface of the GM XI wheel to form the GM XII. The grousers were V-belts, approximately 3/4 in. high and 3/4 in. wide at the base, mounted perpendicular to the direction of travel. Deflections, contact pressures, and other wheel data are given in table 4.

### Wheel-Soil Interaction Test Procedures

26. A programmed-slip technique was used in all the single-wheel tests. The test was started when the wheel was in the negative slip range, i.e. the translational speed of the carriage was greater than that of the wheel. The carriage was decelerated at a programmed, uniform rate (wheel speed was approximately constant) to cause the wheel to pass through the zero-torque point, the 0% slip point, the self-propelled point, etc., as slip progressively increased to 100%. Wheel performance data are shown in table 5.

## PART III: PRESENTATION AND ANALYSIS OF RESULTS

### Data Presentation

27. The relations of torque and pull to slip can be shown by two plots, such as those in figs. 10, 12, 14, and 16 that represent data obtained with the 50 percent covered wheels (GM X and GM XIII). As indicated in these figures, torque and pull increase at a decreased rate for wheel slips greater than about 20%. Although all tests were not identical, torque and pull in nearly all of them appear to reach a significantly lower rate of increase at a wheel slip of 50%, so data for comparing performance of the wheels were read at 20% and 50% slips.

28. It should be noted that whereas the increase in pull at slips greater than 20% is small, the increase in specific power requirements as depicted by the power number  $M\omega/Wv_a$  is quite large (figs. 11, 13, 15, and 17). Because a slip scale is not shown in these figures, it should be mentioned that the 20% slip point generally falls in the area where the power number versus pull coefficient  $t/W$  relation changes sharply in slope. This is shown on a representative computer print out (table 3).

29. The relations in figs. 10-17 indicate that it is unsafe to allow a vehicle to operate at high slip (>20%), except for brief intervals. Therefore, it appears reasonable to compare the relative performance of the wheels at slips of 20% or less and to estimate maximum slope-climbing capability on the basis of performance at the 20% slip level, thus providing a margin of safety.

30. All the wheel performance plots shown herein reflect the assumption that the pull coefficient measured at a given slip on a level surface with a single wheel is roughly equivalent to the tangent of the angle of the slope that a vehicle equipped with similar wheels can climb. This assumption is based on the fact that the P/W versus slip curve in this report is generally similar in shape to those shown by Freitag, Green, and Melzer (1970a), where the correspondence between the results from tests with single wheels on a level surface and the results from tests with vehicles equipped with similar wheels was shown. This

comparis included two vehicles, the Surveyor Lunar Rover Vehicle and a 4x4 vehicle equipped with very flexible pneumatic wheels.

31. The plot of the power number versus the pull coefficient (figs. 11, 13, 15, and 17) is especially important, since it expresses the energy consumed per unit of distance per unit of wheel or vehicle weight in relation to drawbar pull or slope-climbing ability.  $PN_{sp}$  (PN at 0 pull),  $PN_{150}$  (corresponding to 15-deg slope, or  $P/W = 0.27$ ),  $PN_{20\%}$  (the value at 20% slip), and  $PN_{50\%}$  (the value at 50% slip) were recorded. To obtain whr/km conforming to a particular slope, say 15 deg, read the value of  $PN_{150}$ , and multiply this value by the desired wheel load or vehicle weight in newtons and the fraction 1000/3600.

#### Wheel-Soil Performance Evaluation

32. In the discussion that follows, performance indicators, such as power number, torque coefficient, pull coefficient, slope-climbing capability, and wheel slip, are used to illustrate the performance of each of the versions of the GM wheel. Discussions of the performance of the individual wheels is followed by a comparative analysis of the performance of all versions of the GM wheel included in this report.

#### GM IX

33. Two tests were conducted with the GM IX wheel in soil condition  $LSS_1$  ( $G = 0.8$  pci). This wheel had a 75 percent chevron cover as shown in fig. 8. The relations of torque and pull coefficients, respectively, to slip are shown in fig. 18; fig. 19 shows the relation of power number and power consumption rate to pull coefficient on a slope. Results of a simple linear regression on the initial portion of the curve in fig. 19 are:

$$PN = 1.45 (P/W) + 0.182$$

$$\text{Standard error of estimate} = 0.048$$

$$\text{Coefficient of correlation} = 0.949$$

#### GM X and XIII

34. The test data for these two wheels were combined for analysis since each had a 50 percent chevron cover, and their deflection characteristics were essentially the same (table 4). Tests were conducted on each of four soil conditions. The results from these tests are shown in figs. 10 through 17. A simple linear regression was conducted using data

from the initial portion of each plot of power number versus pull coefficient (figs. 11, 13, 15, and 17). The same type of regression was run combining all the data from all four figures. The regression equation is of the form  $y = mx + b$ , and the equation constants and related statistics are as follows:

<u>Conditions</u>	<u>m (Slope)</u>	<u>b (Intercept)</u>	<u>Standard Error of Estimate</u>	<u>Correlation Coefficient</u>
LSS <sub>1</sub>	1.478	0.036	0.104	0.882
LSS <sub>2</sub>	1.400	0.074	0.097	0.897
LSS <sub>3</sub>	1.314	0.053	0.099	0.870
LSS <sub>4</sub>	1.395	0.092	0.057	0.957
Composite	1.403	0.061	0.101	0.884

It is seen that the slope of the regression line decreases as the penetration resistance of the soil increases:

<u>Soil</u>	<u>G</u>	<u>m</u>
LSS <sub>1</sub>	0.8	1.478
LSS <sub>2</sub>	2.2	1.400
LSS <sub>3</sub>	6.5	1.314
LSS <sub>4</sub>	3.7	1.395

35. Since the 50 percent chevron-covered wheel was the one selected for the Lunar Rover Vehicle, six other types of curves were examined fitting the data shown in figs. 11, 13, 15, and 17, and a coefficient of determination (Spiegel, 1961) was used to select the best type. The curve types, soil conditions, and related indices are shown in the following tabulation:

<u>Soil Conditions</u>	<u>Coefficient of Determination</u>					
	$y = mx + b$	$y = be^{*mx}$	$y = bx^m$	$y = \frac{m}{x} + b$	$y = \frac{1}{b} + mx$	$y = \frac{x}{b} + mx$
LSS <sub>1</sub>	0.578	0.821	0.694	0.037	0.493	0.588
LSS <sub>2</sub>	0.496	0.756	0.630	0.011	0.542	0.432
LSS <sub>3</sub>	0.478	0.820	0.687	0.040	0.599	0.412
LSS <sub>4</sub>	0.476	0.731	0.534	0.027	0.714	0.395

\* e is base of Napierian logarithm.

Without exception, the exponential form was indicated to be the best type of curve (highest index of determination) to express the relation of  $y$  (power number) to  $x$  (pull coefficient). The constants for the equation and the related statistics are as follows:

Soil Conditions	m (Exponent Term)	b (Coefficient Term)	Standard Error of Estimate	Correlation Coefficient
LSS <sub>1</sub>	5.250	0.095	0.357	0.906
LSS <sub>2</sub>	4.830	0.121	0.409	0.870
LSS <sub>3</sub>	5.401	0.088	0.363	0.906
LSS <sub>4</sub>	4.939	0.139	0.381	0.855
Composite	5.102	0.108	0.395	0.879

36. Constant-slip tests were conducted with the GM X wheel at 25% slip on soil condition LSS<sub>2</sub> and at 50% slip on LSS<sub>1</sub> to evaluate the reliability of the programmed-slip techniques and the inertia correction system for the horizontal force measurement (pull). Comparative data are as follows:

Soil Conditions	Pass No.	Slip %	Test Type*	P/W	M/Wr <sub>e</sub>	PN
LSS <sub>2</sub>	1	25	CS	0.30	0.41	0.56
	2	24	CS	0.35	0.45	0.50
	1	25	PS	0.30	0.40	0.51
	2	24	PS	0.38	0.48	0.59
LSS <sub>1</sub>	1	50	CS	0.35	0.68	1.38
	1	50	PS	0.43	0.54	1.08

\* CS: constant slip; PS: programmed slip.

There is a relatively good agreement between programmed-slip and constant-slip test results for the two types of soil at 25% slip, but the comparison is poor at 50% slip. At this higher slip, the amount of soil retained in the wheel may have been different for the two types of tests, possibly affecting the comparison.

#### GM XI and XII

37. To obtain a measure of performance of a covered version of the GM wheel, an inner tube was split and stretched over the GM IX wheel's

wire-mesh framework. The performance of this version (GM XI) was very poor in soil conditions LSS<sub>1</sub> and LSS<sub>2</sub>, and the flow of soil observed around the wheel gave some indication of the development of air pore pressures, so grousers were added (paragraph 25). The addition of the grousers (GM XII) caused a slight increase in performance, but did not bring the performance level up to that of the GM IX, X, or XIII. The relations of the torque and pull coefficients to slip are shown in figs. 20, 22, and 24; figs. 21, 23, and 25 show the relations of the power number and power consumption rate to the pull coefficient or slope.

GM XIV

38. The chevron tread was removed from the GM X wheel to produce an open-mesh version (GM XIV) without treads or cover of any type. Two tests were conducted on soil condition LSS<sub>1</sub>, and since the performance level did not match or exceed that of the 50 percent chevron-covered version, testing was limited to the one soil condition. The relations of the torque and pull coefficients to slip for this wheel are shown in fig. 26; fig. 27 shows the relations of power number and power consumption rates to the pull coefficient or slope. A simple linear regression for the initial portion of the curve yielded the following:

$$PN = 1.675(P/W) + 0.076$$

Standard error of estimate: 0.111

Coefficient of correlation: 0.882

Comparative performance (GM IX-XIV)

39. This brief summary is intended to show the effect that the percentage of cover had on wheel performance. A condensation of the data appearing in table 5 follows. The soil condition for each wheel represented was LSS<sub>1</sub>, and the information shown represents the average of the first and second passes of all tests with each of the wheels.

Wheel	Cover %	P <sub>20%</sub> /W	P <sub>T</sub> /W	PN <sub>sp</sub>	PN <sub>15%</sub>	PN <sub>20%</sub>	M <sub>20</sub> /W <sub>r<sub>e</sub></sub>
XIV	J	0.22	0.13	0.12	0.63	0.51	0.40
X and XIII*	50	0.30	0.14	0.11	0.43	0.48	0.39
IX	75	0.21	0.15	0.19	0.90	0.52	0.39
XI	100	0.02	0.14	0.18	(No <sup>∞</sup> Go)	0.23	0.18
XII	100**	0.11	0.19	0.18	(No <sup>∞</sup> Go)	0.42	0.34

\* Averaged.

\*\* With grousers.

The above tabulation offers evidence that the 50 percent covered wheel may be a near-optimum design. It also shows that the performance of the 0 percent covered version is not greatly different from that of the 75 percent covered version. The motion resistance ( $P_T/W$ ) is comparable for all wheels except the GM XII. The power required to propel the wheel, either on a level surface ( $PN_{sp}$ ) or on a 15-deg slope ( $PN_{150}$ ), is the lowest for the 50 percent covered wheel. Its slope-climbing ability when operating at 20% slip is the highest of the group, i.e. approximately 17 deg, as opposed to 12 deg for the 0 and 75 percent covered versions and even less for the fully covered version. Here  $P/W$  is assumed to be approximately equal to the tangent of the angle of the slope being climbed.

#### Soil retained in wheel

40. Soil accumulated in the wheels during the tests; but unlike in the previous tests in sand (Green and Melzer, 1970), where the wheel retained soil only during tests in the  $C_0$  soil condition ( $G \approx 0.8$  psi,  $D_r \rightarrow 0$ , and  $w = 1.4\%$ ), the wheels retained approximately the same amount of crushed basalt in each soil condition tested. The wheels with a 50 percent chevron-tread cover (GM X and XIII) and the one with a 75 percent cover (GM IX) retained from 21 to 24 lb at 100% slip. At 10% slip, they retained approximately 3 lb. The amount of retained soil was observed to increase approximately linearly with slip. The wheel with the tread removed (GM XIV) retained approximately 44 lb of soil at 100% slip. The soil trapped in the GM X wheel at approximately 100% wheel slip is shown in fig. 9. It was further observed that while a wheel was operating at low slips ( $\approx 5\%$ ), it would not retain soil, but would dump any that might have accumulated at higher slips.

41. It is common practice for farmers and earthmoving contractors to fill tires with water or other fluids to increase traction. The added fluid does represent an increase in wheel load, and on some soils the desired increase in the traction force is achieved.\* Such is not necessarily the case for the open or partially open GM wheel. The mechanics involved is not clearly understood. However, little, if any, of the

---

\* U. S. Department of Agriculture, Auburn University, Auburn, Alabama.

weight of retained soil was sensed by the vertical load-measuring device in the test program reported herein, and the weight of this material was not considered in computing the various performance parameters. Before the effect of the retained soil on performance can be evaluated adequately, some means must be devised for determining what percentage of the retained soil represents an increase in wheel load. For this determination, two basic facts must be known or estimated analytically: (a) the extent to which soil bridging occurs in a vibrating, flexing wheel; and (b) the portion of the retained soil that has a large horizontal velocity component. These problems are beyond the scope of this report.

## PART IV: CONCLUSIONS AND RECOMMENDATIONS

### Conclusions

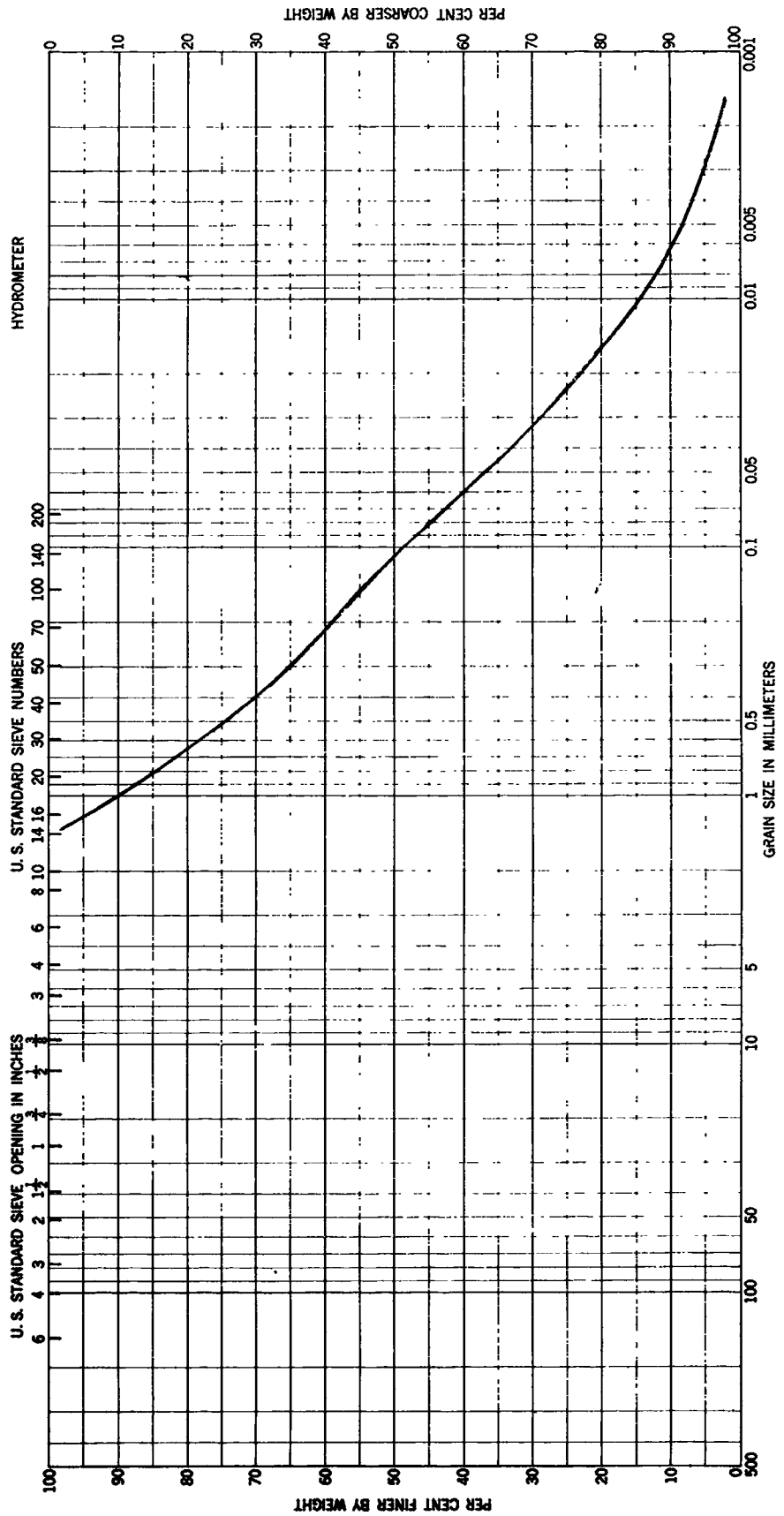
42. It can be concluded that:
- a. The performance of the 50 percent covered wheel in LSS appears to be equal to or slightly superior to that of the other versions on the basis of the performance parameters evaluated (paragraph 39).
  - b. The 0 and 75 percent covered versions displayed similar performance levels.
  - c. There appears to be a relatively good agreement between programmed-slip and constant-slip test results at a slip of 25% (paragraph 36).
  - d. Soil accumulated in the open and partially covered wheels and the amount increased with slip. The wheels with the chevron treads (50 and 75 percent covered) retained an average of 22 lb at 100% slip, whereas the open wheel retained an average of 44 lb (paragraph 40).
  - e. The maximum slope-climbing capability should be estimated on the basis of the pull coefficient developed at 20% slip (paragraph 29). Accordingly, on this basis the maximum slope-climbing capability of the 50 percent chevron-covered wire-mesh GM wheel is estimated to be of the order of 20 deg.

### Recommendations

43. It is recommended that studies be made of:
- a. The effects of velocities up to 10 fps on wheel performance.
  - b. The effects on wheel performance of roughening the present treads (metal-to-soil rather than soil-to-soil failures may have occurred in some instances).
  - c. The incremental increase in battery power consumption required to steer.
  - d. The influence of the direction of the treads on wheel performance.

LITERATURE CITED

- Costes, N. C., Carrier, W. D., Mitchell, J. K., and Scott, R. F. (1969), "Apollo 11 Soil Mechanics Investigation," Apollo 11 Preliminary Science Report, NASA SP-214, National Aeronautics and Space Administration, George C. Marshall Space Flight Center, Ala., pp 85-122.
- Freitag, D. R., Green, A. J., and Melzer, K.-J. (1970a), "Performance Evaluation of Wheels for Lunar Vehicles," Technical Report No. M-70-2, U. S. Army Engineer Waterways Experiment Station, CE, Vicksburg, Miss.
- \_\_\_\_\_ (1970b), "Performance Evaluation of Wheels for Lunar Vehicles (Summary Report)," Miscellaneous Paper No. M-70-4, U. S. Army Engineer Waterways Experiment Station, CE, Vicksburg, Miss.
- Green, A. J. and Melzer, K.-J. (1970), "The Performance of Two Boeing-GM Wheels (GM VII and GM VIII) for the Manned Lunar Rover Vehicle," Miscellaneous Paper No. M-71-3, Feb 1971, U. S. Army Engineer Waterways Experiment Station, CE, Vicksburg, Miss.
- Green, A. J., Smith, J. L., and Murphy, N. R. (1964), "Measuring Soil Properties in Vehicle Mobility Research; Strength-Density Relations of an Air-Dry Sand," Technical Report No. 3-652, Report 1, U. S. Army Engineer Waterways Experiment Station, CE, Vicksburg, Miss.
- Scott, R. F., Carrier, W. D., Costes, N. C., and Mitchell, J. K. (1970), "Mechanical Properties of the Lunar Regolith," Apollo 12 Preliminary Science Report, NASA SP-235, Section 10, Part C, National Aeronautics and Space Administration, George C. Marshall Space Flight Center, Ala., pp 161-182.
- Scott, R. F. and Roberson, F. I. (1968), "Soil Mechanics Surface Sampler," Surveyor Project Final Report; Part II: Science Results, Technical Report No. 32-1265, Chapter V, California Institute of Technology, Jet Propulsion Laboratory, Pasadena, Calif.
- Spiegel, M. R. (1961), "Schaum's Outline of Theory and Problems of Statistics," Schaum Publishing Co., New York, N. Y., p 253.
- Taylor, D. W. (1948), Fundamentals of Soil Mechanics, J. Wiley and Sons, New York, N. Y.



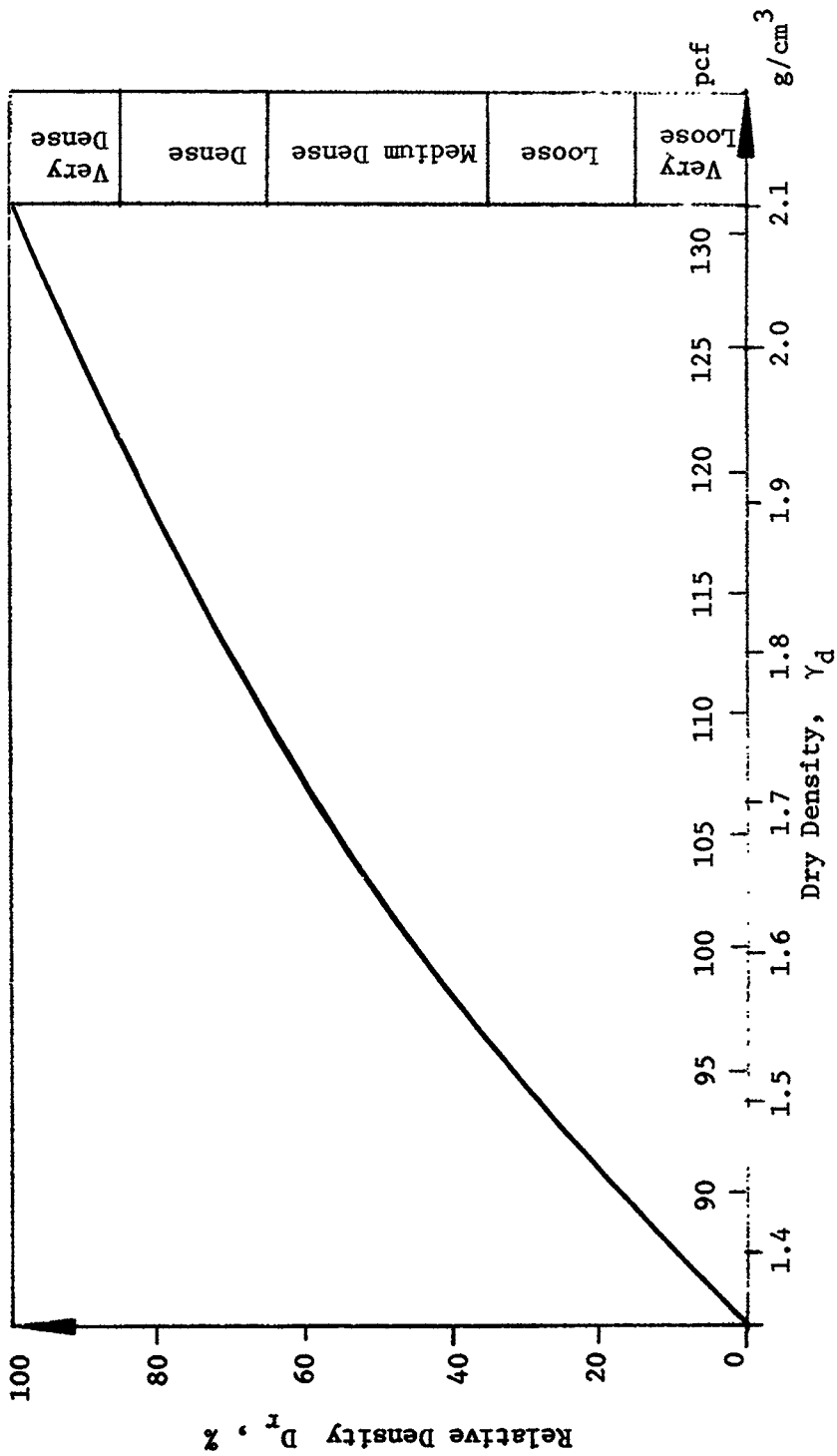


Fig. 2. Relation between dry density and relative density for the lunar soil simulant

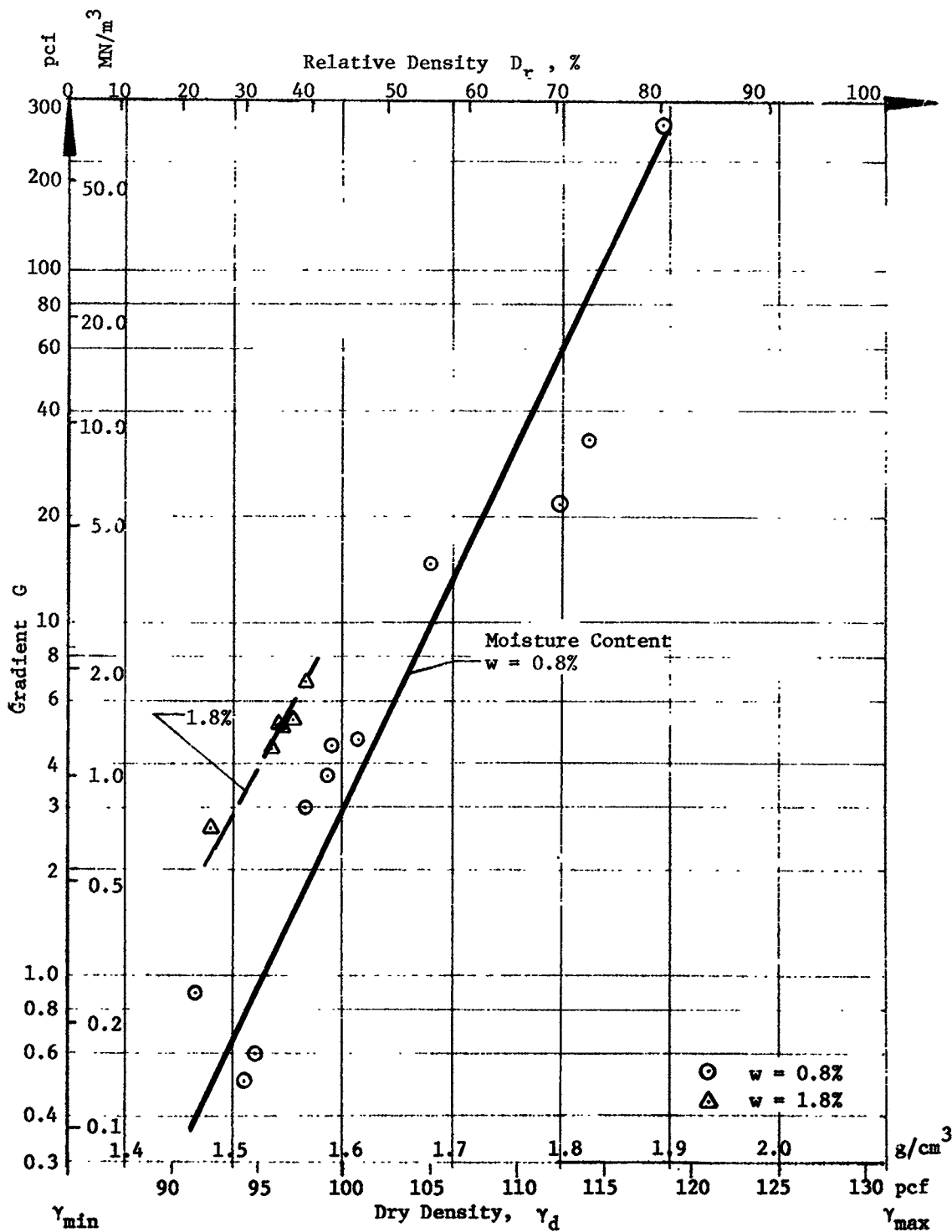


Fig. 3. Relations among cone penetration resistance gradient, dry density, relative density, and moisture content for the lunar soil simulant



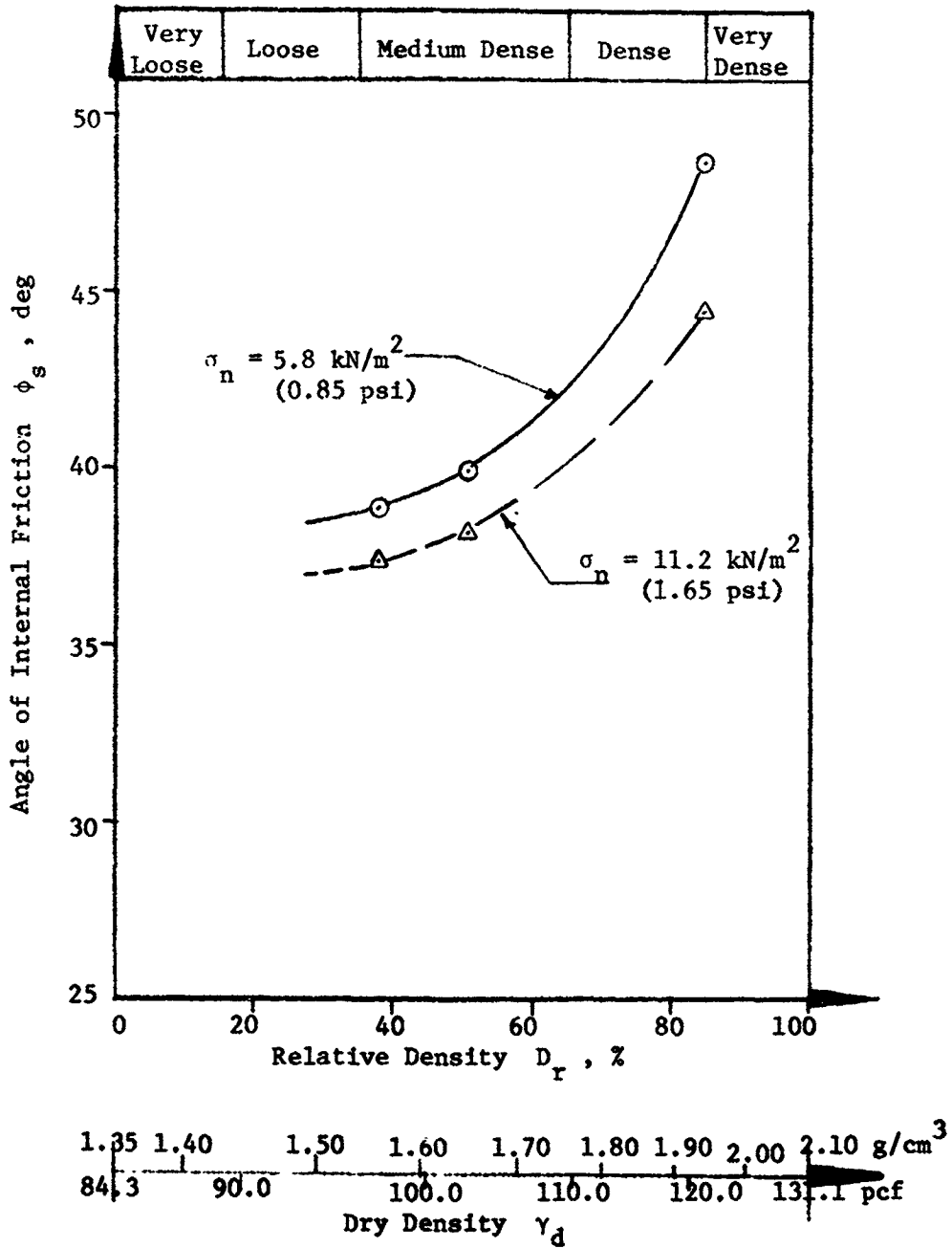


Fig. 5. Relations between angle of internal friction and relative density

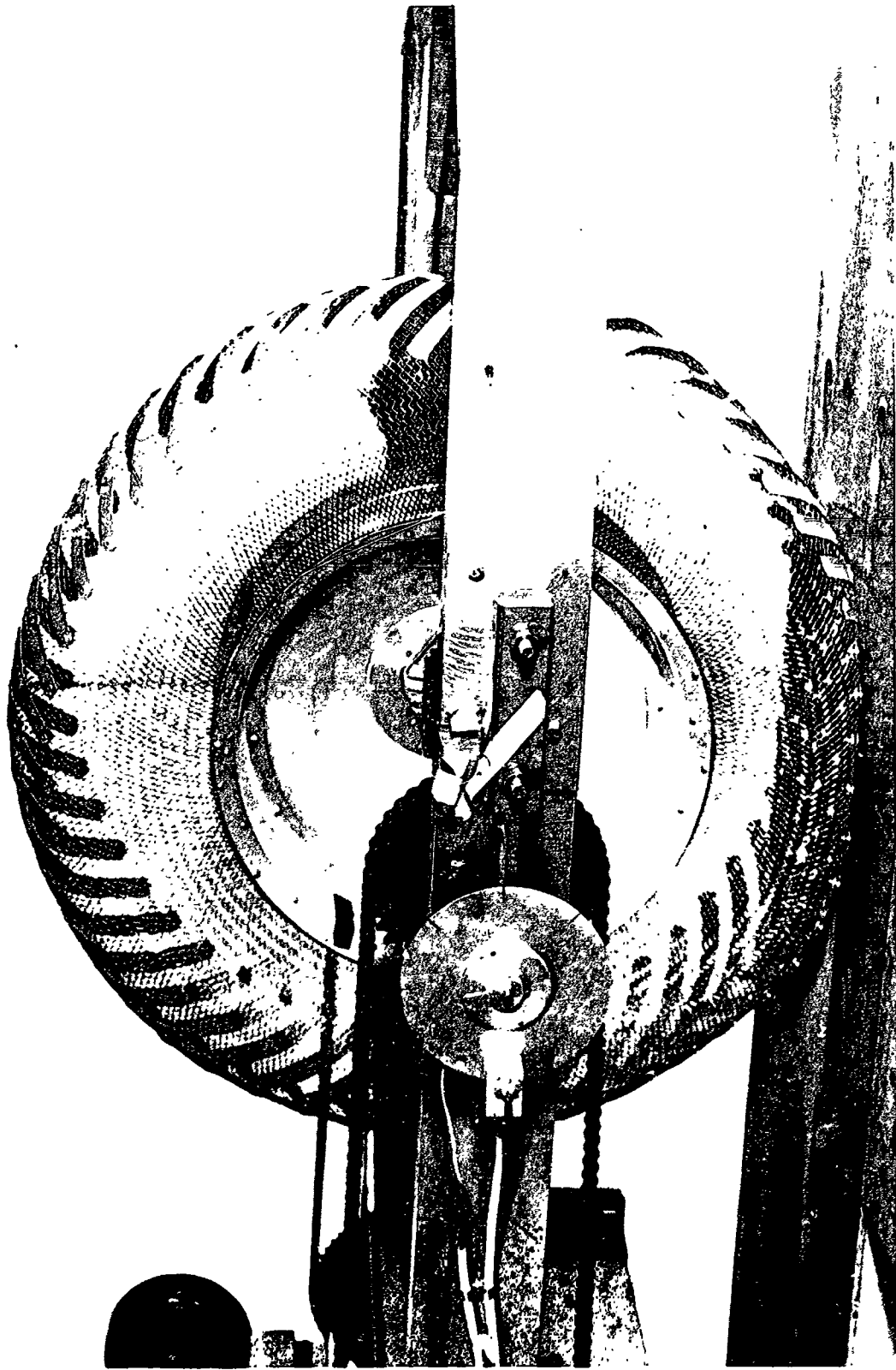
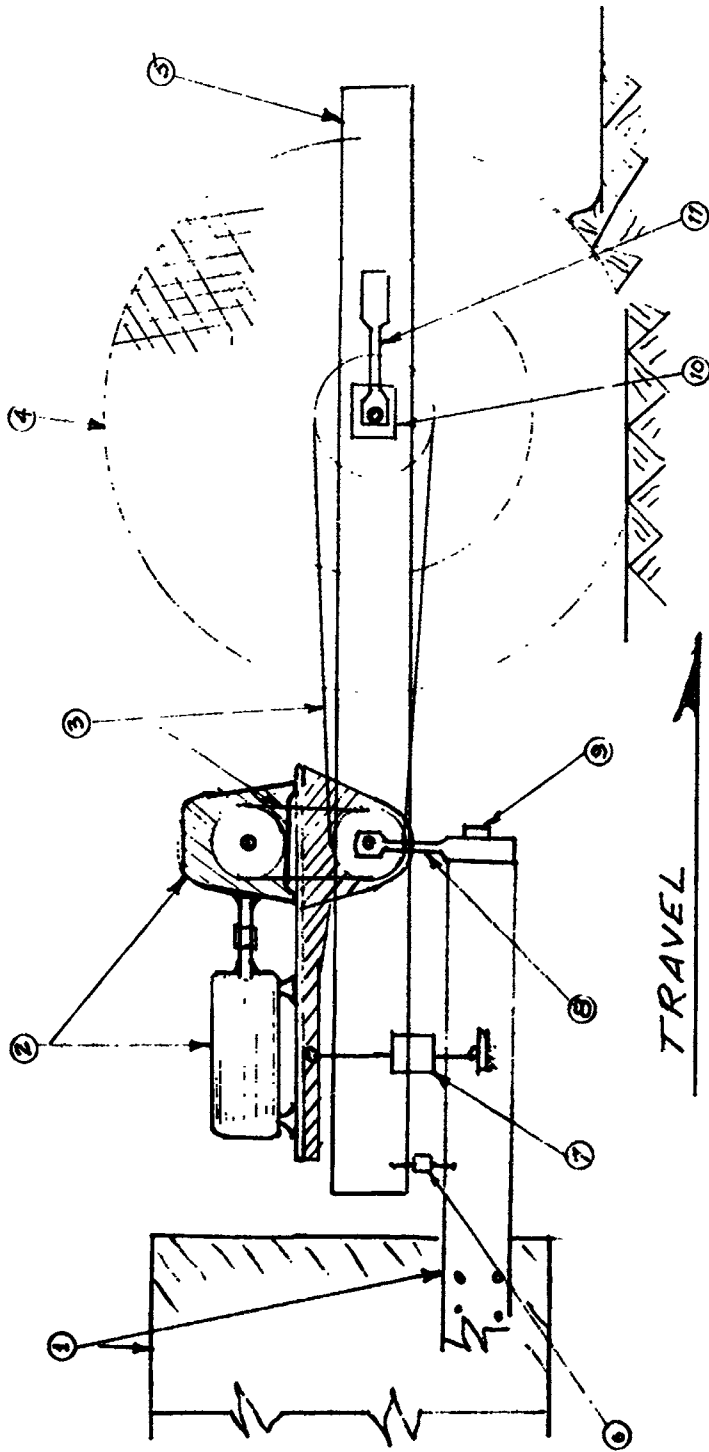
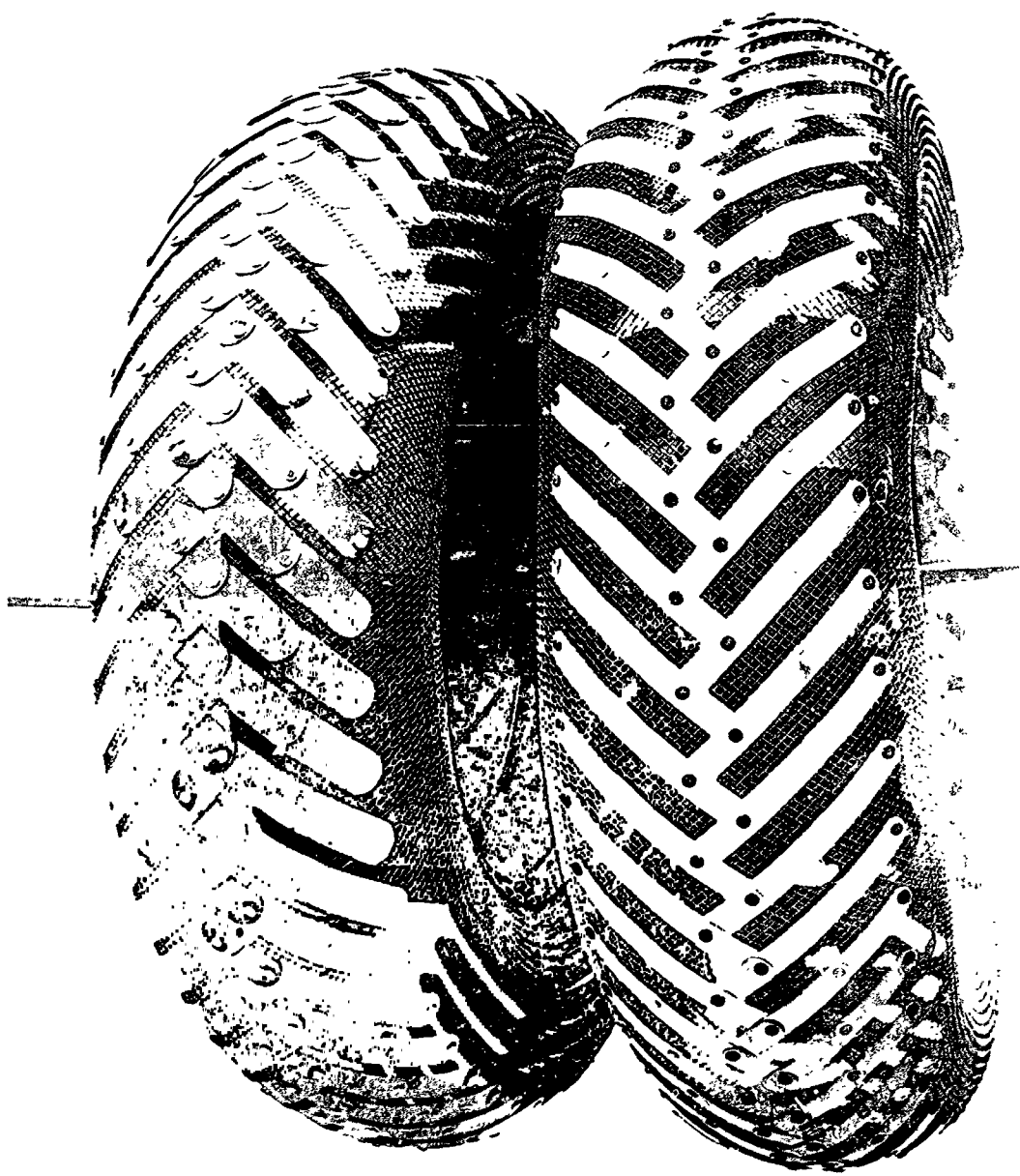


Fig. 6. Test wheel in dynamometer carriage



- |   |   |    |                                |
|---|---|----|--------------------------------|
| 1 | Support frame and carriage drive system | 7  | Torque sensor                  |
| 2 | Wheel drive system                      | 8  | Horizontal force-pull sensor   |
| 3 | Drive chains                            | 9  | Horizontal acceleration sensor |
| 4 | Wheel                                   | 10 | Wheel tachometer               |
| 5 | Wheel support structure                 | 11 | Vertical force (load) sensor   |
| 6 | Sinkage sensor                          |    |                                |

Fig. 7. Wheel dynamometer system



4505-290

Fig. 8. GM IX (left) and GM X (right) wheels



Fig. 9. GM X wheel in soil bin

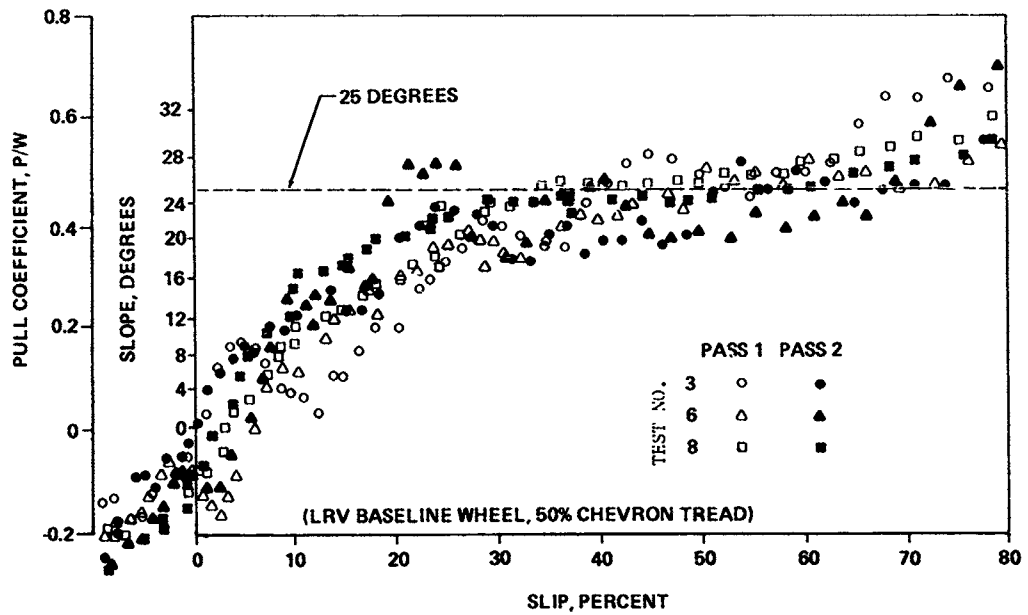
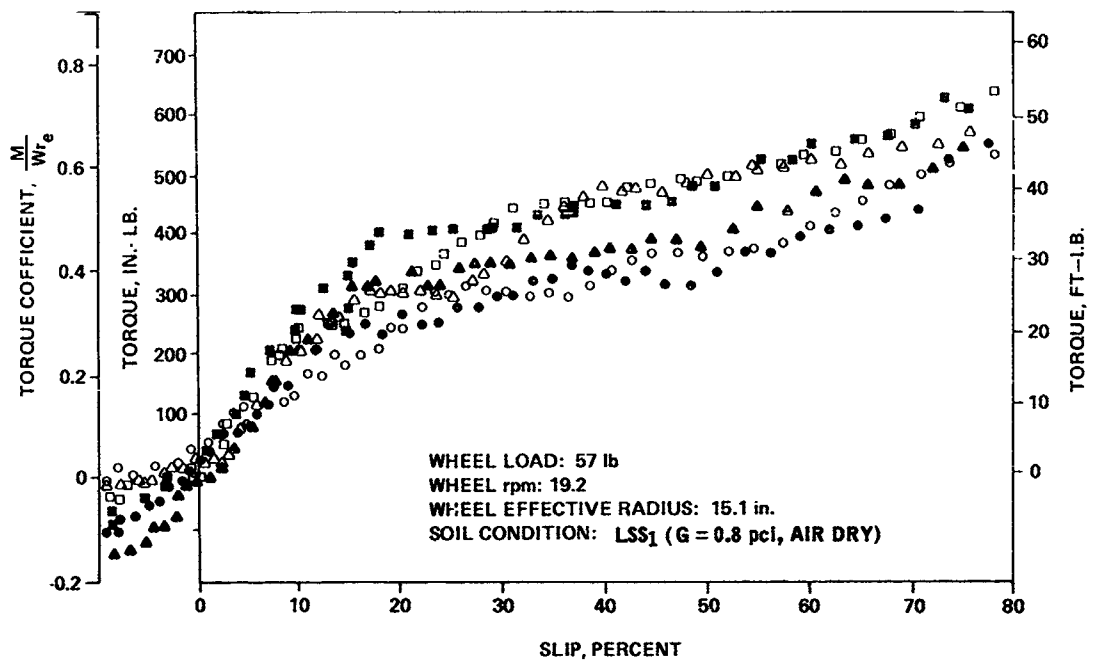


Fig. 10. Data for 50 percent chevron-covered wheel (GM X)

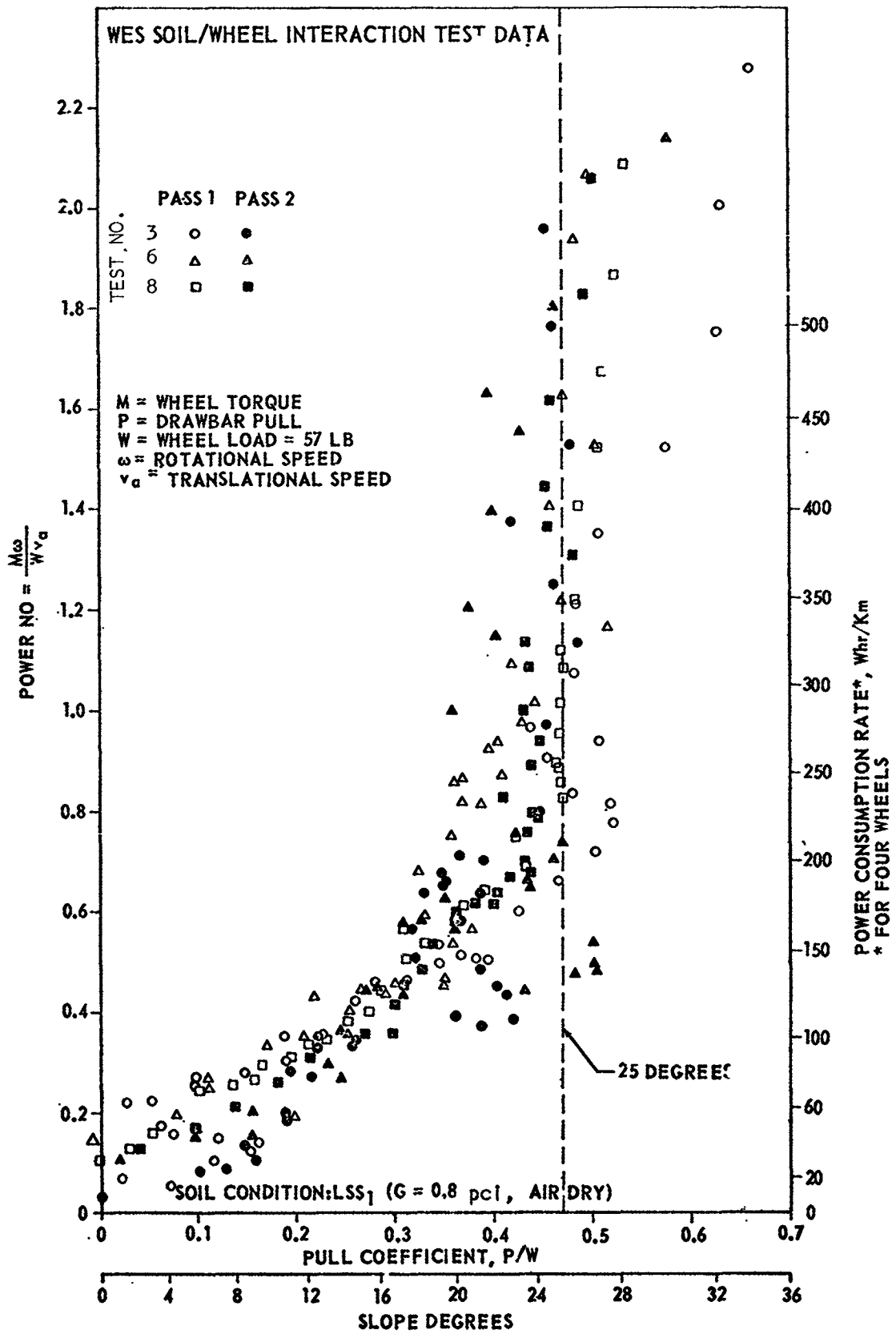


Fig. 11., Data for 50 percent chevron-covered wheel (GM X)

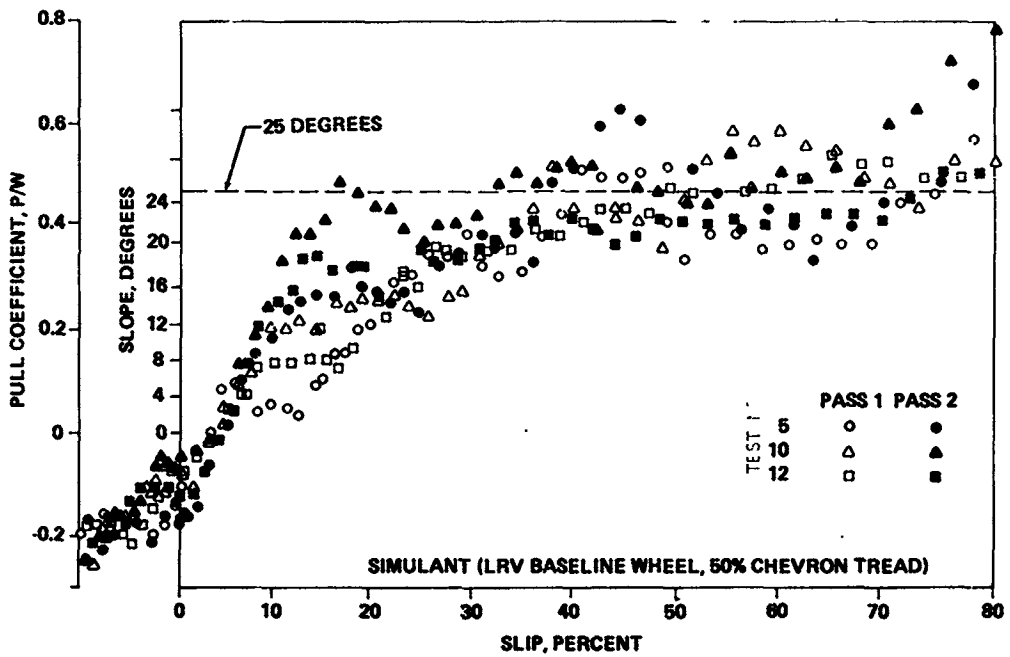
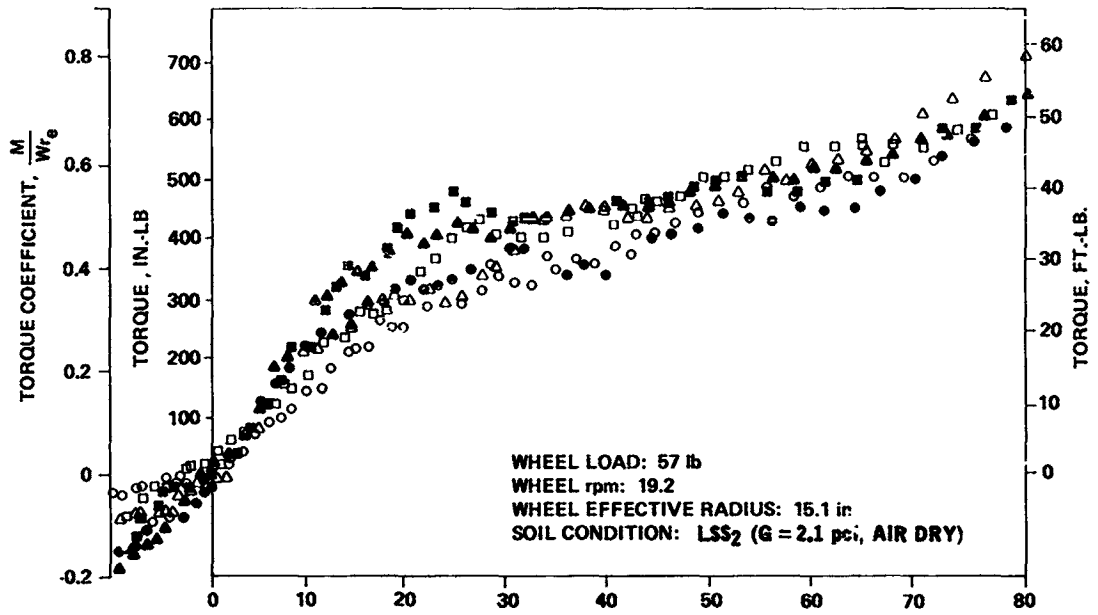


Fig. 12. Data for 50 percent chevron-covered wheel (GM X)

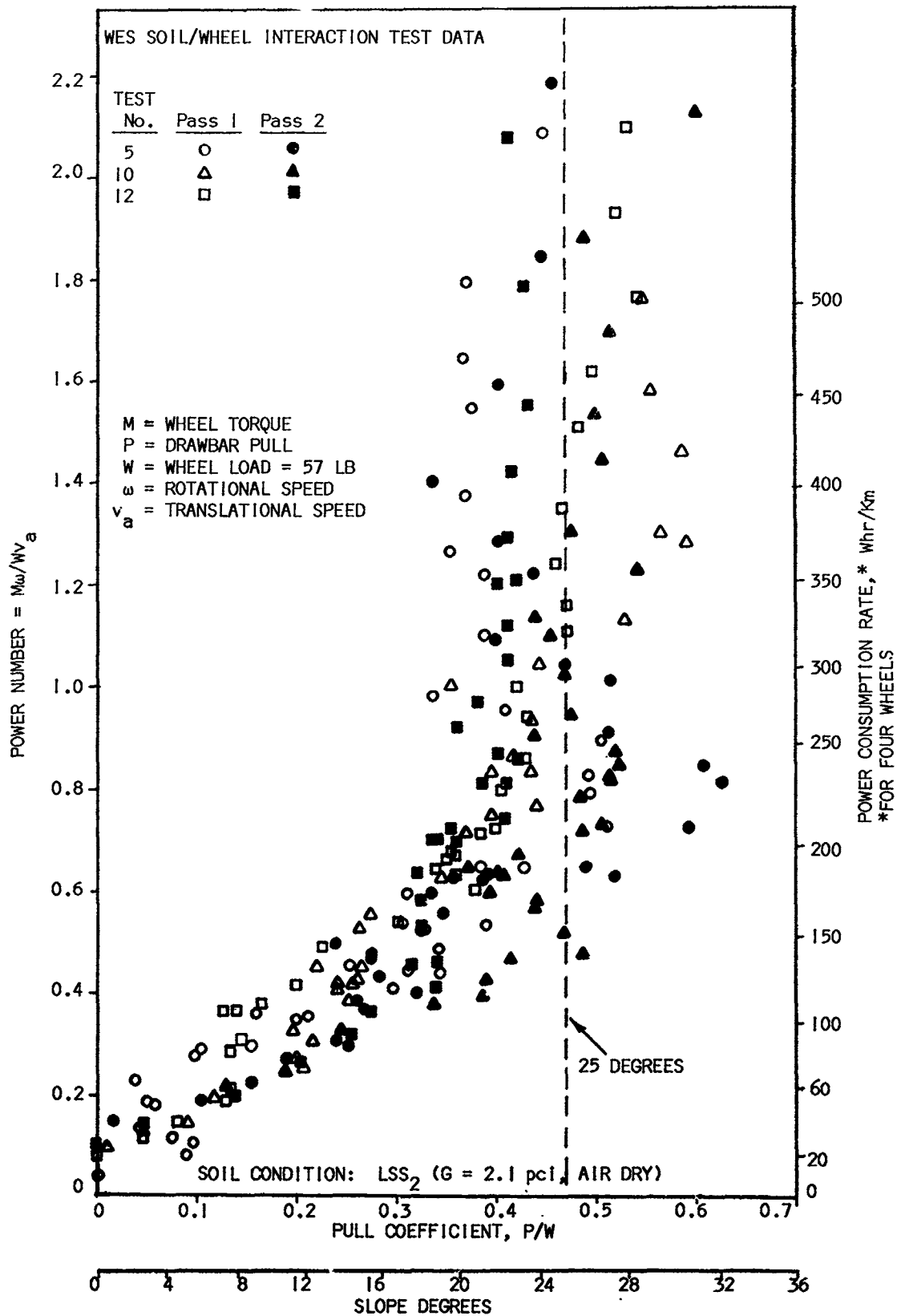


Fig. 13. Data for 50 percent chevron-covered wheel (GM X)

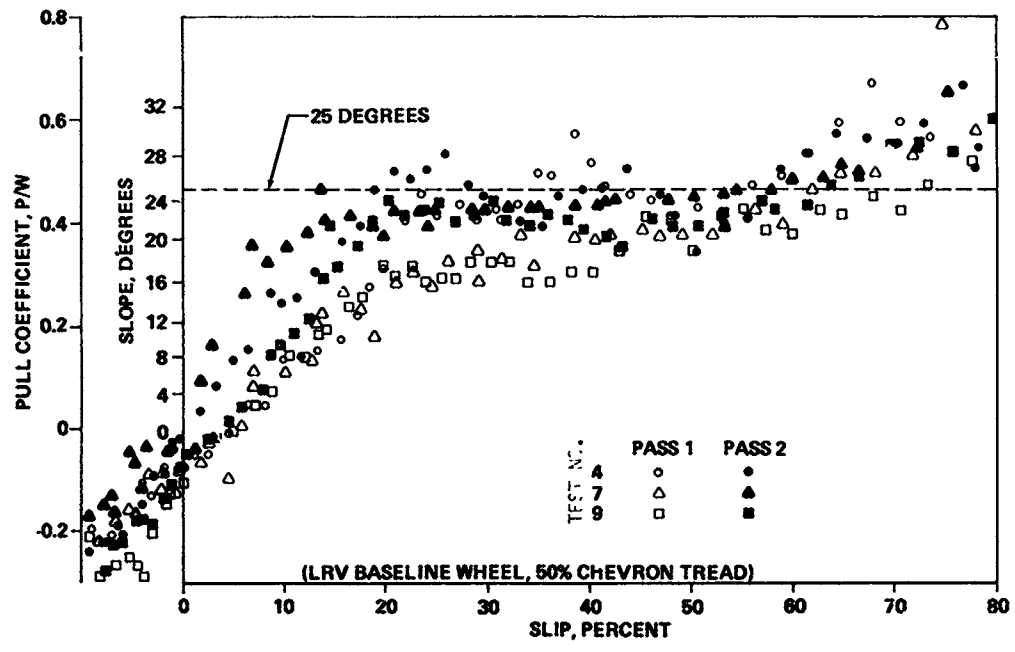
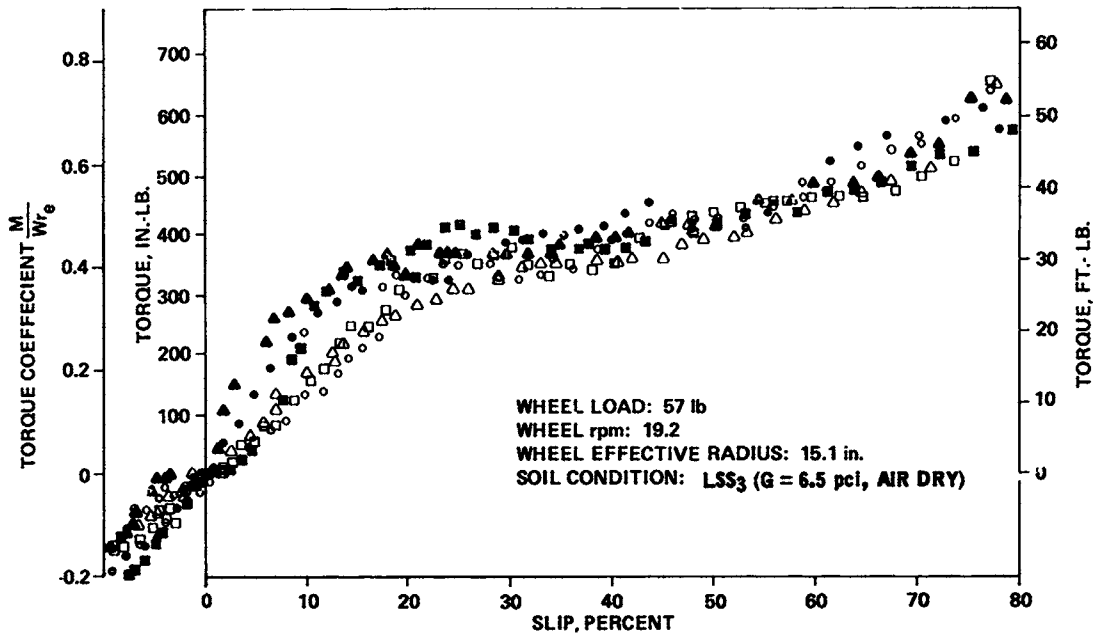


Fig. 14. Data for 50 percent chevron-covered wheel (GM X)

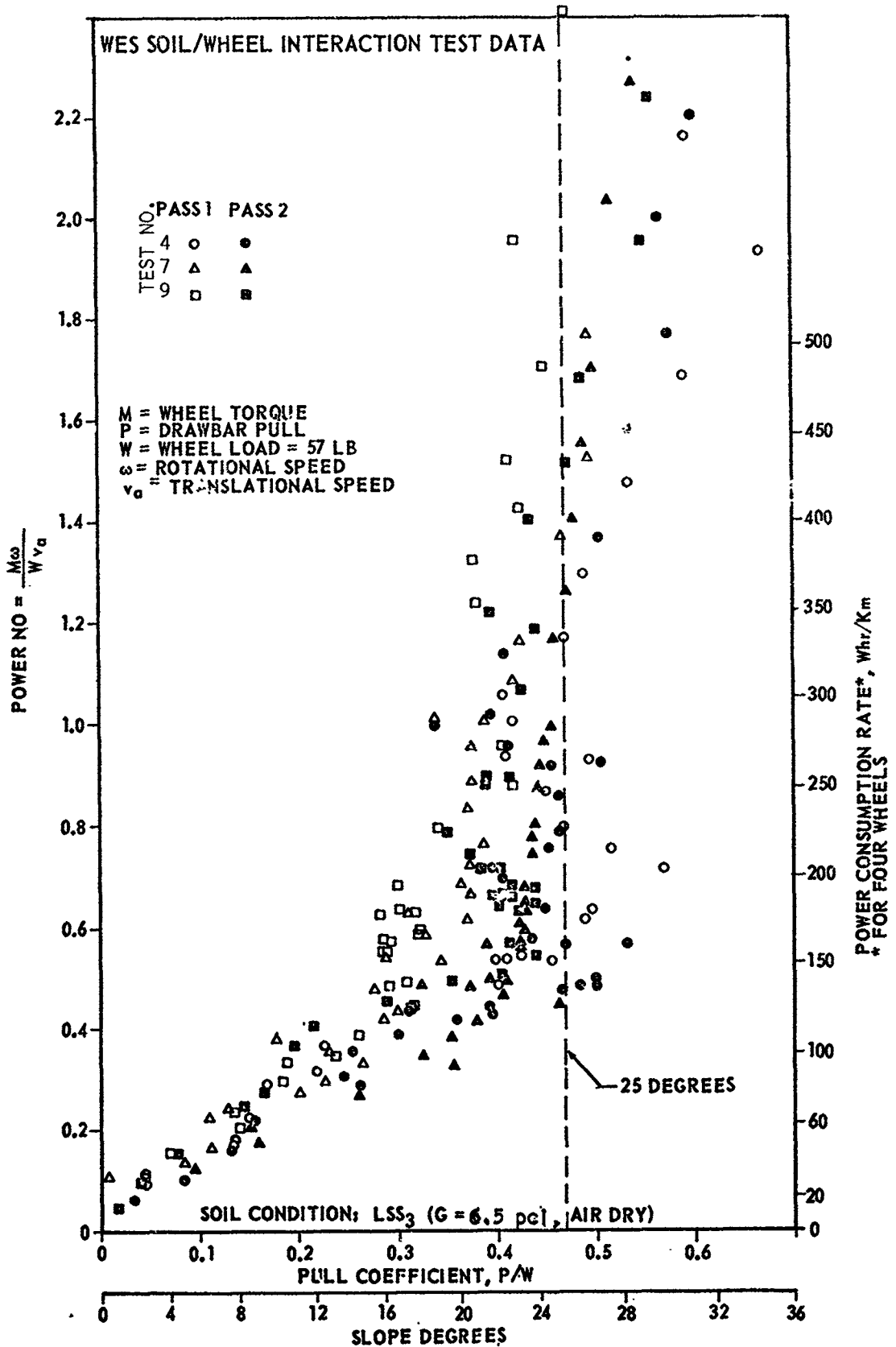


Fig. 15. Data for 50 percent chevron-covered wheel (GM X)

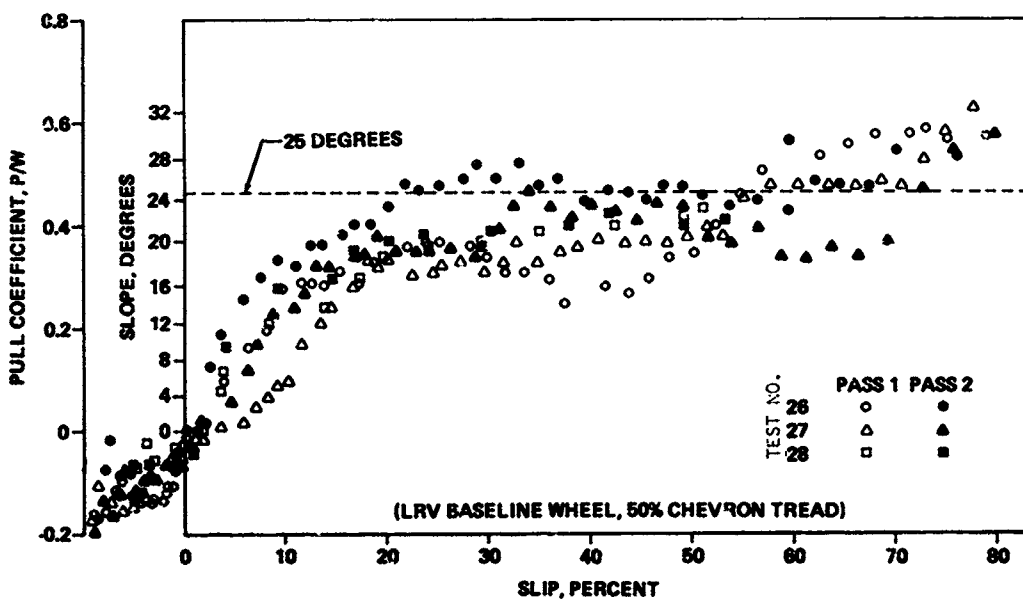
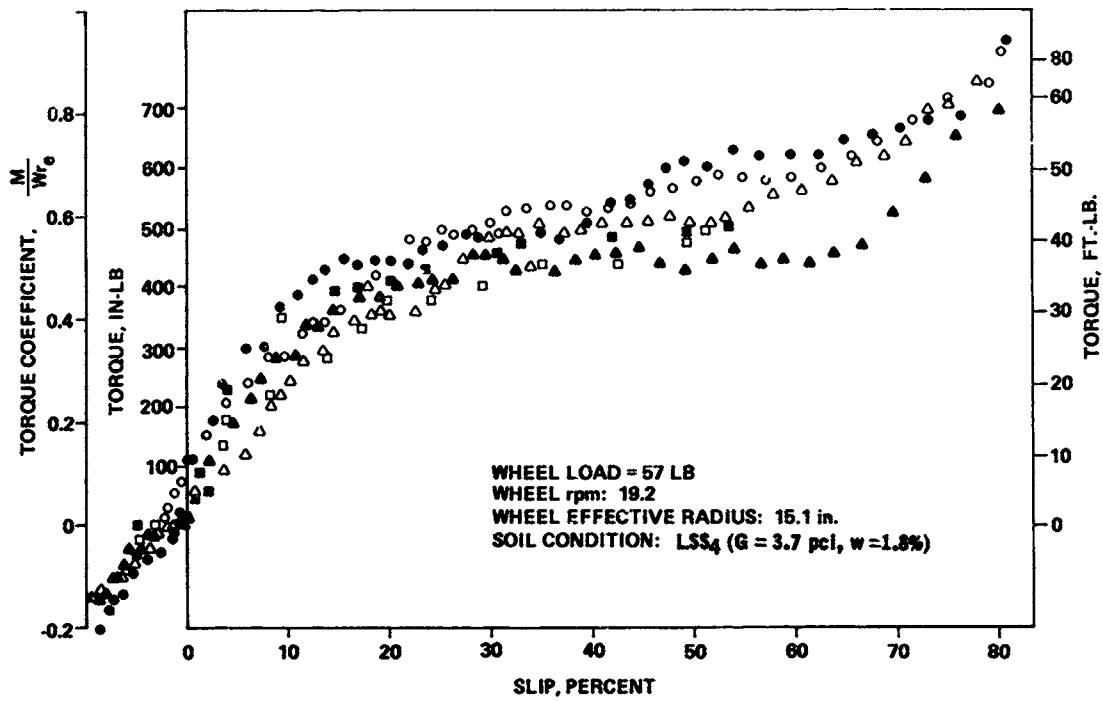


Fig. 16. Data for 50 percent chevron-covered wheel (GM XIII)

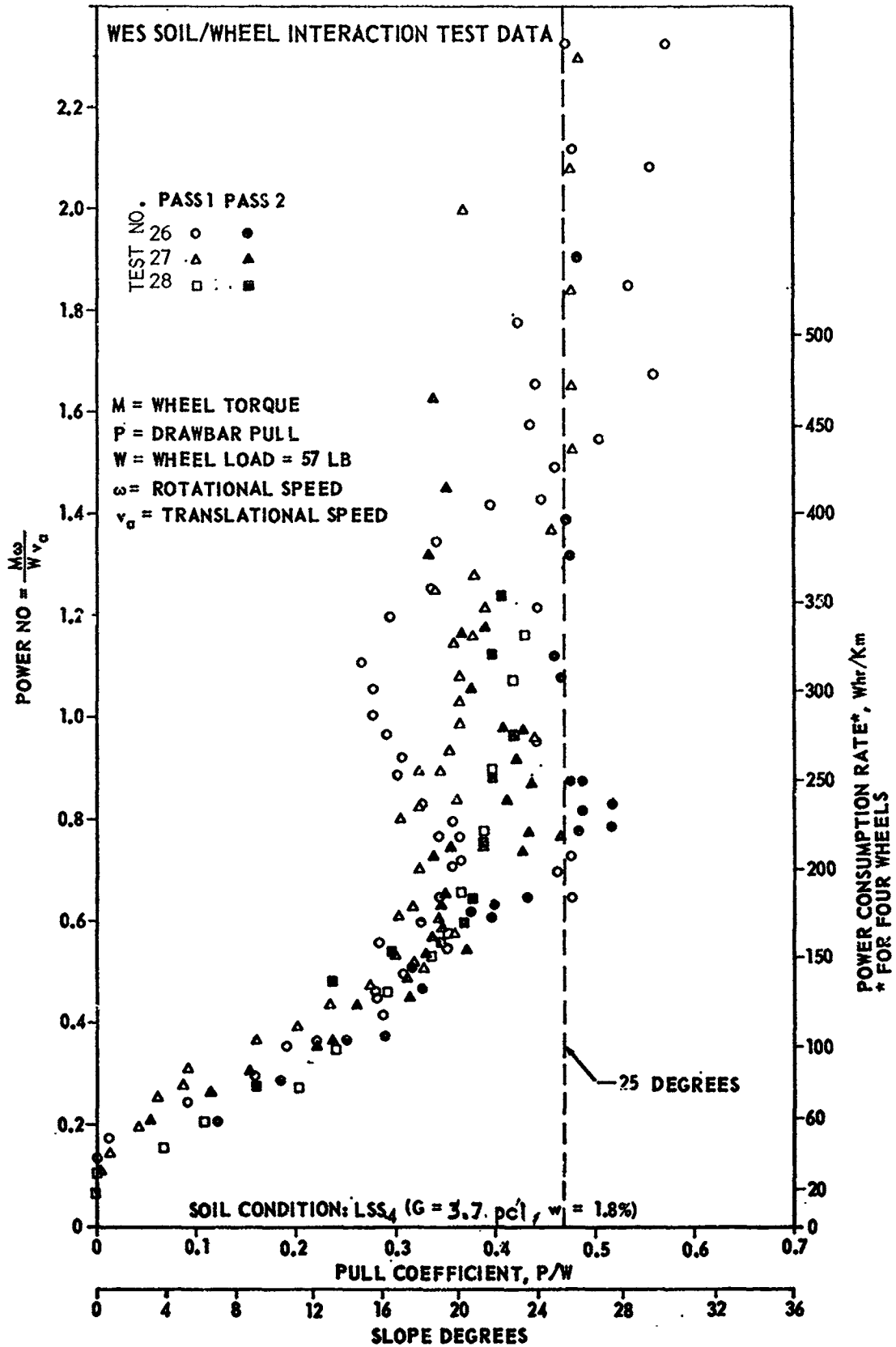


Fig. 17. Data for 50 percent chevron-covered wheel (GM XIII)

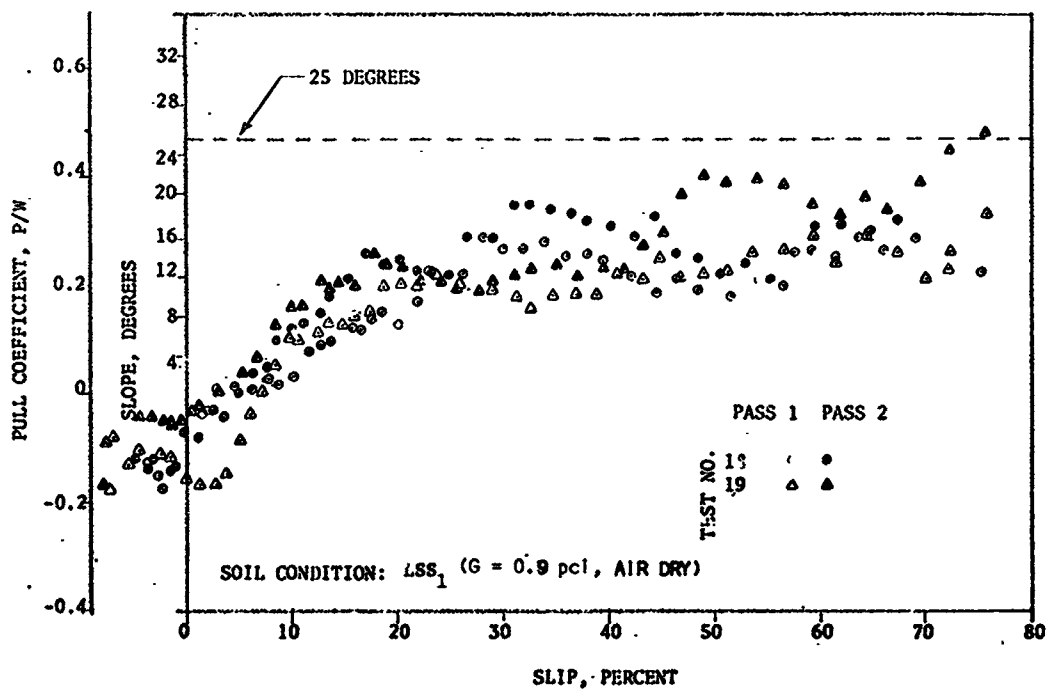
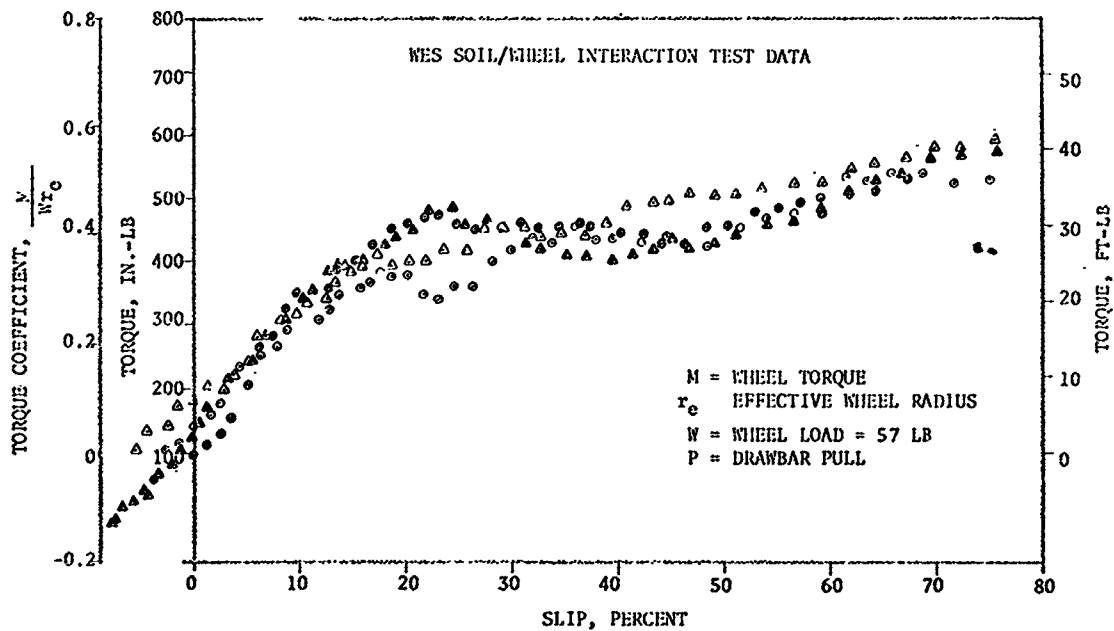


Fig. 18. Data for 75 percent chevron-covered wheel (GM IX)

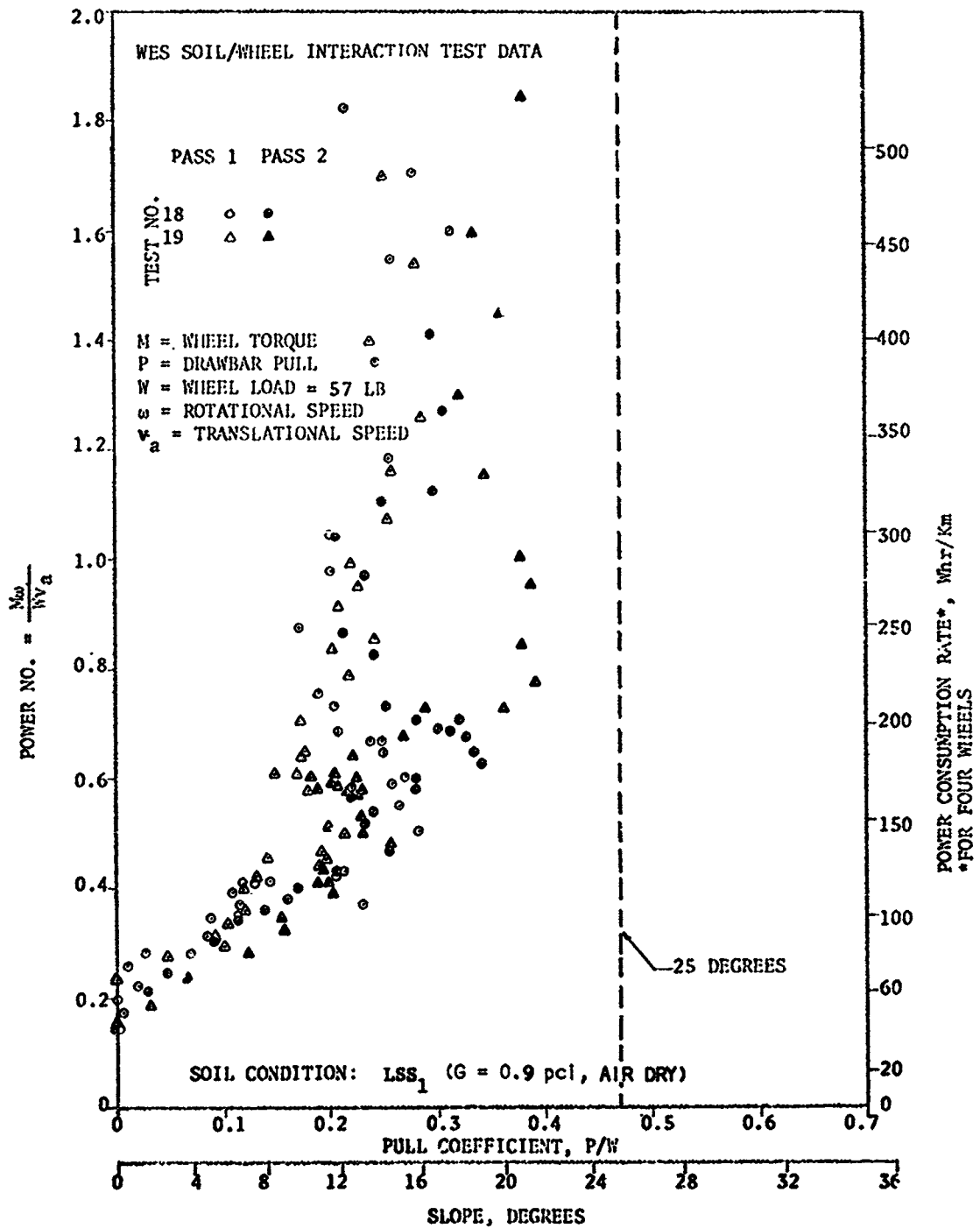


Fig. 19. Data for 75 percent chevron-covered wheel (GM IX)

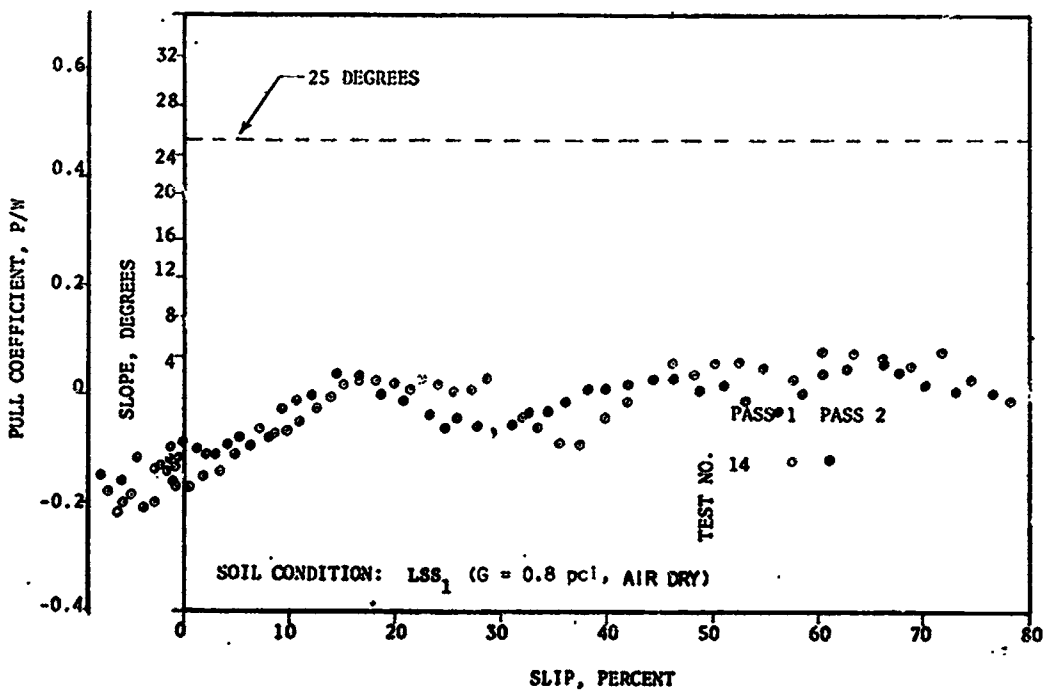
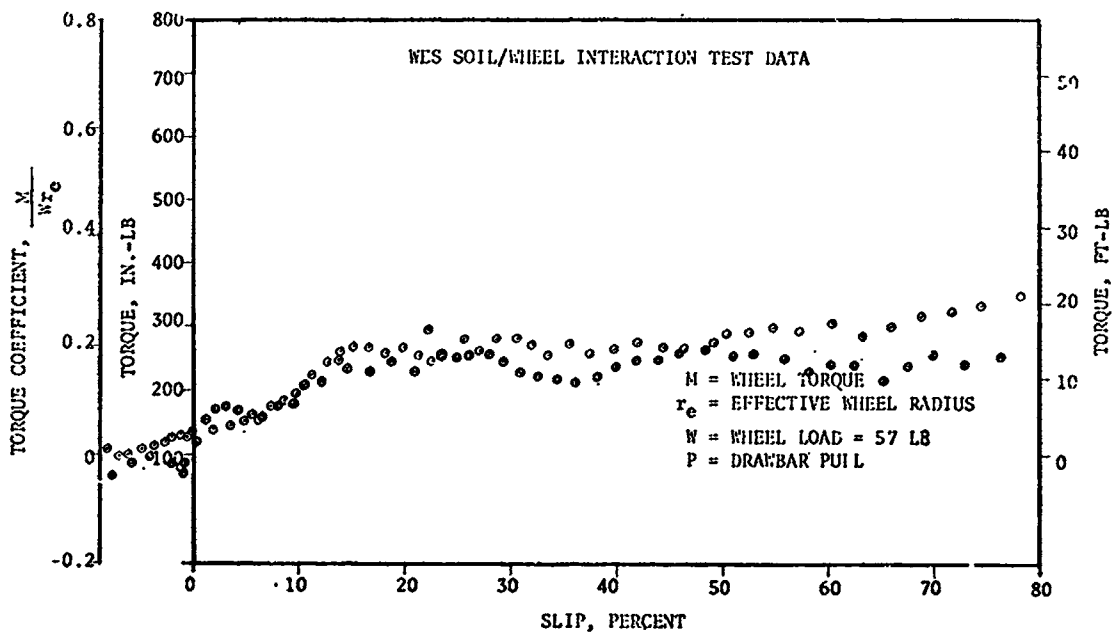


Fig. 20. Data for inner-tube covered wheel (GM XI)

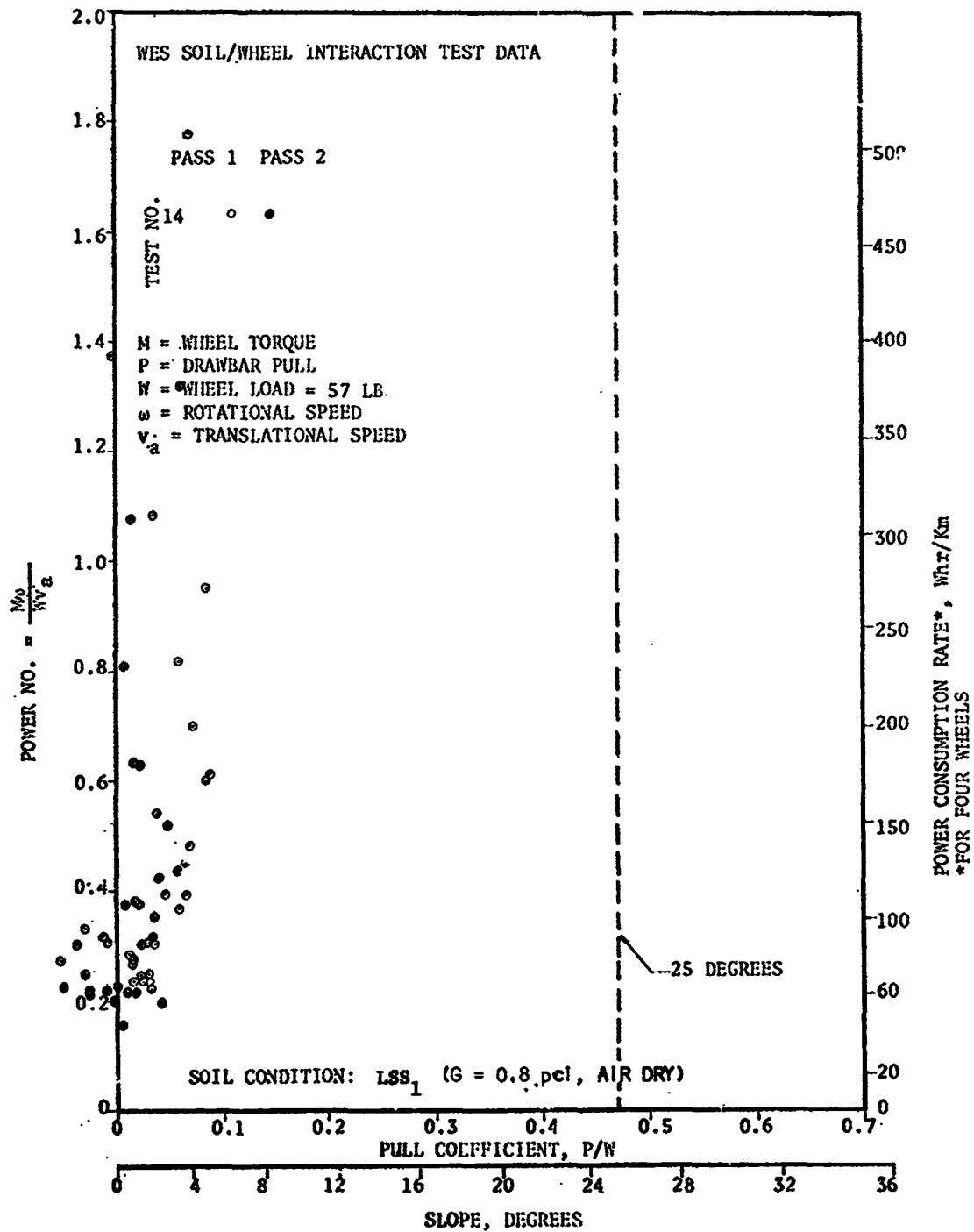


Fig. 21. Data for inner-tube-covered wheel (GM X1)

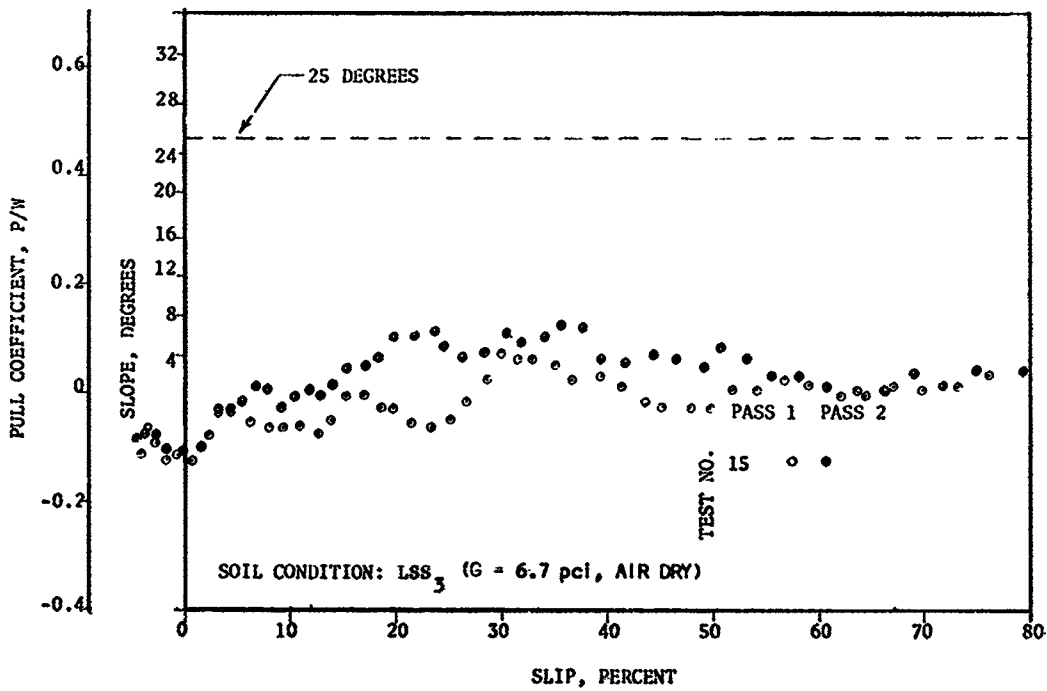
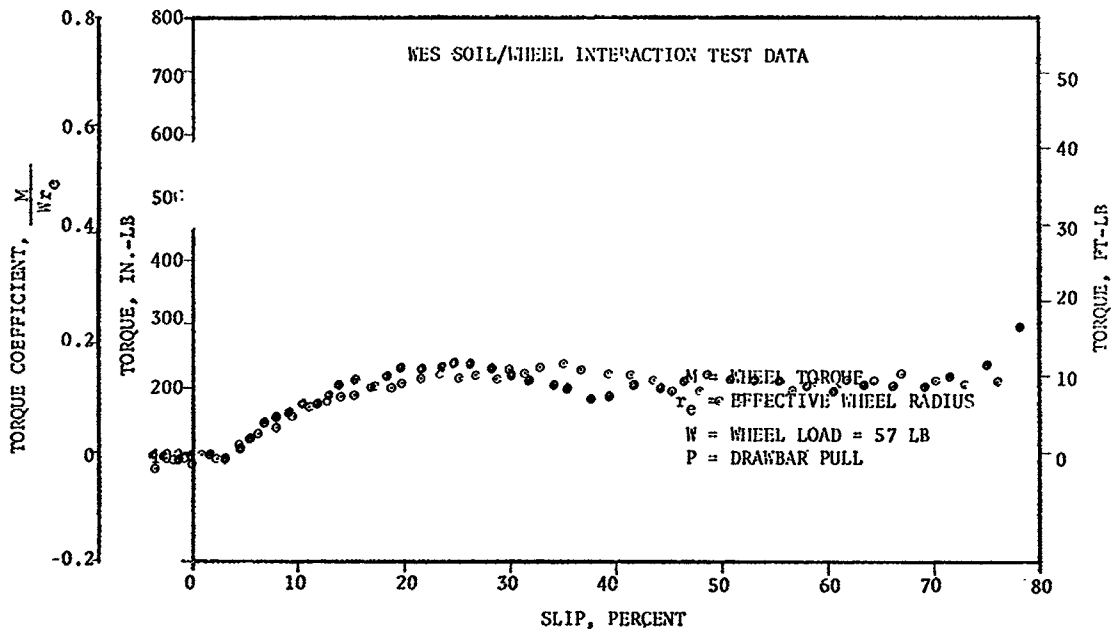


Fig. 22. Data for inner-tube-covered wheel (GM XI)

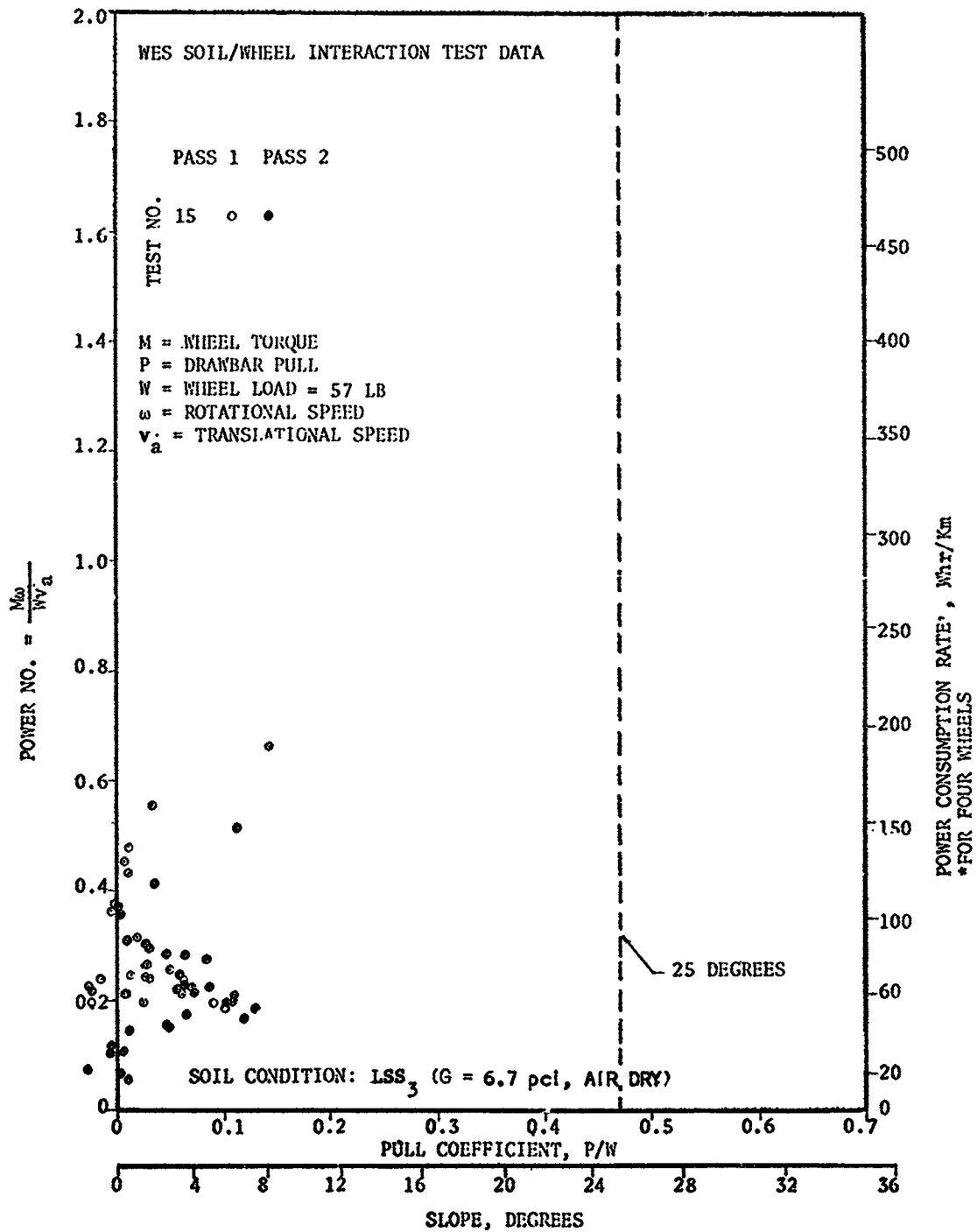


Fig. 23. Data for Inner-tube-covered wheel (GM XI)

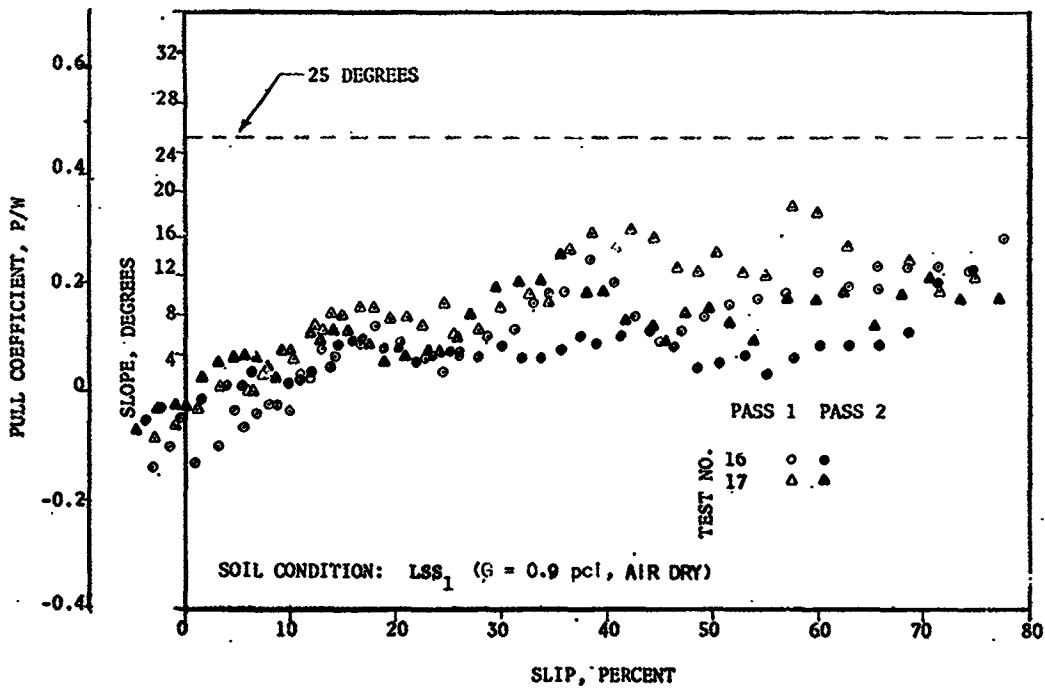
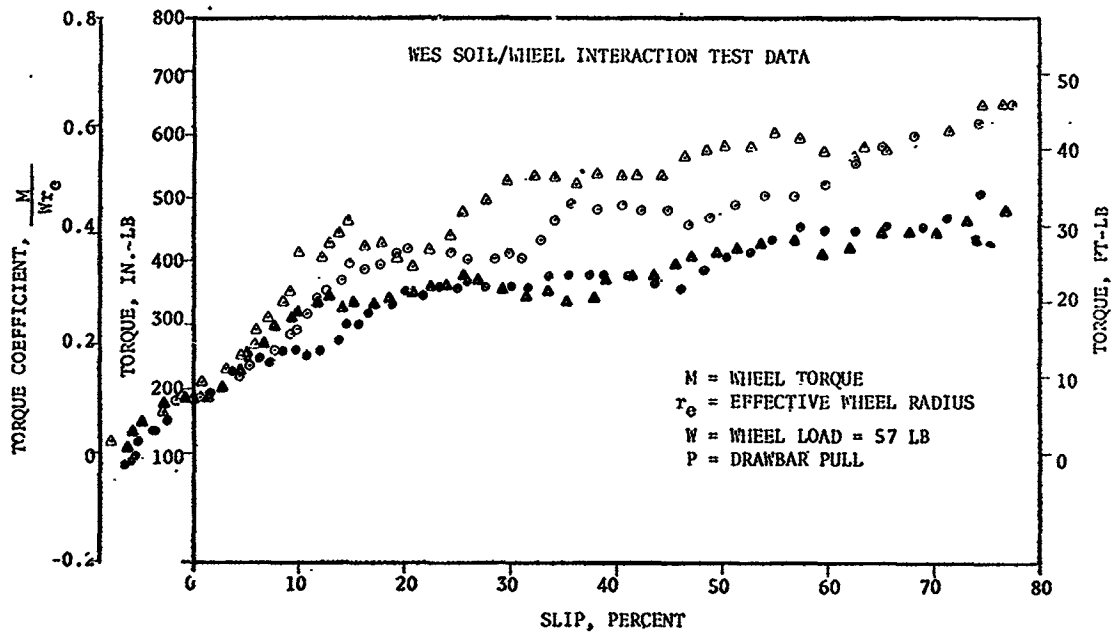


Fig. 24. Data for inner-tube-covered wheel with grousers (GM XII)

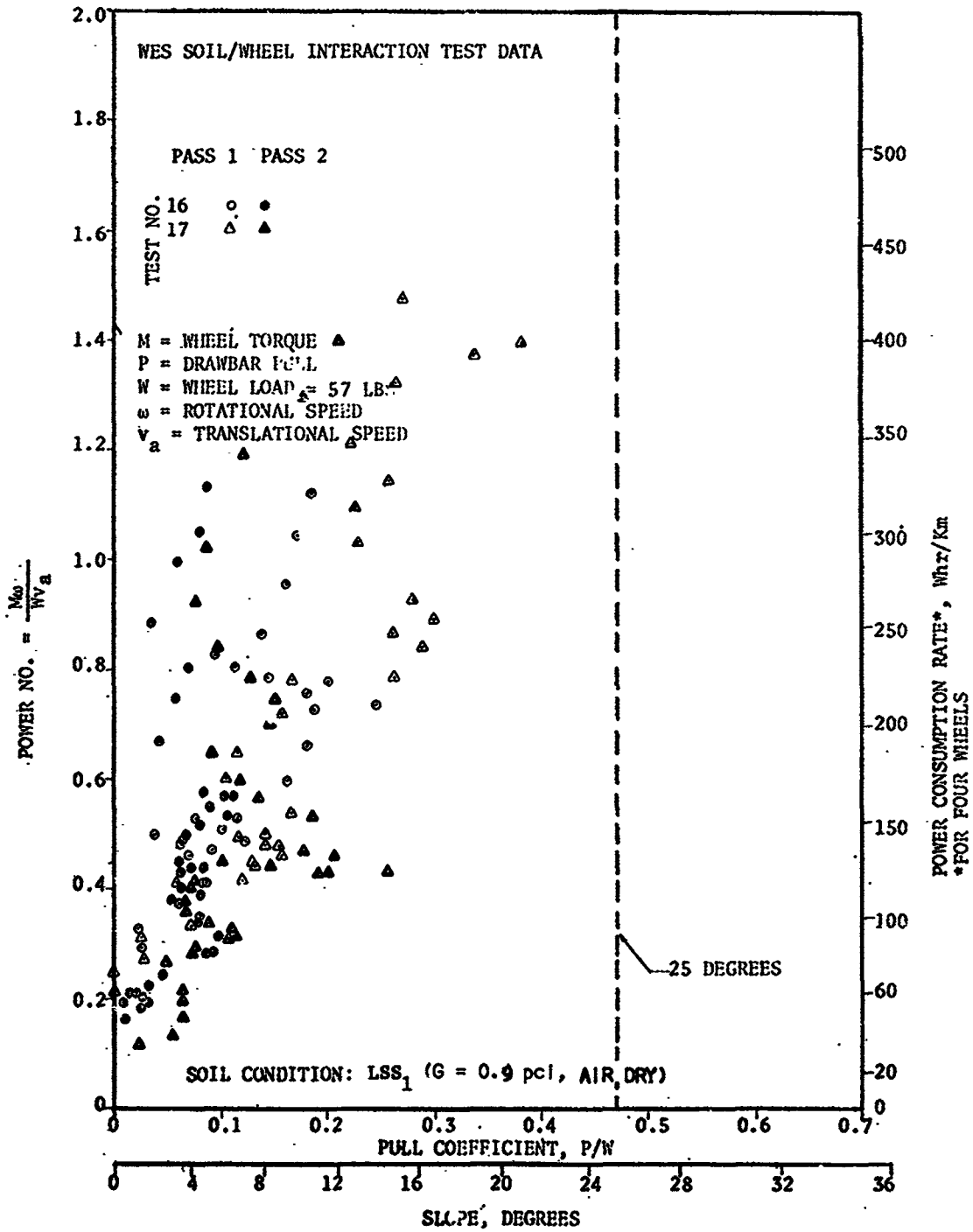


Fig. 25. Data for inner-tube-covered wheel with grousers (GM XII)

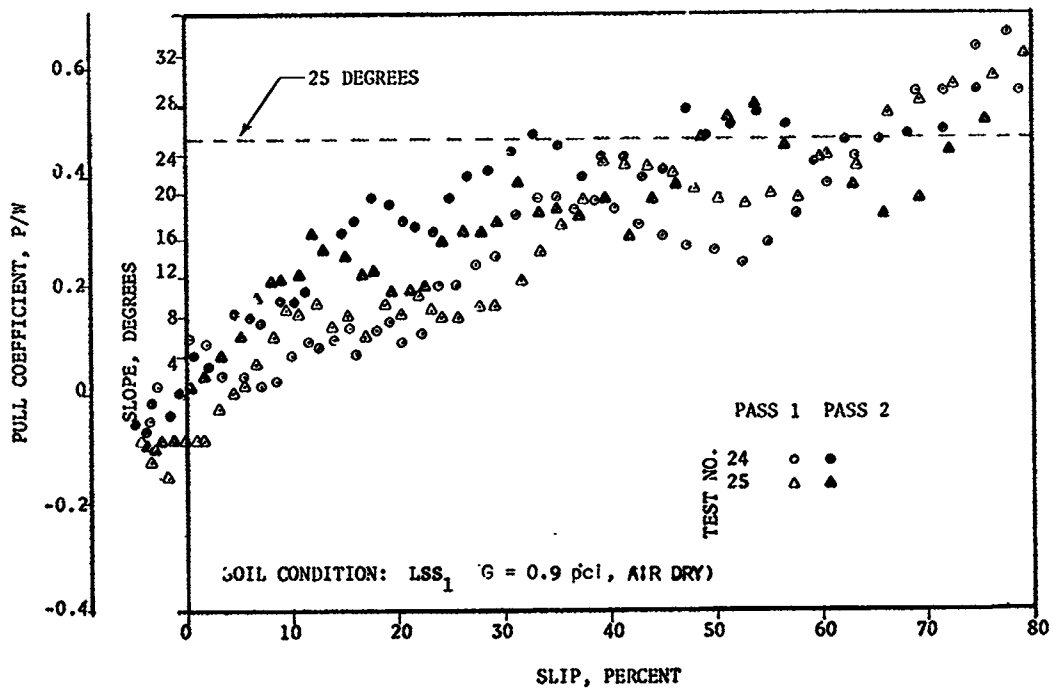
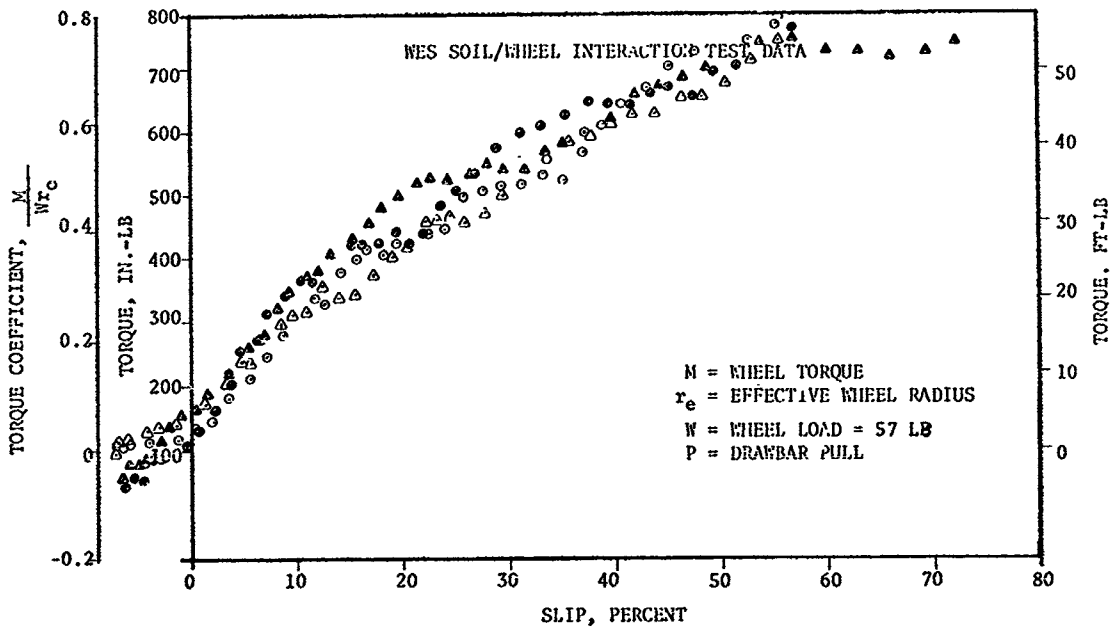


Fig. 26. Data for open-mesh wheel (GM XIV)

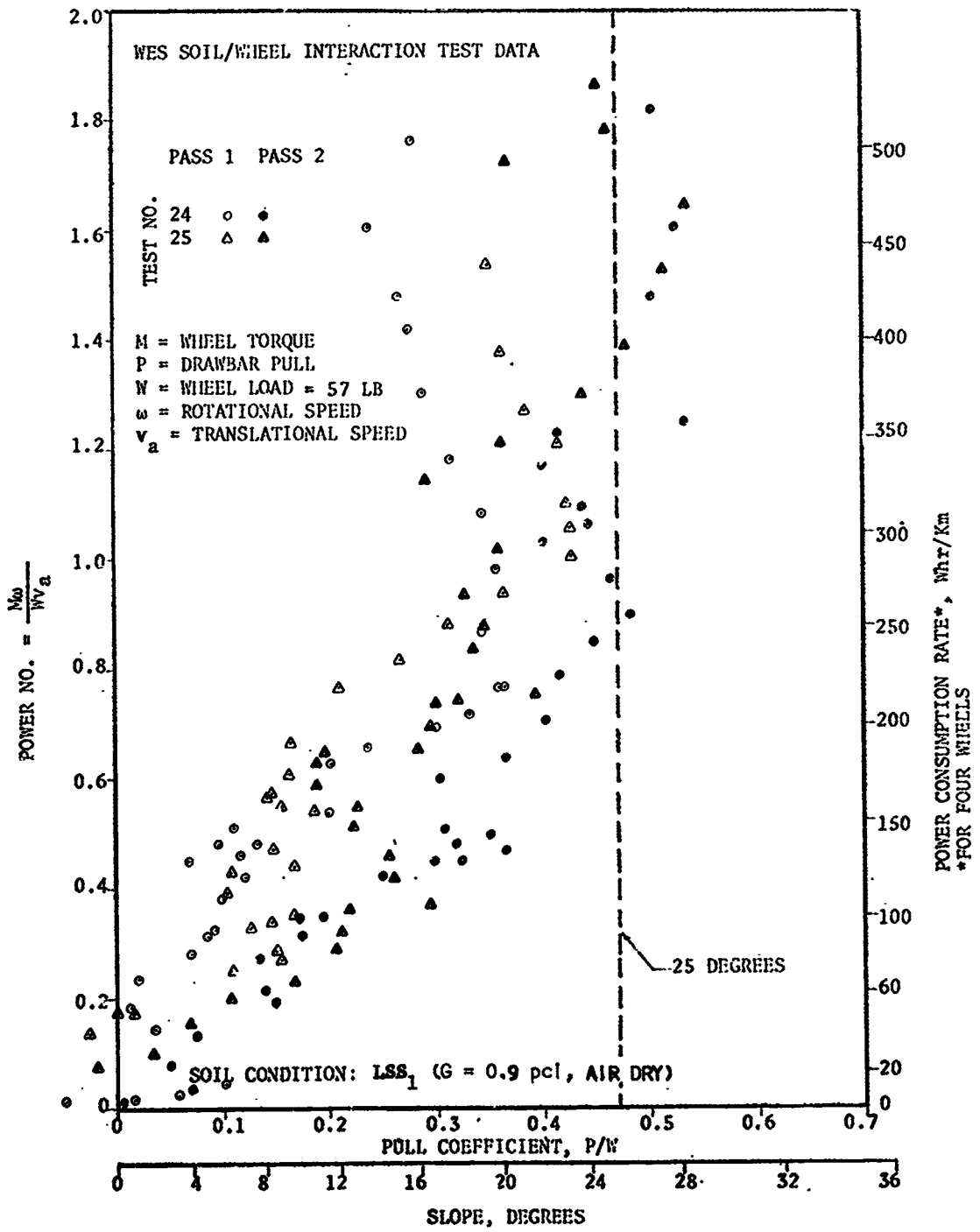


Fig. 27. Data for open-mesh wheel (GM XIV)

Table 1

Soil Properties and Parameters for Single-Wheel Tests; Before-Traffic Data

Soil Condition ISS <sub>1</sub>				
	No. of Tests	Maximum	Minimum	Average
Penetration Resistance Gradient, pci	75	1.2	0.6	0.8
Dry Density, pcf(g/cm <sup>3</sup> )				
Gradient G	15	95.95(1.537)	94.08(1.507)	94.77(1.518)
Gravimetric	6	107.25(1.718)	101.14(1.620)	104.45(1.673)
Moisture Content, %	6	1.0	0.9	0.9
Relative Density, %				
Gradient G	15	34	29	31
Gravimetric	3	60	47	54
Average Friction Angle, deg				
$\phi_g^*$	-	-	-	38.5
$\phi_{pl}^{**}$	-	-	-	34.0
$\phi_b$	4	33.5	25.5	29.0
$\phi_c$	4	23.0	13.5	19.8
Average Cohesion, psi				
$c_{tr}$	-	-	-	-
$c_b$	4	0.26	0.0	0.14
$c_c$	4	0.58	0.17	0.32
Bekker Soil Values				
$k_c$ (lb/in. <sup>1+n</sup> )	4	1.28	-0.76	0.42
$k_\phi$ (lb/in. <sup>2+n</sup> )	4	5.25	3.50	4.32
n	4	1.13	0.70	0.90

\* $\sigma_n = 0.85$  psi.      \*\* $\sigma_n = 1.06$  psi.

Table 1 (Continued)

		Soil Condition ISS <sub>2</sub>		
	No. of Tests	Maximum	Minimum	Average
Penetration Resistance Gradient, pci	20	2.6	1.7	2.2
Dry Density, pcf (g/cm <sup>3</sup> )				
Gradient G	4	99.01(1.586)	98.20(1.573)	98.76(1.582)
Gravimetric	4	105.07(1.683)	103.01(1.650)	104.13(1.668)
Moisture Content, %	4	1.0	0.9	0.9
Relative Density, %				
Gradient G	4	42	40	42
Gravimetric	2	55	52	54
Average Friction Angle, deg				
$\phi_s^*$	-	-	-	39
$\phi_{ps}^{**}$	-	-	-	35.0
$\phi_b$	1	-	-	29.0
$\phi_c$	1	-	-	23.0
Average Cohesion, psi				
$c_{tr}$	-	-	-	0.05
$c_b$	1	-	-	0.15
$c_c$	1	-	-	0.36
Bekker Soil Values				
$k_c$ (lb/in. 1+ $n$ )	1	-	-	0.13
$k_\phi$ (lb/in. 2+ $n$ )	1	-	-	5.34
$n$	1	-	-	1.15

\* $\sigma_n = 0.85$  psi.   \*\* $\sigma_n = 1.06$  psi.   (2 of 4 Sheets)

Table 1 (Continued)

Soil Condition LSS <sub>3</sub>					
	No. of Tests	Maximum	Minimum	Average	
Penetration Resistance Gradient, pci	20	7.0	5.7	6.5	
Dry Density, pcf (g/cm <sup>3</sup> )					
Gradient G	4	103.45(1.657)	103.07(1.651)	103.32(1.655)	
Gravimetric	6	106.13(1.700)	103.70(1.661)	104.82(1.679)	
Moisture Content, %	6	1.0	0.9	0.9	
Relative Density, %					
Gradient G	4	52	52	52	
Gravimetric	3	57	54	55	
Average Friction Angle, deg					
$\phi_{s^*}$	-	-	-	40	
$\phi_{pl}$	-	-	-	35.5	
$\phi_b$	3	30.0	26.5	28.8	
$\phi_c$	3	23.5	20.0	21.8	
Average Cohesion, psi					
$c_{tr}$	-	-	-	0.08	
$c_b$	3	0.20	0.10	0.15	
$c_c$	3	0.41	0.04	0.22	
Bekker Soil Values					
$k_c$ (lb/in. <sup>1+n</sup> )	3	-0.94	-2.44	-1.58	
$k_\phi$ (lb/in. <sup>2+n</sup> )	3	9.46	7.10	8.83	
n	3	1.65	1.38	1.48	

(3 of 4 Sheets)

\* $\phi_n = 0.85$  psi. \*\* $\phi_n = 1.06$  psi.

Table 1 (Continued)

	No. of Tests	Soil Condition LSS <sub>4</sub>		
		Maximum	Minimum	Average
Penetration Resistance Gradient, pci	15	4.5	3.2	3.7
Dry Density, pcf(g/cm <sup>3</sup> )	Gradient G	95.52(1.532)	94.46(1.516)	95.14(1.524)
	Gravimetric	95.71(1.533)	81.16(1.300)	89.77(1.438)
Moisture Content, %	4	1.9	1.7	1.8
Relative Density, %	Gradient G	33	31	32
	Gravimetric	34	0	17
Average Friction Angle, deg	$\phi_{s^*}$	-	-	38.5
	$\phi_p^{**}$	-	-	34.0
	$\phi_b$	1	-	29.0
	$\phi_c$	1	-	19.5
Average Cohesion, psi	$c_{tr}$	-	-	0.11
	$c_b$	1	-	0.12
	$c_c$	1	-	0.36
Bekker Soil Values	$k_c$ (lb/in. <sup>1+n</sup> )	1	-	1.76
	$k_\phi$ (lb/in. <sup>2+n</sup> )	1	-	5.04
	$n$	1	-	1.18

\* $\sigma_n = 1.85$  psi. \*\* $\sigma_n = 1.06$  psi.

(4 of 4 Sheets)

Table 2  
Soil Properties and Parameters for Single-Wheel Tests  
During-Traffic Data

Test No.	Soil Condition	Pass No.	Penetration Resistance Gradient G, pci			$\gamma_d$ based on G pcf(g/cm <sup>3</sup> )	D <sub>r</sub> , % based on G
			Max	Min	Avg		
003-6	LSS <sub>1</sub>	0	0.9	0.7	0.8	94.54(1.516)	30
		0*	-	-	-	-	-
		1	2.4	2.2	2.3	99.14(1.586)	42
		3	3.7	3.5	3.6	100.87(1.616)	47
004-6	LSS <sub>3</sub>	0	6.7	5.7	6.3	103.07(1.651)	52
		0*	-	-	-	-	-
		1	7.6	6.7	7.2	103.70(1.661)	53
		3	9.5	6.3	8.5	104.38(1.672)	54
005-6	LSS <sub>2</sub>	0	2.0	1.7	1.9	97.20(1.573)	40
		0*	-	-	-	-	-
		1	3.0	2.8	3.1	100.26(1.606)	45
		3	4.2	3.8	3.9	101.20(1.621)	47
006-6	LSS <sub>1</sub>	0	1.1	0.7	0.9	95.14(1.524)	32
		0*	1.6	0.7	1.1	95.95(1.537)	32
		1	2.5	2.2	2.3	99.01(1.586)	42
		3	4.1	3.5	3.6	100.88(1.616)	47
007-6	LSS <sub>3</sub>	0	7.0	6.7	6.7	103.45(1.657)	52
		0*	10.5	6.3	9.0	104.63(1.676)	55
		1	-	8.2	8.4	104.32(1.671)	54
		3	-	6.4	8.1	104.20(1.669)	54
008-6	LSS <sub>1</sub>	0	0.9	0.6	0.8	94.64(1.516)	30
		0*	1.9	0.7	1.5	97.27(1.558)	33
		1	8.5	1.8	2.0	98.45(1.577)	40
		3	3.1	2.3	2.9	99.25(1.601)	44
009-6	LSS <sub>3</sub>	0	6.8	6.2	6.4	103.26(1.654)	52
		0*	14.5	6.3	9.6	104.88(1.680)	56
		1	8.7	7.1	7.8	104.07(1.667)	54
		3	9.9	7.2	8.4	104.32(1.671)	54
010-6	LSS <sub>2</sub>	0	2.3	2.1	2.2	98.82(1.583)	42
		0*	3.6	2.1	2.8	99.83(1.599)	44
		1	3.9	3.0	3.3	100.51(1.610)	46
		3	4.8	3.7	4.2	101.51(1.626)	48
011-6	LSS <sub>2</sub>	0	2.6	2.2	2.3	99.01(1.586)	42
		0*	4.3	2.1	2.8	99.83(1.599)	44
		1	3.6	1.8	3.1	100.26(1.606)	45
		3	4.6	2.0	4.0	101.32(1.623)	48

\*Offset center line.

(1 of 8 Sheets)

Table 2 (Continued)

Test No.	Soil Condition	Pass No.	Penetration Resistance Gradient G, pci			$\gamma_d$ based on G pcf (g/cm <sup>3</sup> )	$D_r$ , % based on G
			Max	Min	Avg		
012-6	LSS <sub>2</sub>	0	2.4	2.2	2.3	99.01(1.586)	42
		0*	3.3	2.2	2.6	99.51(1.594)	44
		1	3.6	3.1	3.5	100.76(1.614)	46
		3	4.4	4.0	4.2	101.51(1.626)	48
013-6	LSS <sub>1</sub>	0	1.1	0.7	1.0	95.58(1.531)	33
		0*	-	-	-	-	-
		1	2.8	2.2	2.5	99.39(1.592)	43
		3	-	-	-	-	-
014-6	LSS <sub>1</sub>	0	0.9	0.8	0.8	94.64(1.516)	30
		0*	-	-	-	-	-
		1	2.5	2.2	2.4	99.20(1.589)	43
		3	4.2	3.4	3.8	101.07(1.619)	47
015-6	LSS <sub>3</sub>	0	6.9	6.4	6.7	103.45(1.657)	52
		0*	7.8	6.9	7.3	103.76(1.662)	53
		1	8.6	6.3	7.8	104.07(1.667)	54
		3	10.8	9.7	10.2	105.13(1.684)	56
016-6	LSS <sub>1</sub>	0	1.2	1.0	1.1	95.95(1.537)	34
		0*	1.4	1.2	1.3	96.64(1.548)	36
		1	3.7	2.8	3.2	100.39(1.608)	46
		3	5.6	4.4	4.9	102.14(1.636)	49
017-6	LSS <sub>1</sub>	0	0.8	0.6	0.7	94.08(1.507)	29
		0*	-	-	-	-	-
		1	2.7	2.3	2.5	99.39(1.592)	43
		3	5.0	1.6	4.0	101.32(1.623)	48
018-6	LSS <sub>1</sub>	0	1.1	1.0	1.0	95.58(1.531)	33
		0*	-	-	-	-	-
		1	2.6	2.1	2.4	99.20(1.589)	43
		3	4.3	3.8	4.1	101.39(1.624)	48
019-6	LSS <sub>1</sub>	0	1.0	0.7	0.8	94.64(1.516)	30
		0*	-	-	-	-	-
		1	2.7	2.4	2.5	99.39(1.592)	43
		3	4.2	3.2	3.8	101.07(1.619)	47
020-6	LSS <sub>1</sub>	0	0.9	0.5	0.7	94.08(1.507)	29
		0*	-	-	-	-	-
		1	2.8	1.8	2.2	98.83(1.583)	42
		3	6.4	2.7	2.4	99.20(1.581)	43
021-6	LSS <sub>1</sub>	0	0.8	0.7	0.7	94.08(1.507)	29
		0*	-	-	-	-	-
		1	2.1	1.9	2.0	98.45(1.577)	40
		3	3.6	3.0	3.3	100.51(1.610)	46

C-2

Table 2 (Continued)

Test No.	Soil Condition	Pass No.	Penetration Resistance Gradient G, pci			$\gamma_d$ based on G pcf (g/cm <sup>3</sup> )	D <sub>r</sub> , % based on G
			Max	Min	Avg		
024-6	LSS <sub>1</sub>	0	1.1	0.8	1.0	95.58(1.531)	33
		0*	-	-	-	-	-
		1	4.4	1.9	2.6	99.51(1.594)	44
		3	3.9	2.7	3.5	100.76(1.614)	46
025-6	LSS <sub>1</sub>	0	0.9	0.8	0.8	94.64(1.516)	30
		0*	-	-	-	-	-
		1	3.6	1.8	2.5	99.39(1.592)	43
		3	4.7	3.2	3.9	101.20(1.621)	47
026-6	LSS <sub>4</sub>	0	4.6	3.6	4.2	95.52(1.530)	33
		0*	-	-	-	-	-
		1	5.7	4.9	5.4	96.70(1.549)	36
		3	6.3	5.5	5.9	97.14(1.556)	37
027-6	LSS <sub>4</sub>	0	3.6	3.2	3.5	94.64(1.516)	31
		0*	-	-	-	-	-
		1	4.6	3.6	4.3	95.64(1.532)	33
		3	5.6	2.7	4.7	96.02(1.538)	34
028-6	LSS <sub>4</sub>	0	3.7	3.3	3.5	94.64(1.516)	31
		0*	-	-	-	-	-
		1	5.4	2.7	4.1	95.39(1.528)	32
		3	5.3	5.0	5.2	96.52(1.546)	36

Table 2 (Continued)

Test No.	Soil Condition	Pass No.	Moisture Content w , % From Density Measurement		
			Maximum	Minimum	Average
003-6	LSS <sub>1</sub>	0	-	-	-
		3	-	-	-
004-6	LSS <sub>3</sub>	0	-	-	-
		3	-	-	-
005-6	LSS <sub>2</sub>	0	-	-	-
		3	-	-	-
006-6	LSS <sub>1</sub>	0	0.9	0.9	0.9
		3	-	-	0.9
007-6	LSS <sub>3</sub>	0	0.9	0.9	0.9
		3	-	-	0.9
008-6	LSS <sub>1</sub>	0	0.9	0.9	0.9
		3	-	-	0.9
009-6	LSS <sub>3</sub>	0	1.0	0.9	0.9
		3	-	-	-
010-6	LSS <sub>2</sub>	0	0.9	0.9	0.9
		3	-	-	0.9
011-6	LSS <sub>2</sub>	0	-	-	-
		3	-	-	-
012-6	LSS <sub>2</sub>	0	1.0	0.9	1.0
		3	-	-	0.9
013-6	LSS <sub>1</sub>	0	1.0	0.9	0.9
		3	-	-	-
014-6	LSS <sub>1</sub>	0	-	-	-
		3	-	-	-
015-6	LSS <sub>3</sub>	0	0.9	0.9	0.9
		3	-	-	-
026-6	LSS <sub>4</sub>	0	1.9	1.7	1.8
		3	-	-	-
028-6	LSS <sub>4</sub>	0	1.9	1.8	1.8
		3	-	-	-

Table 2 (Continued)

Test No.	Soil Condition	Pass No.	$\gamma_d$ Measured Gravimetrically, pcf(g/cm <sup>3</sup> )			D <sub>r</sub> %
			Maximum	Minimum	Average	
003-6	LSS <sub>1</sub>	0	-	-	-	-
		3	-	-	-	-
004-6	LSS <sub>3</sub>	0	-	-	-	-
		3	-	-	-	-
005-6	LSS <sub>2</sub>	0	-	-	-	-
		3	-	-	-	-
006-6	LSS <sub>1</sub>	0	105.49(1.690)	101.12(1.620)	103.30(1.655)	52
		3	-	-	105.80(1.695)	57
007-6	LSS <sub>3</sub>	0	104.08(1.667)	103.90(1.664)	104.00(1.666)	54
		3	-	-	106.25(1.702)	58
008-6	LSS <sub>1</sub>	0	107.24(1.718)	104.89(1.680)	106.05(1.699)	58
		3	-	-	108.19(1.733)	62
009-6	LSS <sub>3</sub>	0	106.03(1.699)	103.67(1.661)	104.86(1.680)	55
		3	-	-	-	-
010-6	LSS <sub>2</sub>	0	105.07(1.683)	104.70(1.677)	104.88(1.680)	55
		3	-	-	109.00(1.746)	64
011-6	LSS <sub>2</sub>	0	-	-	-	-
		3	-	-	-	-
012-6	LSS <sub>2</sub>	0	103.63(1.660)	103.01(1.650)	103.32(1.655)	52
		3	-	-	108.38(1.736)	63
013-6	LSS <sub>1</sub>	0	105.01(1.682)	102.76(1.646)	103.88(1.664)	53
		3	-	-	-	-
014-6	LSS <sub>1</sub>	0	-	-	-	-
		3	-	-	-	-
015-6	LSS <sub>3</sub>	0	106.13(1.700)	104.88(1.680)	105.51(1.690)	57
		3	-	-	-	-
026-6	LSS <sub>4</sub>	0	86.78(1.390)	81.16(1.300)	83.97(1.345)	0
		3	-	-	86.78(1.390)	8
028-6	LSS <sub>4</sub>	0	95.71(1.533)	95.46(1.529)	95.58(1.531)	34
		3	-	-	-	-

Table 2 (Continued)

Test No.	Soil Condition	Pass No.	Bevamer Plate Test Results		
			$k_c$ (lb/in. <sup>1+n</sup> )	$k_\phi$ (lb/in. <sup>2+n</sup> )	n
003-6	LSS <sub>1</sub>	0	-	-	-
		3	-	-	-
004-6	LSS <sub>3</sub>	0	-	-	-
		3	-	-	-
005-6	LSS <sub>2</sub>	0	-	-	-
		3	-	-	-
006-6	LSS <sub>1</sub>	0	0.97	3.50	1.13
		3	1.20	1.89	1.07
007-6	LSS <sub>3</sub>	0	-1.35	9.46	1.41
		3	0.12	11.91	0.99
008-6	LSS <sub>1</sub>	0	-0.76	4.54	1.00
		3	5.37	2.66	0.71
009-6	LSS <sub>3</sub>	0	-0.94	9.93	1.38
		3	-1.18	9.86	1.24
010-6	LSS <sub>2</sub>	0	0.13	5.34	1.05
		3	-0.45	6.01	1.15
011-6	LSS <sub>2</sub>	0	-	-	-
		3	-	-	-
012-6	LSS <sub>1</sub>	0	1.28	5.25	0.78
		3	4.00	5.62	0.66
013-6	LSS <sub>1</sub>	0	-	-	-
		3	-	-	-
014-6	LSS <sub>1</sub>	0	0.18	3.99	0.70
		3	5.69	1.64	0.64
015-6	LSS <sub>3</sub>	0	-2.44	7.10	1.65
		3	1.10	10.63	0.99
028-6	LSS <sub>4</sub>	0	1.76	5.04	1.18
		3	1.44	5.08	1.10

Table 2 (Continued)

Test No.	Soil Condition	Pass No.	Bevamer Ring Shear Test Results					
			$s_b$	psi			$c_b$	$\phi_b$
			1.1	2.2	3.4	psi	deg	
003-6	LSS <sub>1</sub>	0	-	-	-	-	-	
		3	-	-	-	-	-	
004-6	LSS <sub>3</sub>	0	-	-	-	-	-	
		3	-	-	-	-	-	
005-6	LSS <sub>2</sub>	0	-	-	-	-	-	
		3	-	-	-	-	-	
006-6	LSS <sub>1</sub>	0	0.80	1.40	1.81	0.26	25.9	
		3	0.65	1.38	1.89	0.00	30.5	
007-6	LSS <sub>3</sub>	0	0.65	1.51	1.94	0.10	30.0	
		3	0.69	1.46	1.78	0.19	25.0	
008-6	LSS <sub>1</sub>	0	0.71	1.44	2.24	0.00	33.5	
		3	0.75	1.38	2.09	0.13	30.0	
009-6	LSS <sub>3</sub>	0	0.73	1.33	2.18	0.15	30.0	
		3	0.78	1.55	2.00	0.06	32.0	
010-6	LSS <sub>2</sub>	0	0.76	1.40	1.94	0.15	29.0	
		3	0.77	1.38	1.81	0.22	26.0	
011-6	LSS <sub>2</sub>	0	-	-	-	-	-	
		3	-	-	-	-	-	
012-6	LSS <sub>1</sub>	0	0.69	1.23	2.04	0.20	27.0	
		3	0.73	1.38	1.74	0.28	25.0	
013-6	LSS <sub>1</sub>	0	-	-	-	-	-	
		3	-	-	-	-	-	
014-6	LSS <sub>1</sub>	0	0.73	1.46	2.11	0.10	30.0	
		3	0.78	1.23	1.96	0.19	27.5	
015-6	LSS <sub>3</sub>	0	0.75	1.44	2.11	0.20	26.5	
		3	0.75	1.42	1.85	0.19	27.5	
028-6	LSS <sub>4</sub>	0	0.73	1.36	1.97	0.12	29.0	
		3	0.67	1.33	1.70	0.10	26.5	

Table 2 (Concluded)

Test No.	Soil Condition	Pass No.	Cohron Sheargraph Test Results				
			$s_c$ 1.6	psi 3.3	psi 4.9	$c_c$ psi	$\phi_c$ deg
003-6	LSS <sub>1</sub>	0	-	-	-	-	-
		3	-	-	-	-	-
004-6	LSS <sub>3</sub>	0	-	-	-	-	-
		3	-	-	-	-	-
005-6	LSS <sub>2</sub>	0	-	-	-	-	-
		3	-	-	-	-	-
006-6	LSS <sub>1</sub>	0	0.98	1.36	-	0.58	13.5
		3	1.12	1.87	2.28	0.51	21.0
007-6	LSS <sub>3</sub>	0	0.96	1.61	2.18	0.41	20.0
		3	0.76	1.52	2.18	0.03	24.0
008-6	LSS <sub>1</sub>	0	0.87	1.63	2.12	0.17	23.0
		3	1.09	1.63	2.12	0.58	17.5
009-6	LSS <sub>3</sub>	0	0.99	1.19	2.15	0.04	23.5
		3	0.95	1.52	2.07	0.41	18.5
010-6	LSS <sub>2</sub>	0	0.92	1.44	2.02	0.36	18.5
		3	0.92	1.65	2.47	0.15	25.0
011-6	LSS <sub>2</sub>	0	-	-	-	-	-
		3	-	-	-	-	-
012-6	LSS <sub>1</sub>	0	0.90	1.52	2.12	0.29	20.5
		3	1.00	1.50	2.01	0.46	18.0
013-6	LSS <sub>1</sub>	0	-	-	-	-	-
		3	-	-	-	-	-
014-6	LSS <sub>1</sub>	0	0.87	1.80	2.28	0.22	22.0
		3	1.05	1.38	2.18	0.58	17.0
015-6	LSS <sub>3</sub>	0	0.86	1.51	2.09	0.22	22.0
		3	1.09	1.62	2.18	0.48	18.5
028-6	LSS <sub>4</sub>	0	0.92	1.41	2.09	0.36	19.5
		3	0.81	1.45	2.07	0.22	21.0

Table 3

Representative Data from Computer Recording System

<u>P/W</u>	<u>M/R W e</u>	<u>Slip %</u>	<u><math>\eta^*</math></u>	<u>Power No.</u>
.054	.071	-1.7	-37.255	.001
.037	.021	-2.3	-1.020	.021
.035	.035	-3.1	-1.056	.034
.064	.057	-1.9	-1.134	.057
.046	.026	-.6	-.545	.025
.032	.110	-.1	-.099	.100
.017	.141	1.1	-.129	.143
.037	.162	3.5	.212	.174
.115	.272	4.2	.547	.213
.140	.246	6.2	.569	.262
.204	.276	7.4	.659	.300
.250	.295	2.2	.771	.324
.279	.357	11.2	.693	.402
.270	.352	12.6	.652	.415
.337	.376	13.7	.775	.436
.322	.397	15.2	.625	.470
.335	.437	16.3	.637	.525
.340	.422	17.1	.669	.500
.335	.439	17.3	.622	.532
.332	.431	19.2	.617	.532
.377	.405	21.5	.729	.516
.369	.414	22.6	.629	.536
.371	.454	24.5	.634	.602
.390	.473	26.4	.606	.644
.371	.473	22.2	.567	.673
.337	.512	30.0	.460	.732
.347	.517	32.6	.451	.762
.327	.422	34.6	.432	.746
.306	.492	36.6	.394	.777
.223	.491	32.2	.352	.203
.224	.423	40.7	.342	.216
.272	.462	42.9	.339	.221
.301	.494	45.5	.332	.207
.310	.510	47.2	.317	.277
.349	.520	50.3	.333	1.047
.352	.532	53.0	.210	1.162
.372	.550	55.7	.204	1.264
.405	.565	57.6	.303	1.335
.444	.591	60.1	.292	1.426
.430	.615	62.7	.260	1.652
.440	.622	65.4	.245	1.709
.437	.655	62.1	.213	2.057
.440	.705	71.3	.172	2.463
.427	.732	74.7	.162	2.972
.532	.720	72.0	.143	3.711

\* Efficiency = ratio of recoverable energy to total energy input.

Table 4

Wheel Data

Tire Code No.	Tire Print		Contact Area in. <sup>2</sup>	Radius, in.		Section Height: Unloaded h, in.	Section Height: Loaded h', in.	Carcass Diameter d, in.	Load lb	Contact Pressure psi	Deflection	
	Length in.	Width in.		r <sub>r</sub>	r <sub>e</sub> *						Computed in.	%
GM IX	-	-	-	13.65	14.95	7.150	5.310	31.74	57	-	1.840	11.59
GM X	11.00	6.85	62.00	13.68	15.13	7.330	5.400	32.10	57	0.92	1.93	12.02
GM XI	-	-	-	13.46	14.56	6.497	4.988	30.43	57	-	1.509	9.92
GM XII	-	-	-	13.46	15.13	6.939	5.884	31.32	57	-	1.055	6.74
GM XIII	-	-	-	13.36	15.13	7.453	5.350	32.35	57	-	2.103	13.00
GM XIV	-	-	-	13.31	15.00	7.232	5.335	31.90	57	-	1.897	11.89

$$*r_e = \frac{d}{2} - \frac{h-h'}{2}$$

Table 5

## Wheel Performance Data

Test No.	Pass No.	Soil Condition	$P_T/W$	Slip* %	PN <sub>sp</sub>	Slip* %	PN <sub>15°</sub>	Slip* %	$P_{20\%/W}$	$\frac{M_{20}}{Wre}$	PN <sub>20%</sub>	$P_{50\%/W}$	$\frac{M_{50}}{Wre}$	PN <sub>50%</sub>
<u>GM IX</u>														
018-6	1	LSS <sub>1</sub>	0.17	6.0	0.16	3.0	0.63	30.3	0.15	0.33	0.46	0.19	0.39	0.90
019-6	1		0.20	6.3	0.26	7.2	1.60	63.0	0.20	0.36	0.41	0.22	0.48	1.08
018-6	2	LSS <sub>1</sub>	0.17	2.0	0.16	5.2	0.60	26.5	0.24	0.43	0.61	0.23	0.43	0.97
019-6	2		0.06	1.5	0.17	3.2	0.76	43.7	0.23	0.42	0.58	0.39	0.40	0.89
Avg			0.15	3.4	0.19	4.6	0.90	40.9	0.21	0.39	0.52	0.26	0.42	0.95
<u>GM X</u>														
003-6	1	LSS <sub>1</sub>	0.18	6.4	0.06	0.5	0.44	23.0	0.26	0.30	0.38	0.45	0.45	0.90
006-6	1		0.13	4.5	0.15	4.5	0.43	19.0	0.29	0.35	0.44	0.47	0.57	1.17
008-6	1		0.13	0.8	0.10	2.9	0.40	18.0	0.29	0.35	0.45	0.47	0.57	1.12
003-6	2	LSS <sub>1</sub>	0.05	1.5	0.04	0.5	0.35	19.0	0.32	0.31	0.38	0.37	0.37	0.75
006-6	2		0.07	0.5	0.06	4.0	0.44	16.5	0.37	0.38	0.47	0.36	0.45	0.90
008-6	2		0.18	3.2	0.09	2.4	0.36	9.8	0.37	0.47	0.59	0.43	0.55	1.10
Avg			0.12	2.8	0.08	2.5	0.42	17.6	0.33	0.36	0.45	0.43	0.49	0.99
005-6	1	LSS <sub>2</sub>	0.11	0.3	0.06	3.1	0.39	20.5	0.25	0.30	0.38	0.34	0.49	0.98
010-6	1		0.06	1.0	0.08	4.0	0.55	27.0	0.26	0.34	0.43	0.48	0.55	0.11
012-6	1		0.15	3.0	0.08	3.4	0.51	21.5	0.23	0.39	0.49	0.47	0.57	1.16

(Continued)

\*Slip at which  $P_T/W$ , PN<sub>sp</sub>, and PN<sub>15°</sub>, respectively, occurred.

(1 of 4 Sheets)

Table 5 (Continued)

Test Pass No.	Soil Condition	P <sub>T</sub> /W	Slip %	PN <sub>sp</sub>	Slip %	PN <sub>15°</sub>	Slip %	GM X (Cont'd)			M <sub>20</sub>			M <sub>50</sub>		
								P <sub>20%/W</sub>	Wr <sub>e</sub>	PN <sub>20%</sub>	P <sub>50%/W</sub>	Wr <sub>e</sub>	PN <sub>50%</sub>			
005-6	LSS <sub>2</sub>	0.16	0.5	0.12	4.0	0.27	20.0	0.27	0.37	0.46	0.44	0.49	1.01			
010-6		0.05	1.0	0.10	4.0	0.33	9.2	0.42	0.46	0.57	0.47	0.55	1.12			
012-6		0.12	0.0	0.10	4.2	0.34	10.7	0.32	0.51	0.63	0.41	0.56	1.12			
AVG		0.11	1.0	0.09	3.8	0.40	18.1	0.29	0.40	0.49	0.44	0.54	1.09			
004-6	LSS <sub>3</sub>	0.03	1.0	0.07	4.7	0.36	18.0	0.31	0.34	0.43	0.43	0.49	1.00			
007-6		0.07	0.4	0.08	4.5	0.40	20.0	0.27	0.32	0.40	0.38	0.45	0.92			
009-6		0.10	0.5	0.08	6.0	0.39	18.0	0.30	0.37	0.47	0.40	0.47	0.95			
004-6		0.02	1.0	0.06	1.5	0.36	12.0	0.38	0.38	0.48	0.41	0.49	0.99			
007-6		0.03	3.6	0.07	1.4	0.28	6.2	0.38	0.40	0.50	0.45	0.48	0.96			
009-6		0.05	0.5	0.05	0.4	0.43	13.2	0.41	0.43	0.55	0.41	0.48	0.97			
AVG		0.05	1.3	0.07	3.1	0.3	14.6	0.34	0.38	0.47	0.41	0.48	0.96			
011-6	LSS <sub>2</sub>	Constant Slip Average = 25.0 P <sub>25%/W</sub> = 0.30; M <sub>25</sub> /Wr = 0.41; PN <sub>25°</sub> = 0.56														
		Constant Slip Average = 24.0 P <sub>24%/W</sub> = 0.35; M <sub>24</sub> /Wr = 0.45; PN <sub>24</sub> = 0.50														
013-6	LSS <sub>1</sub>	Constant Slip Average = 50; P/W = 0.35; M <sub>50</sub> /Wr = 0.68; PN <sub>50</sub> = 1.38														
GM XI																
014-6	LSS <sub>1</sub>	0.15	14.0	0.22	14.0	---	No Go	---	0.03	0.20	0.25	0.06	0.22	0.45		
014-6		0.13	0.8	0.15	11.5	---	No Go	---	0.00	0	0.21	0.02	0.19	0.38		
AVG		0.14	7.4	0.18	12.8	---	No Go	---	0.02	0.18	0.23	0.04	0.20	0.42		

Table 5 (Continued)

Test Pass No.	Soil Condition	P <sub>T</sub> /W	Slip %	PN <sub>sp</sub>	Slip %	PN <sub>15°</sub>	Slip %	P <sub>20%/W</sub>	M <sub>20</sub> Wr e	PN <sub>20%</sub>	P <sub>50%/W</sub>	M <sub>50</sub> Wr e	PN <sub>50%</sub>	
														GM XI (Cont'd)
015-6 1	LSS <sub>3</sub>	0.04	3.3	0.20	27.0	--	No Go	--	-0.03	0.13	0.16	-0.02	0.10	0.20
2		0.03	3.2	0.12	13.0	--	No Go	--	0.11	0.16	0.20	0.07	0.14	0.28
AVG		0.04	3.2	0.16	20.0	--	No Go	--	0.04	0.14	0.18	0.03	0.12	0.24
GM XII														
016-6 1	LSS <sub>1</sub>	0.24	10.6	0.27	10.4	--	No Go	--	0.09	0.38	0.48	0.15	0.45	0.90
017-6 1		0.19	12.5	0.19	11.2	--	No Go	--	0.13	0.36	0.45	0.24	0.57	1.16
016-6 2		0.15	5.4	0.14	2.7	--	No Go	--	0.08	0.30	0.38	0.09	0.37	0.75
017-6 2		0.19	7.3	0.11	0.8	--	No Go	--	0.12	0.30	0.37	0.15	0.38	0.76
AVG		0.19	9.0	0.18	6.3	--	No Go	--	0.11	0.34	0.42	0.16	0.44	0.89
GM XIII														
020-6 1	LSS <sub>1</sub>	0.24	7.0	0.14	1.8	0.60	22.0	0.22	0.46	0.58	0.35	0.62	1.25	
021-6 1		0.21	5.5	0.16	5.5	0.67	26.4	0.15	0.40	0.50	0.38	0.57	1.14	
020-6 2		0.10	5.0	0.10	5.0	0.45	14.5	0.35	0.37	0.47	0.41	0.54	1.10	
021-6 2		0.05	1.8	0.15	1.9	0.42	12.6	0.33	0.43	0.54	0.35	0.52	1.05	
AVG		0.15	4.8	0.14	7.1	0.44	18.9	0.26	0.42	0.52	0.37	0.54	1.13	
026-6 1	LSS <sub>4</sub>	0.13	3.1	0.17	1.7	0.36	9.6	0.34	0.51	0.64	0.34	0.67	1.34	
027-6 1		0.06	0.7	0.10	3.3	0.47	16.0	0.33	0.40	0.51	0.38	0.59	1.17	
028-6 1		0.06	1.5	0.10	1.2	0.44	9.4	0.37	0.47	0.59	0.40	0.57	1.12	

Table 5 (Concluded)

Test No.	Pass No.	Soil Condition	P <sub>T</sub> /W	Slip %	PN <sub>sp</sub>	Slip %	PN <sub>15°</sub>	Slip %	P <sub>20%/W</sub>	GM XIII (Cont'd)		GM XIV	
										PN <sub>20%</sub>	F <sub>50%/W</sub>	M <sub>20</sub> W <sub>r</sub> e	M <sub>50</sub> W <sub>r</sub> e
026-6	2	LSS <sub>4</sub>	0.07	0.7	0.13	0.4	0.37	6.7	0.43	0.51	0.64	0.46	0.70
027-6	2		0.06	1.8	0.15	2.8	0.44	12.0	0.35	0.46	0.58	0.40	0.50
028-6	2		0.03	0.7	0.06	1.9	0.40	15.0	0.34	0.43	0.53	0.43	0.57
AVG			0.07	1.4	0.12	1.9	0.41	11.4	0.38	0.48	0.58	0.40	0.60
024-6	1	LSS <sub>1</sub>	0.08	8.4	0.17	2.8	0.68	28.6	0.10	0.38	0.48	0.35	0.74
025-6	1		0.22	7.1	0.17	4.5	0.82	33.8	0.17	0.38	0.47	0.37	0.69
024-6	2		0.02	1.1	0.08	0.0	0.43	14.0	0.34	0.39	0.49	0.51	0.71
025-6	2	0.09	3.2	0.08	0.9	0.59	20.0	0.27	0.47	0.59	0.50	0.73	
AVG			0.13	5.0	0.12	4.0	0.63	24.1	0.22	0.40	0.51	0.43	0.72

## APPENDIX A: WES SINGLE-WHEEL DYNAMOMETER SYSTEM

1. The WES single-wheel dynamometer system is housed in the mobility test facility shown in fig. A1. An overall view of the dynamometer system with the LRV wheel mounted in it is presented in fig. A2. Closeup views and schematic drawings of dynamometer components are displayed in figs. A3-A10.

2. The following tabulation presents the test elements that are controlled and the measurements for each element.

Control	Measurement
Vertical force on wheel	Vertical force on wheel (load) Vertical motion of wheel (sinkage)
Horizontal wheel velocity	Horizontal wheel velocity Horizontal wheel acceleration Horizontal wheel position Horizontal wheel force (pull)
Angular wheel velocity	Angular wheel velocity Angular wheel position Torque
---	Vertical acceleration of wheel drive frame Horizontal acceleration of sinkage frame
Wheel path	---
Side thrust	
Steering moment	
Tilt moment	
Soil conditions	---
Wheel type and conditions	

3. A flow chart for the recording systems is shown in fig. A11. Relations of pull coefficient to slip, obtained with three different recording methods, are compared in fig. A12.

4. The following operational procedures are used to ensure validity of data:

- a. Facility checks
- b. Test carriage checks
- c. Transducer calibration
- d. Electronic checks
- e. System calibration (end-to-end).

REPRODUCIBILITY OF THE ORIGINAL PAGE IS POOR.

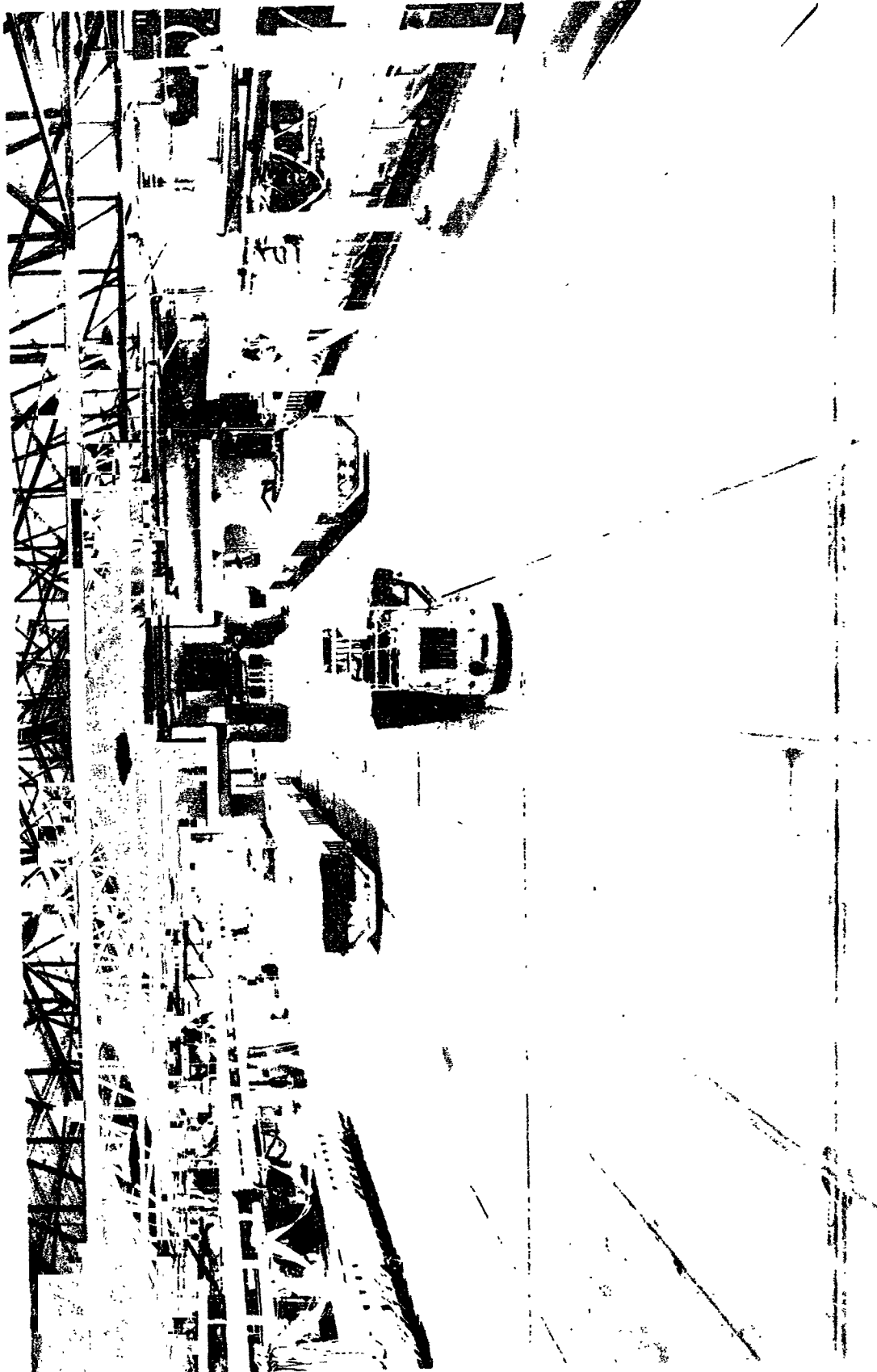


Fig. A1. General view of WES mobility test facility  
(temperature and humidity controlled)

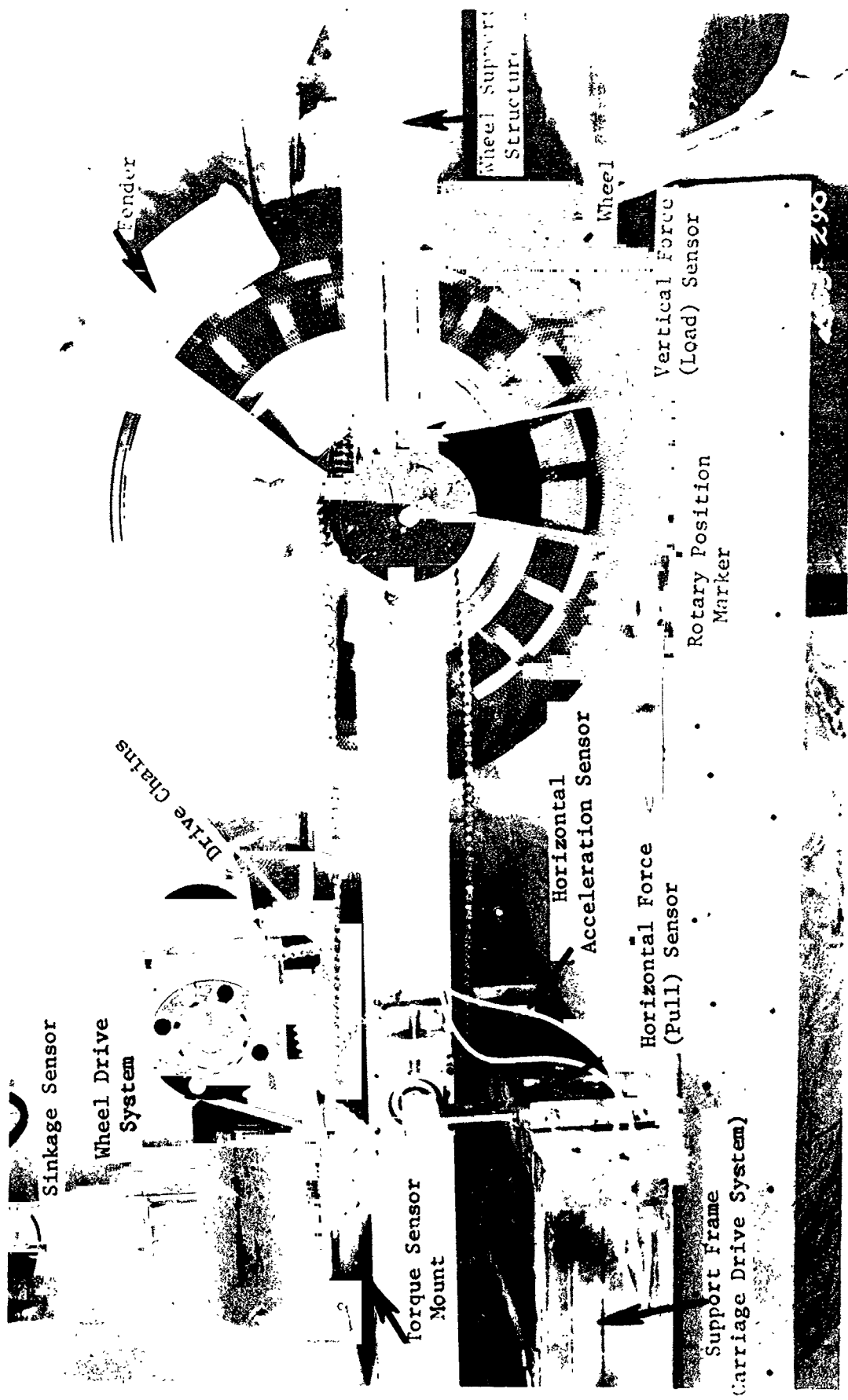


Fig. A2. WES single-wheel dynamometer system

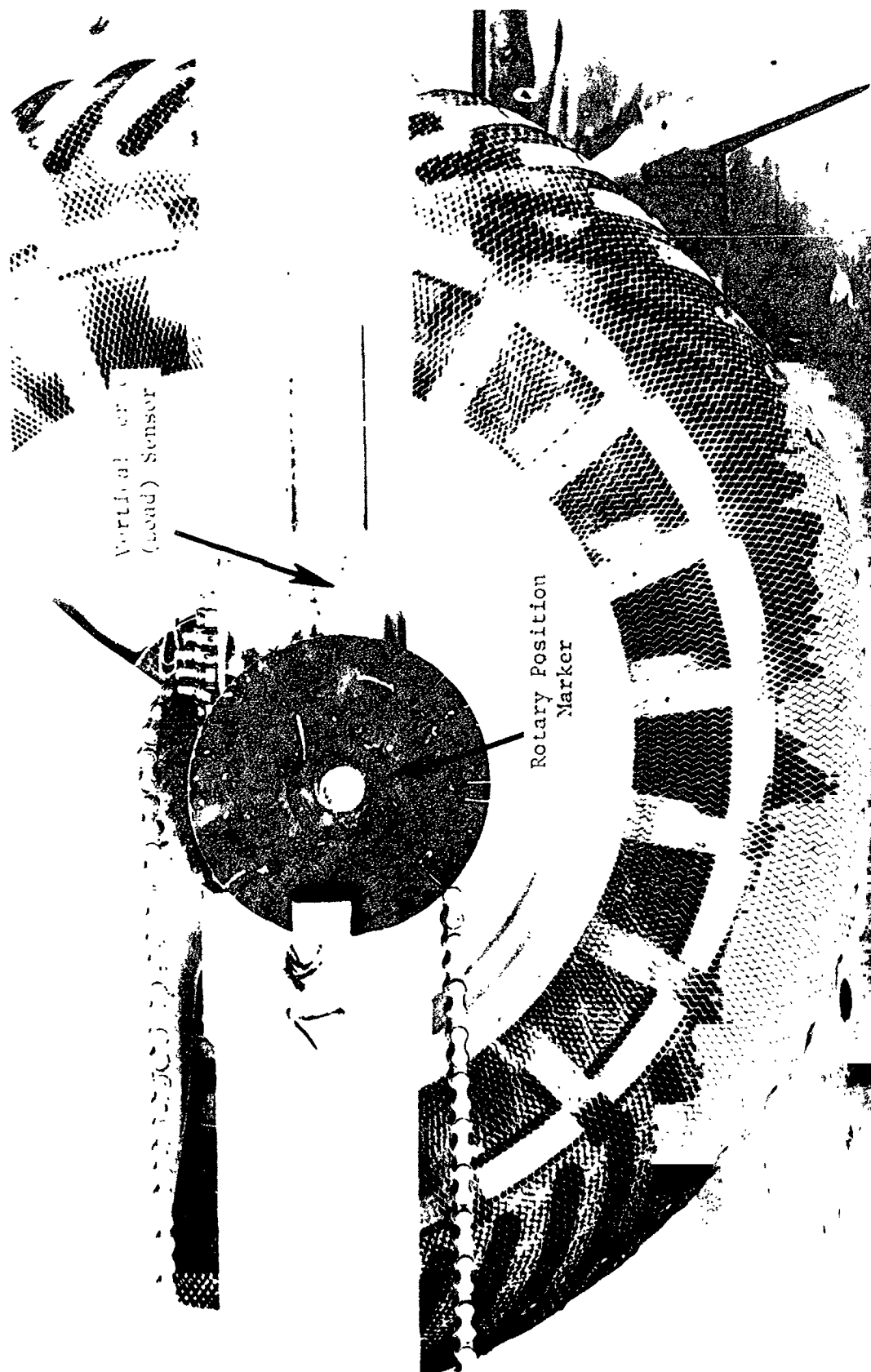
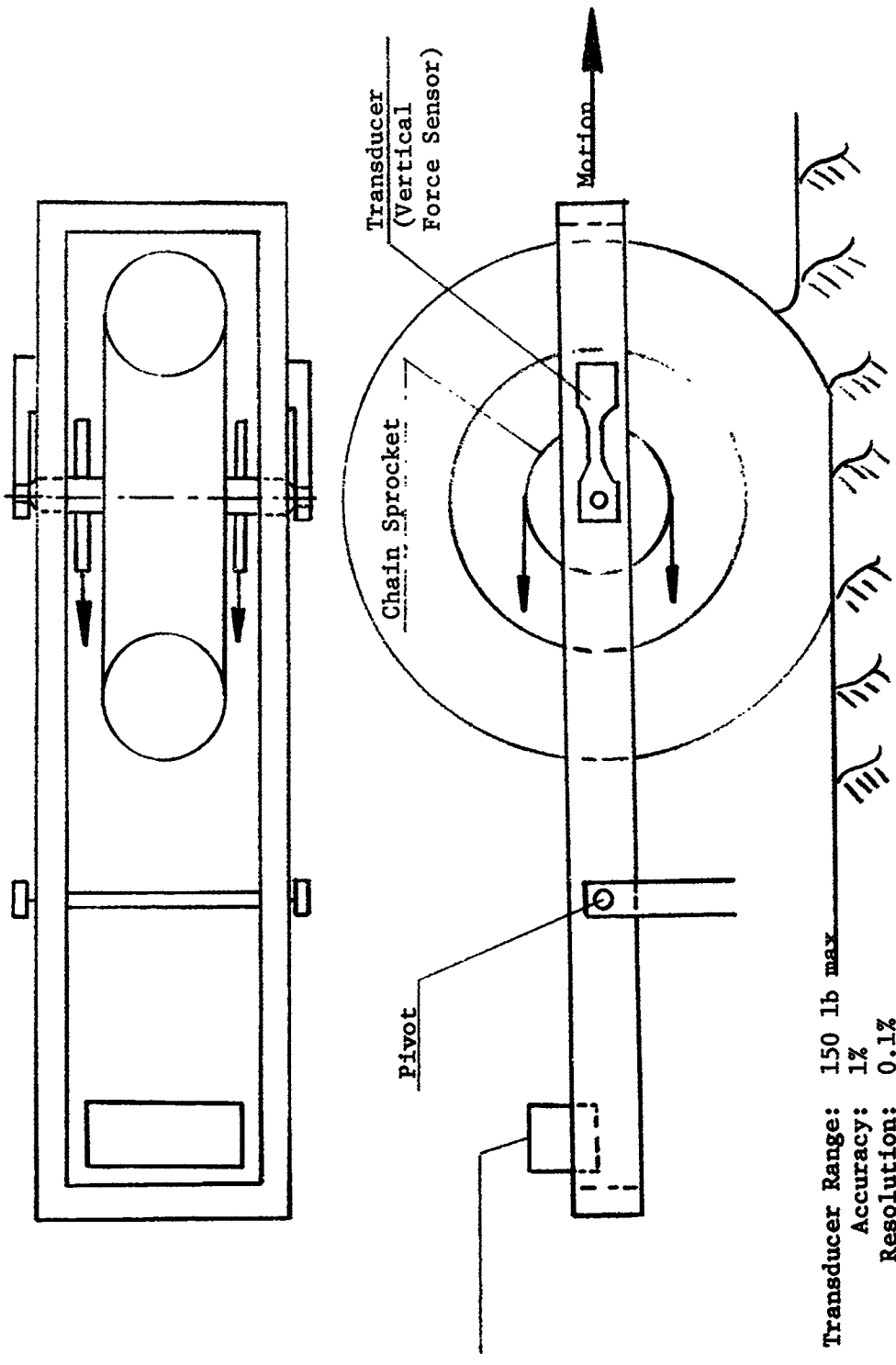


Fig. A3. Close-up view of vertical force (load) sensor and rotary position marker for determination of angular wheel velocity



Transducer Range: 150 lb max  
 Accuracy: 1%  
 Resolution: 0.1%

Fig. A4. Scheme showing principle of vertical force (load) measurement and means of maintaining constant load (counterweighted frame)

REPRODUCIBILITY OF THE ORIGINAL PAGE IS POOR.

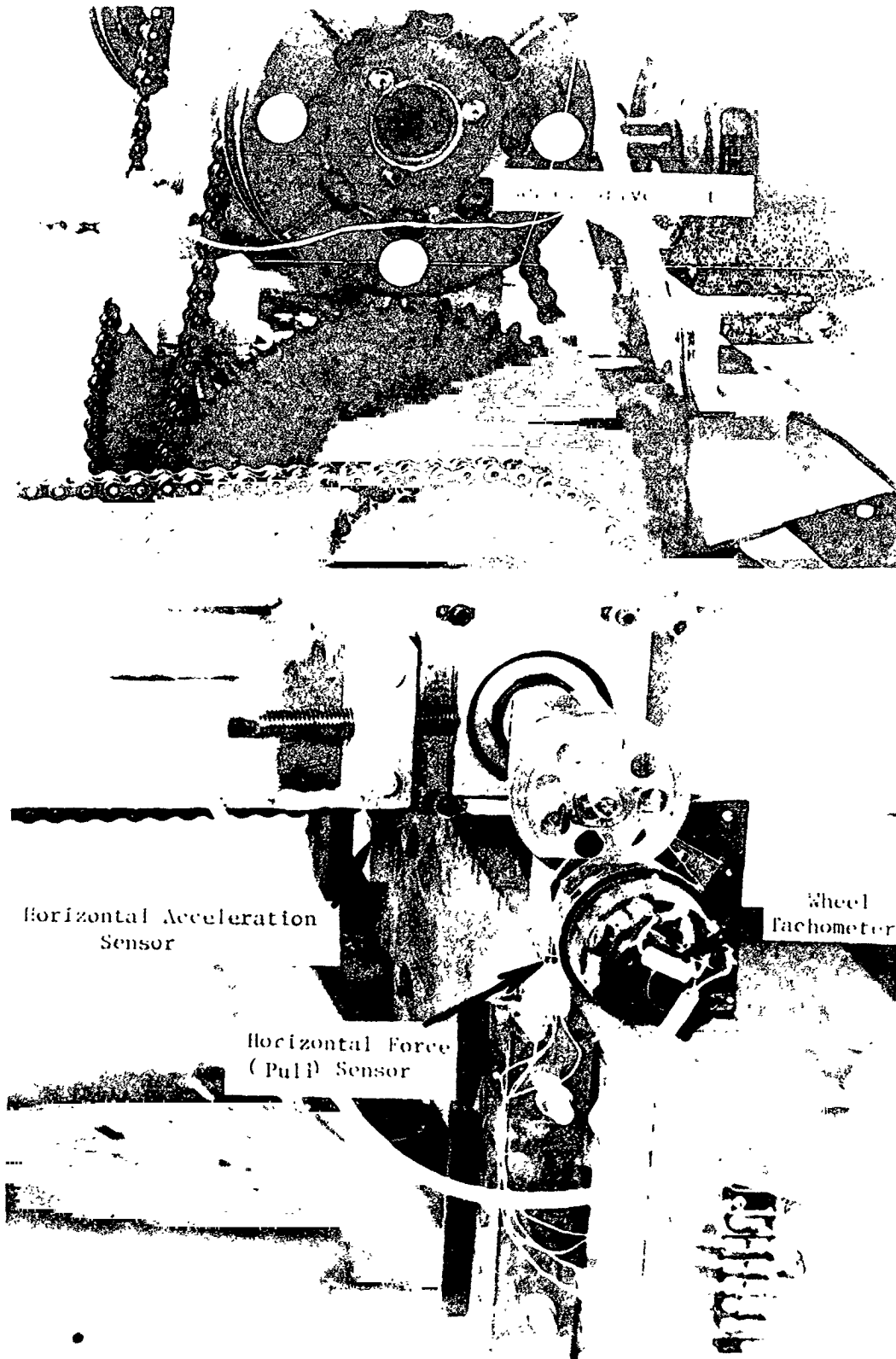


Fig. A5. Close-up view of horizontal force (pull) sensor, horizontal acceleration sensor, and wheel tachometer

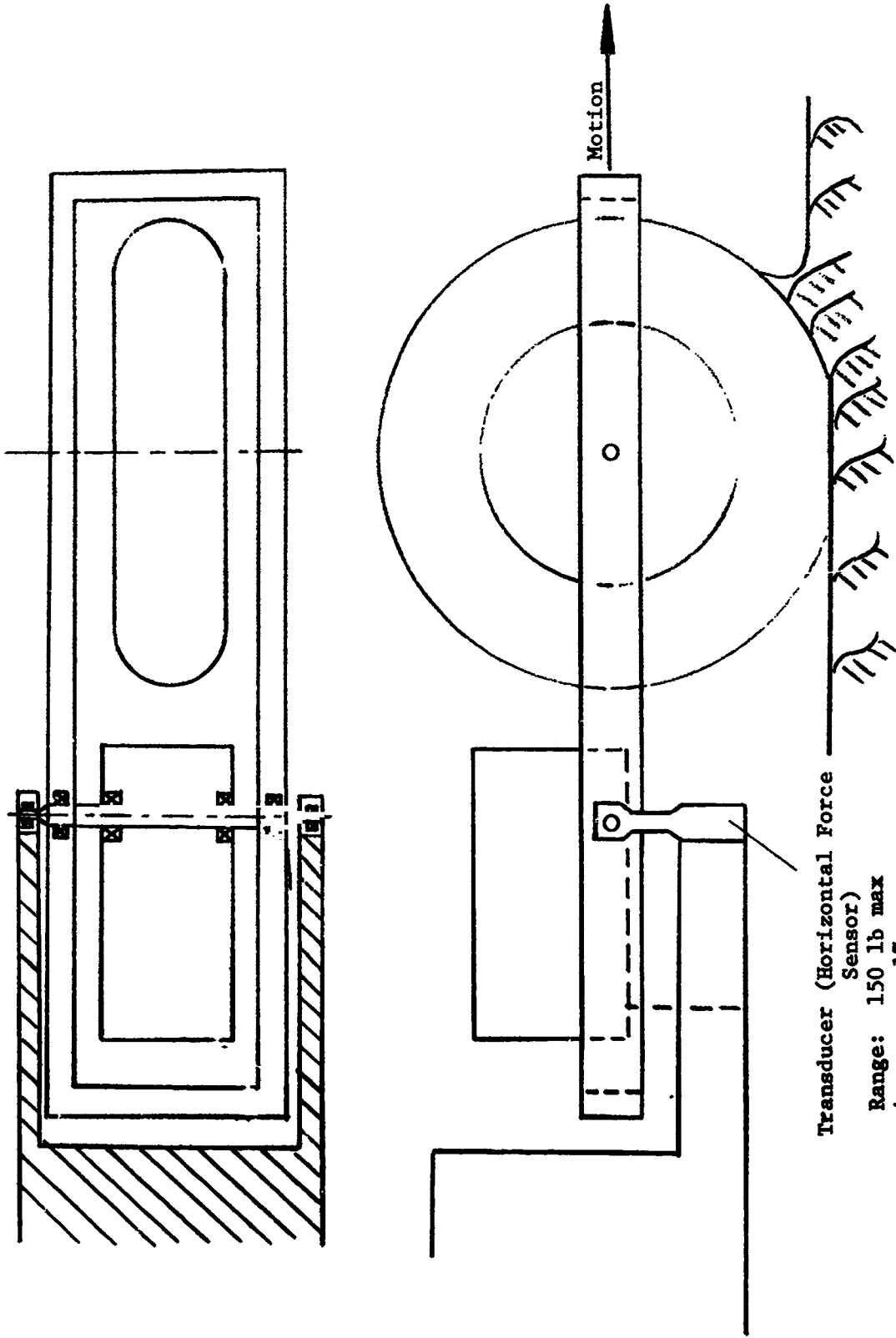


Fig. A6. Scheme showing principle of horizontal force (pull) measurement.

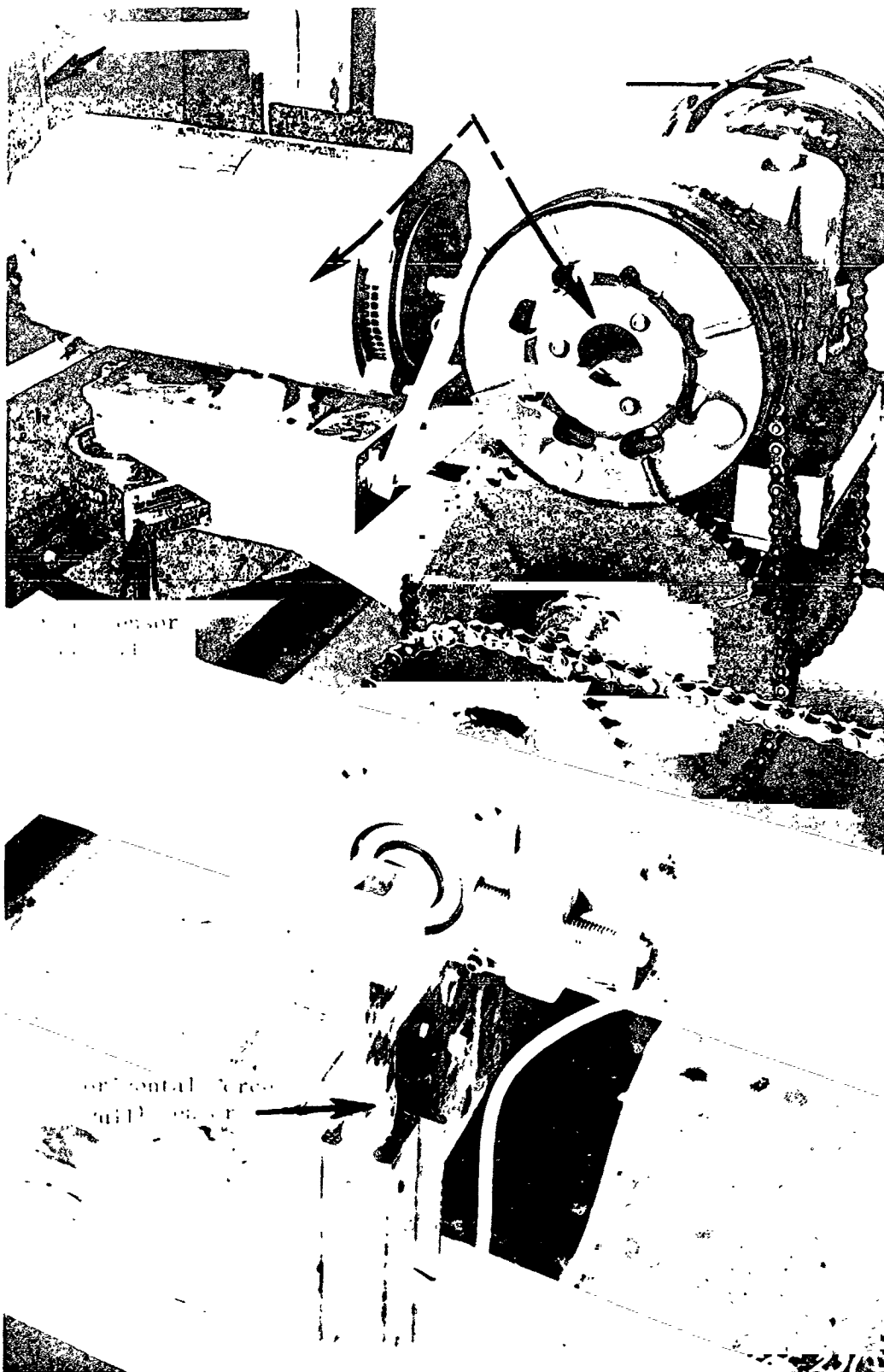


Fig. A7. Close-up view of wheel drive system and torque sensor

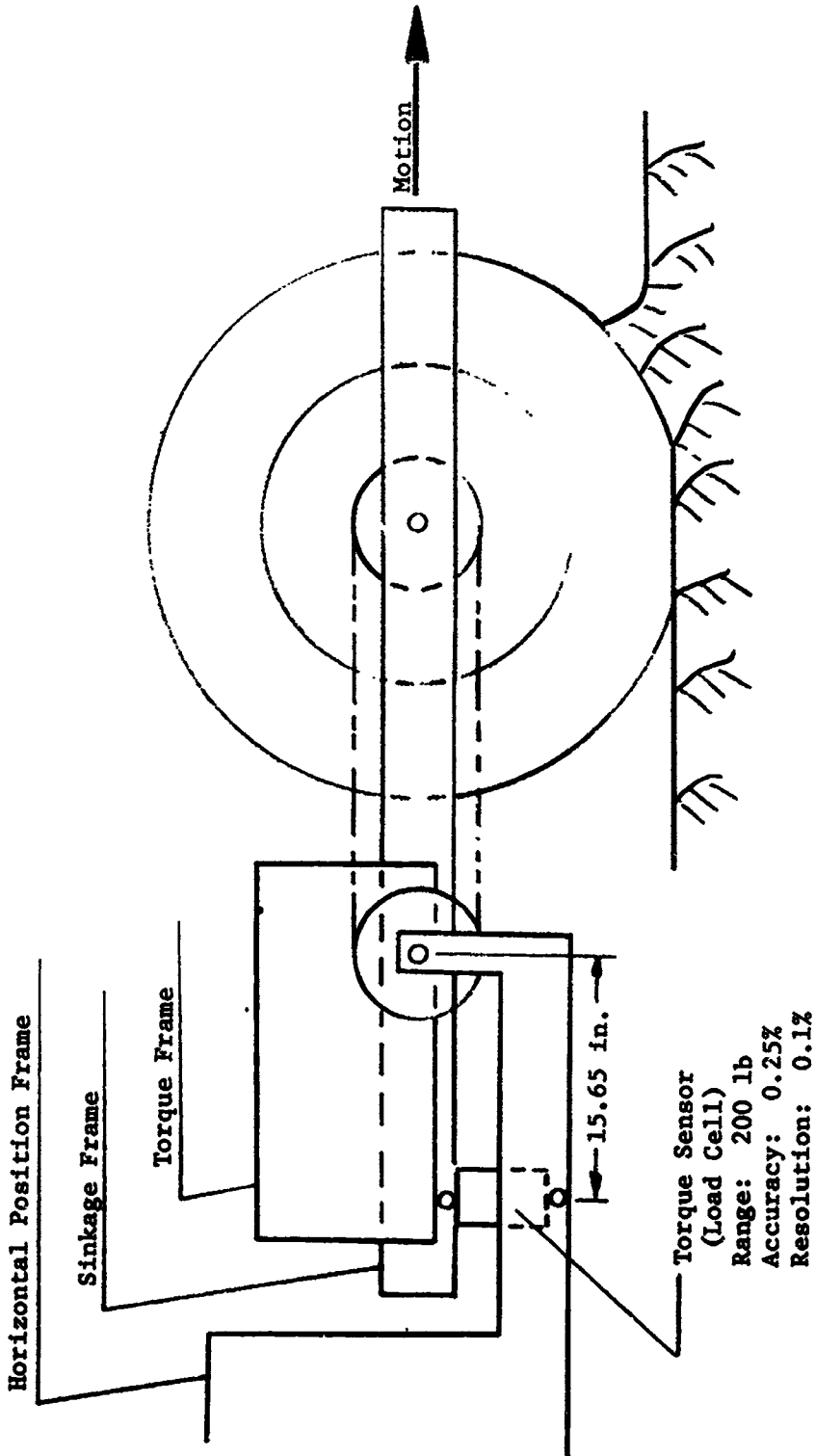
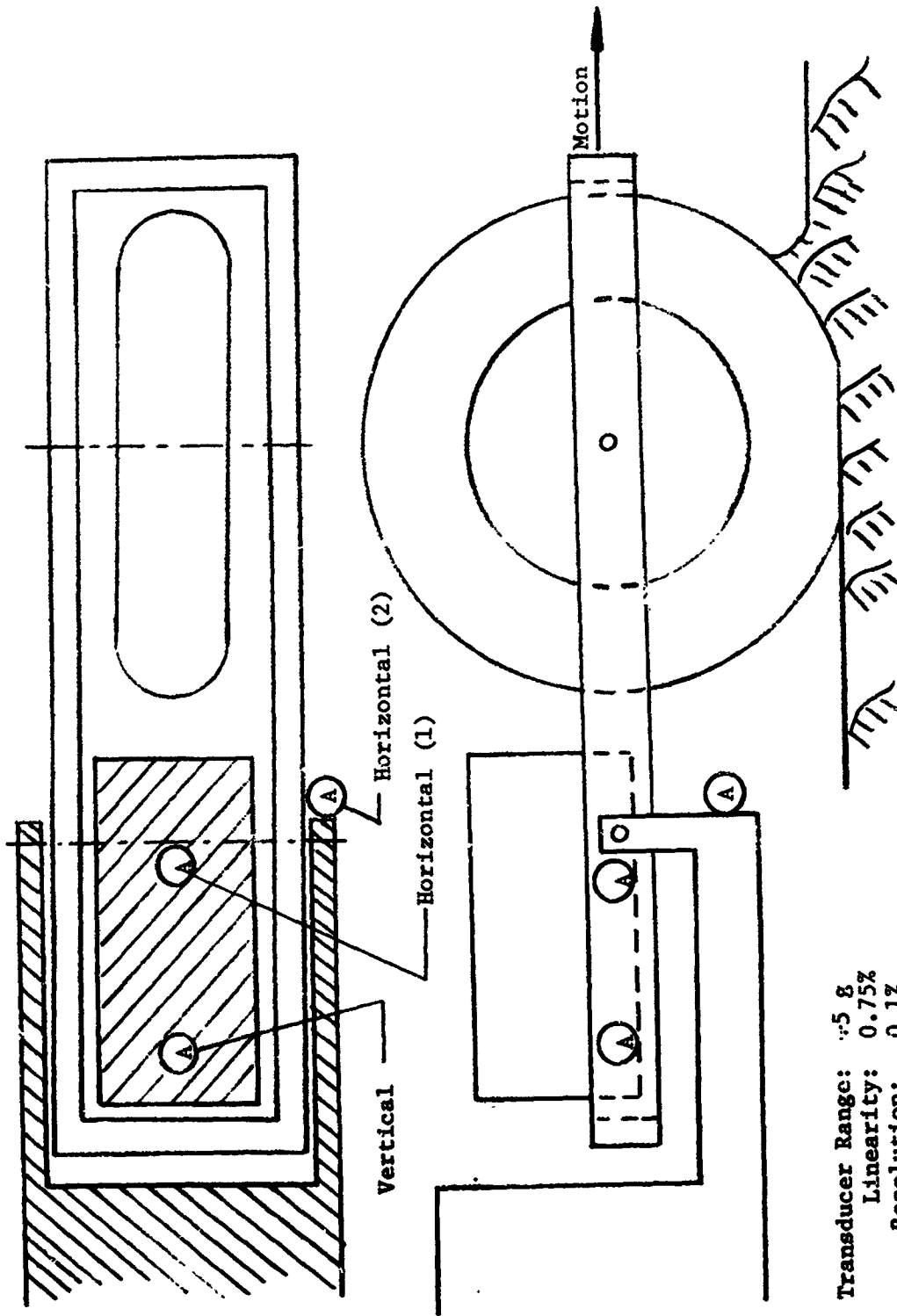
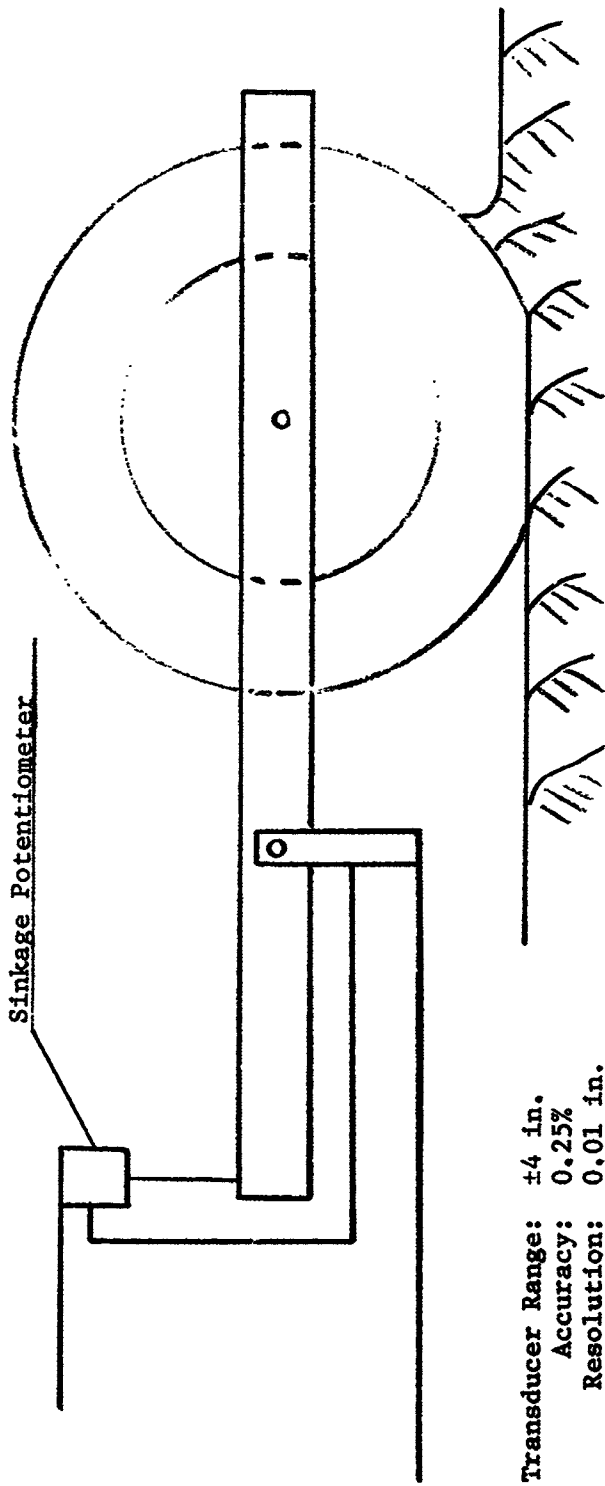


Fig. A8. Scheme showing principle of wheel drive system and torque measurement



Transducer Range:  $\pm 5$  g  
 Linearity: 0.75%  
 Resolution: 0.1%

Fig. A9. Scheme showing location of accelerometers (A), used to correct other measurements (pull, torque) for inertia effects



Transducer Range:  $\pm 4$  in.  
Accuracy: 0.25%  
Resolution: 0.01 in.

Fig. A10. Scheme showing principle of sinkage measurement

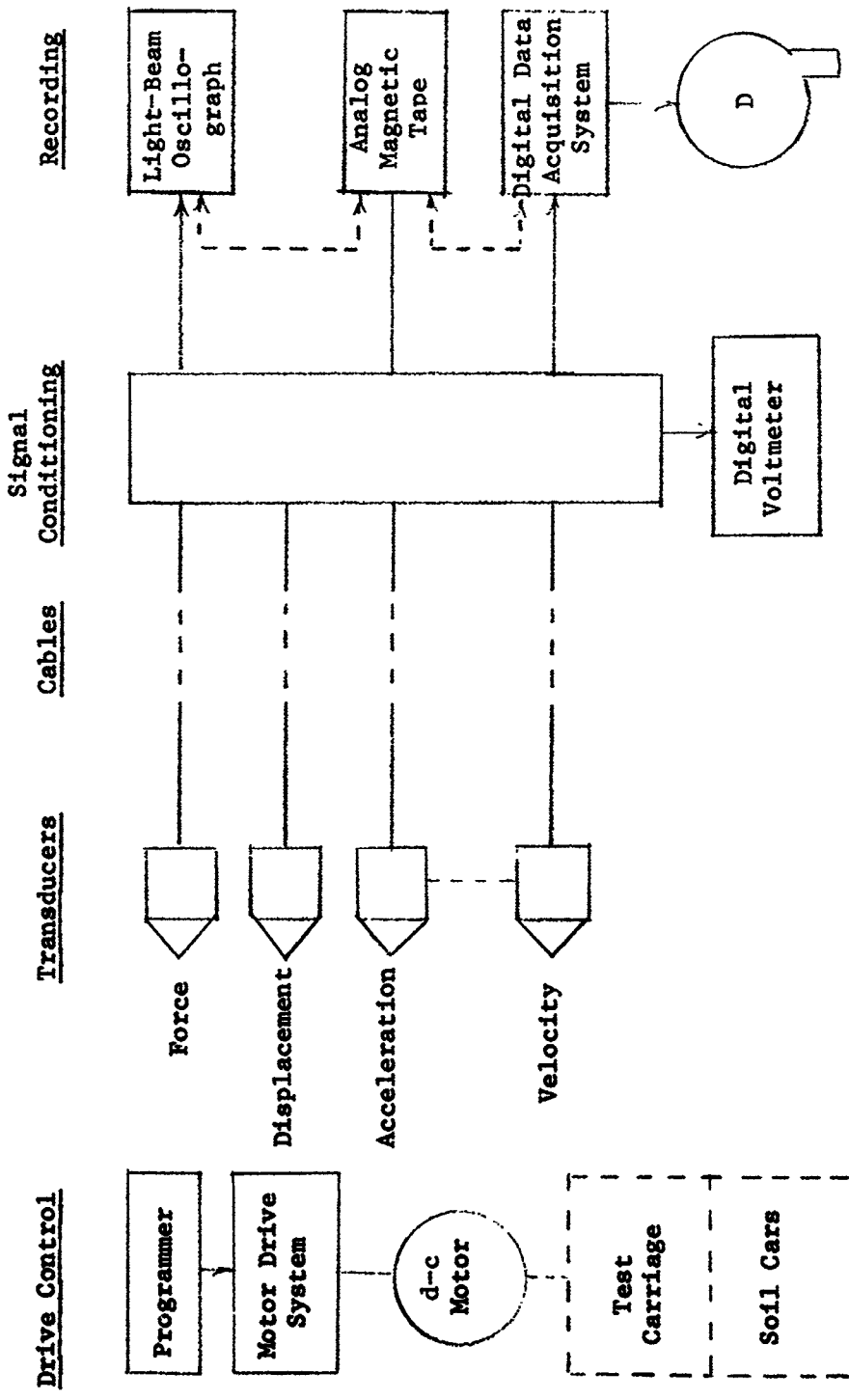


Fig. All. Flow chart for measurement and control systems

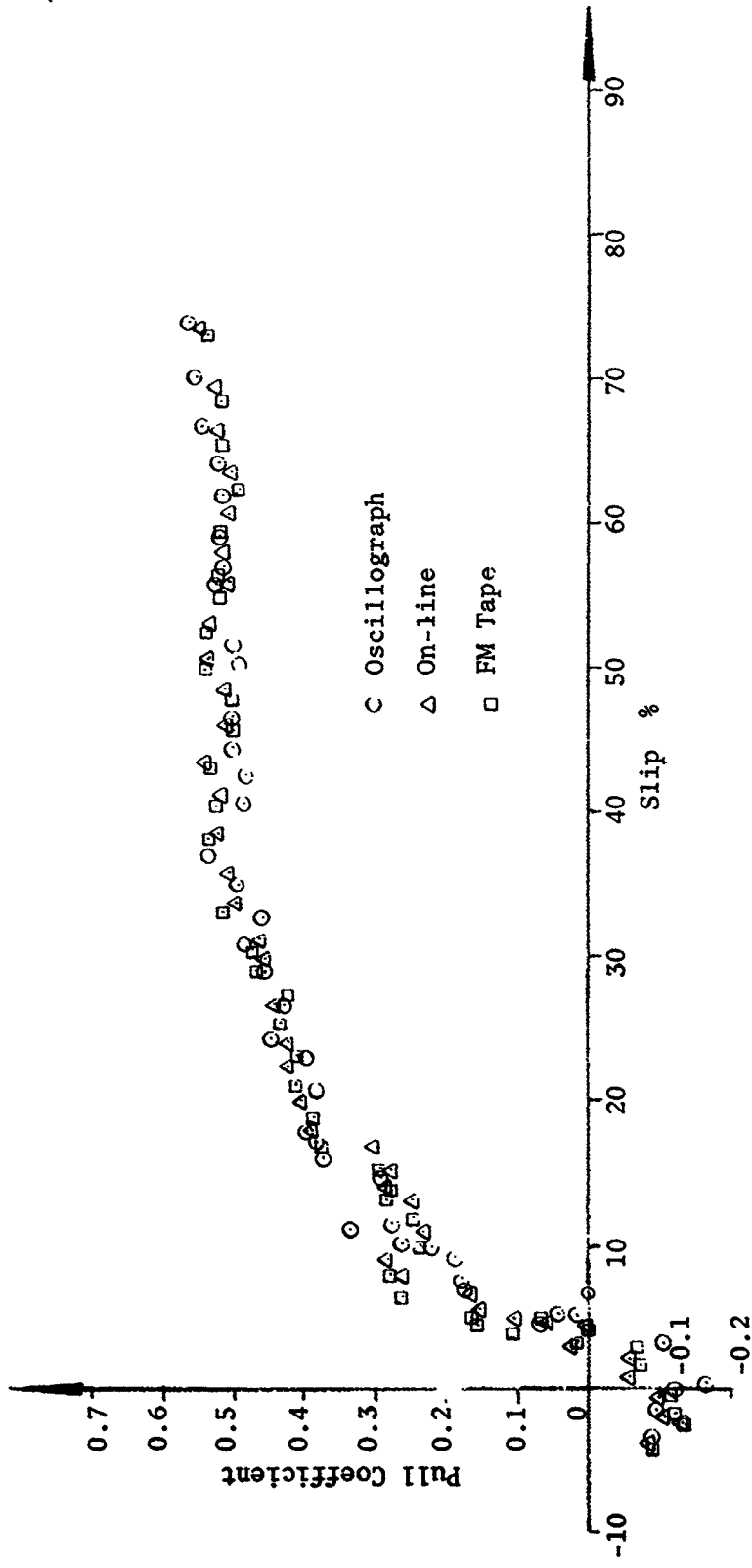


Fig. A12. Comparison of relations of pull coefficient to slip obtained by three different recording methods

Unclassified  
Security Classification

DOCUMENT CONTROL DATA - R & D		
<i>(Security classification of title, body of abstract and indexing annotation must be entered when the overall report is classified)</i>		
1. ORIGINATING ACTIVITY (Corporate author) U. S. Army Engineer Waterways Experiment Station Vicksburg, Mississippi		2a. REPORT SECURITY CLASSIFICATION Unclassified
		2b. GROUP
3. REPORT TITLE PERFORMANCE OF BOEING LRV WHEELS IN A LUNAR SOIL SIMULANT; Report 1, EFFECT OF WHEEL DESIGN AND SOIL		
4. DESCRIPTIVE NOTES (Type of report and inclusive dates) Report 1 of a series		
5. AUTHOR(S) (First name, middle initial, last name) Andrew J. Green Klaus-Jurgen Melzer		
6. REPORT DATE December 1971	7a. TOTAL NO. OF PAGES 83	7b. NO. OF REFS 9
8a. CONTRACT OR GRANT NO.	9a. ORIGINATOR'S REPORT NUMBER(S) Technical Report M-71-10, Report 1 (Supersedes Technical Report M-70-15)	
b. PROJECT NO.	9b. OTHER REPORT NO(S) (Any other numbers that may be assigned this report)	
c.		
d.		
10. DISTRIBUTION STATEMENT Approved for public release; distribution unlimited		
11. SUPPLEMENTARY NOTES		12. SPONSORING MILITARY ACTIVITY George C. Marshall Space Flight Center National Aeronautics and Space Administration Huntsville, Alabama
13. ABSTRACT Six versions of the Boeing-GM wire-mesh wheel were laboratory tested in a lunar soil simulant, consisting of a crushed basalt with a grain-size distribution similar to that of samples collected during Apollo 11 and 12 flights, to determine their relative performance. The consistency of the soil was varied to cover a range of cohesive and frictional properties to simulate soil conditions assumed to exist on the moon. Programmed-slip and constant-slip tests were conducted with the U. S. Army Engineer Waterways Experiment Station single-wheel dynamometer system. The performance of the wheel covered with a metal chevron tread over 50 percent of its contact surface was slightly superior to that of other tread designs. The amount of soil accumulated in the wheels during the tests varied linearly with slip. Less soil accumulated in the 50 and 75 percent chevron-covered wheels than in the open-mesh one. Pull/load increased rapidly with increasing slip to a near maximum at 15 to 25% slip for all wheels, then increased slowly with increasing wheel slip to 100% slip. This behavior suggests that the operation of a vehicle at slips higher than 25% for protracted periods would result in immobilizing the vehicle, as would be the case if the vehicle were required to negotiate a soft soil spot or a steeper slope section. Specific power requirements for all wheels tested, as depicted by the power number, also rose rapidly at slips beyond 15 to 25%. These trends indicate that the wheel performance at 20% wheel slip provides a reasonable measure for comparing the limiting mobility performance capabilities of several versions of the basic GMC (wire-mesh) Lunar Roving Vehicle (LRV) wheel type. Following the selection of the Boeing-GMC wheel for LRV, additional wheel-soil interaction tests were conducted in the lunar soil simulant and are reported in Report 2 of this series. Appendix A describes in detail the WES dynamometer system in which the LRV wheel was tested.		

DD FORM 1473 1 NOV 68 REPLACES DD FORM 1473, 1 JAN 64, WHICH IS OBSOLETE FOR ARMY USE.

Unclassified  
Security Classification

Unclassified  
Security Classification

14. KEY WORDS	LINK A		LINK B		LINK C	
	ROLE	WT	ROLE	WT	ROLE	WT
Lunar roving vehicles						
Lunar soils						
Simulated soils						
Vehicle wheels						

Unclassified  
Security Classification